universität wien

# DISSERTATION

Titel der Dissertation

# In search of the cellular function of a novel adjuvant

How KLK, a unique membrane-interacting peptide, contributes to adjuvant action

angestrebter akademischer Grad

Doktor der Naturwissenschaften (Dr. rer.nat.)


| | |
|---|---|
| Verfasser: | Michael Christoph Aichinger |
| Matrikel-Nummer: | 0001212 |
| Dissertationsgebiet: | Genetik – Mikrobiologie |
| Betreuer: | Prof. Dr. Thomas Decker |
| Wien, im | September 2009 |

# Thesis related publications

*"Adjuvanting the Adjuvant: Facilitated delivery of the immunomodulatory oligonucleotide, ODN1a, to TLR9 by the cationic antimicrobial peptide, KLK, in dendritic cells."* Submitted.

*"Unique membrane-interacting properties of the immunostimulatory cationic peptide KLKL(5)KLK (KLK)."* (Aichinger et al.; Cell Biology International, (2008), 32(11): 1449-58)

# Table of Contents

# 1.1. Summary

In the last years new technologies considerably improved the development of vaccines. Genomics-based, high throughput techniques contributed significantly to antigen identification and selection for many pathogens. However, vaccines consisting of even the most carefully selected antigens only are limited in their application, as immunisation with such preparations does not always lead to an adequate immune response. Therefore, supplementation of vaccines with adjuvants that improve and modulate the immune system is desirable. The number of adjuvants licensed for human application is limited. Currently, only Alum, MF59 and Virosomes are on the market and only Alum is licensed worldwide.

IC31® is a novel potent adjuvant composed of the cationic antimicrobial peptide $NH_2$-KLKLLLLLKLK-COOH (KLK) and the TLR9 agonist oligonucleotide ODN1a (poly(dIdC)$_{13}$).

In this research project we clarified the molecular mechanisms behind the function of IC31®. We demonstrated profound membrane-interacting properties and unique conformational transitions of KLK. Interaction of this peptide with various membrane vesicles as well as cells altered membrane ultrastructure and cell surface morphology.

We showed that KLK forms aggregates with ODN1a. Due to charge attraction and membrane-interacting properties of KLK, these complexes are readily attracted to cell surfaces. We revealed that the presence of KLK considerably increased endocytic uptake of ODN1a into dendritic cells. We localized the nucleotide in both early and late endosomes as well as the endoplasmic reticulum. Further, we observed ODN1a in TLR9 positive compartments while KLK was demonstrated to stay associated with the plasma-membrane.

Our results made significant contributions to better understanding of the molecular action of IC31®. With these contributions IC31® became one of the best understood adjuvants in current vaccine research.

# 1.2. Zusammenfassung

In den letzten Jahren wurde die Entwicklung von Impfstoffen durch neue Methoden vorangetrieben. Die gezielte gentechnische Herstellung von Antigenen ist sicherer in der Verwendung und gezielter in der Aktivität. Dennoch sind diese meist partikulären Impfstoffe entscheidend in der Anwendbarkeit eingeschränkt – schlicht aufgrund der Tatsache, dass die Impfung mit Antigenen alleine nicht immer die notwendige Immunantwort auslöst. Aus diesem Grund wird auf so genannte Adjuvanzien zurückgegriffen, die das Immunsystem stimulieren ohne selbst einen antigenischen Effekt zu haben. Die Zahl der für humane Immunisierung zugelassenen Adjuvanzien (Alum, MF59 und Virosomen) ist gering. Wobei betont werden muss, dass allein Alum weltweit zugelassen.

IC31® ist ein neues Adjuvans, welches aus dem kationischen, antimikrobiellen Peptid $NH_2$-KLKLLLLLKLK-COOH (KLK) und dem Nukleotid ODN1a (oligo-$(dIdC)_{13}$) welches von TLR9 erkannt wird.

Die vorliegende Arbeit legt zum ersten Mal den molekulare Mechanismus hinter der Funktion von IC31® offen. Wir zeigen, dass KLK mit unterschiedlichen Membranen interagiert und darin, ohne Poren zu generieren, interkaliert. Dabei sind eine Lipid-induzierte Änderungen der Konformation des Peptids von random-coil zu einem β-Faltblatt und von einem β-Faltblatt zu α-Helix, sowie KLK induzierte ultrastrukturelle Veränderungen der Membranen zu beobachten.

Wir demonstrieren des Weiteren, dass KLK mit ODN1a aggregiert. Aufgrund der Ladung des Peptids und seiner Fähigkeit mit Membranen zu interagieren, lagert sich der Komplex an der Oberfläche von Zellen an. Wir zeigen weiters, dass die Anwesenheit von KLK die endozytotische Aufnahme von ODN1a in dendritische Zellen erhöht. Wir haben das Nukleotid in frühen und späten Endosomen sowie im Endoplasmatischen Retikulum detektiert und darüber hinaus gezeigt, dass es mit TLR9 positiven Kompartimenten kolokalisiert. KLK sebst wird nicht in die Zellen aufgenommen sondern verbleibt vielmehr an der Plasmamembran.

Durch die vorliegende Arbeit konnte zum ersten Mal die molekulare Wirkungsweise von IC31® dargestellt werden. Die Funktion der beiden Komponenten im Bezug auf die Stimulation des Immunsystems ist klar. Dadurch wird IC31® zu einem der am Besten verstanden Adjuvanzien.


**Figure 1. Early vaccination critics**

Early cartoon showing people with cows growing out of their bodies after being vaccinated with cow-pox. The painting in the upper middle of the picture recalls the worship of the golden calf . (James Gillray, 1802; Library of Congress, Prints & Photographs Division)

# 2. Introduction

Research is most interesting when multiple topics come together to create a new story and a conclusive picture about a particular subject. In the course of this thesis our knowledge about the novel adjuvant IC31® gets more and more detailed, as the story starts from scratch with *in silico* studies of one component and leads to the observation of the fate of IC31® within the target cells. The examination touches diverse research fields that seemingly do not overlap at first, but are necessary to understand the function of IC31®.

The introduction deals first with the history and problems of vaccination in general. At the end of this chapter a short outlook is given where the need for new adjuvants is emphasized. The already licensed adjuvants and some of the most promising substances are described in the next section before the two components of IC31® are detailed. Here, it is quoted that the mode of action of the adjuvant is dependent on the function of a cationic antimicrobial peptide and therefore describe general properties of these peptides in a detailed but important following chapter. Then key properties of dendritic cells, the target cells of IC31® are explained and finally, the introduction concentrates on the different cellular uptake routes that might be involved in the mode of action of the adjuvant.

# 2.1. Vaccination

## 2.1.1. History

Active immunization is one of the greatest success-stories in medical history. The eradication of smallpox and the worldwide reduction of polio are perhaps the best-known achievements of this medical intervention. Additionally, millions of lives were safed by routine vaccination against childhood-diseases such as measles or mumps and against tetanus. The theory of adapted immunity was essential for the development of this health intervention. In 430 B.C. Thukydides described the plaque of Athens. The inhabitants already recognized that people who survived the disease did not suffer from it again.

The empirical roots of vaccination date back to ancient India and China were the technique of inoculation was discovered. People observed that smallpox appear in two distinct forms which were later identified as two different strains. The idea was to introduce a mild infection by blowing crusts of a pustule from a child with a less severe infection into the nostrils of an uninfected child. At the early years of the 18$^{th}$ century Lady Wortley Montague learnt this technique in Constantinople and brought this knownledge back to London. Here, king Georg I could be persuaded after experiments with Newcastle prisoners and orphans to inoculate his grand daughters and later his grand son (for review see Grundy, 2000). In 1796, Edward Jenner, a surgeon in England, realized that people who were in contact with cows suffering from cowpox did not sicken from smallpox. So he started what we now call vaccination (vacca in Latin means cow) by inducing mild cowpox in humans that protected them against the disease. This approach turned out to be safer than inoculation which caused in a large percentage of treated people the severe form of smallpox (for review see Bazin, 2003).

Very soon authorities realized that for the first time in history there was a tool at hand that could not treat but already prevent life threatening diseases and quickly introduced vaccination for whole population use.

## 2.1.2. Problems

The major problems regarding vaccination today are not scientific restrictions – some will be mentioned at the end of this chapter – but the public opinion toward this medical technique. Interestingly, from the beginning of vaccination-history the emergence of vaccination critics and opponents can be observed. Not only because inoculation was unsafe, but for example because people feared the injection of material from cows as they expected to turn into cows themselves (Figure 1A). Vaccination is still a constant matter of debate. Every year discussions about the usefulness of the Influenza-vaccine fill the Austrian media. In the anglo-american countries vaccination opponents claim a link between immunisation and autism. Most of these critics are marked by an enormous distrust of health autorities and pharmaceutical companies. Various scientific approaches were taken to examine the reasons for this opposition (Campbell et al., 2000; Sturm et al., 2005; Zimet et al., 2006; Marckmann, 2008; Maurer, 2008).

Especially, immunisation of children has to face an increasing opposition of laymen groups but also of people with scientific background endangering not only the health of their children – a fact that DDr. Wolfgang Maurer, a well known Austrian vaccinologist calls child-maltreatment (Maurer, 2008) – but also a high number susceptible persons that can not be vaccinated as increasing numbers of unvaccinated people weakens the herd immunity (Fine, 1993). As a matter of course, health authorities try to fight this negative development.

Here, to keep the vaccination-levels high, some countries go for compulsory immunisations referring to ethics and fairness (May and Silverman, 2005; Asveld, 2008). Others reject their introduction as they would harm the "trust, choice and openness" of doctor-patient relationships (British Medical Association: Bord of Science and Education. 2003. Childhood Immunisation: A Guide for Healthcare Professionals). The problems caused by vaccination-opposition seem to be increasing. The outbreak of measles in a school in Salzburg in the year 2008 (Schmid D., 2008) is just the tip of the iceberg. In Germany the herd immunity regarding measles is decreasing and large outbreaks are reported regularly (Wichmann et al., 2007; Muscat et al., 2009; Poethko-Müller et al., 2009). An easy solution is not in view, but a truthful publication even of problems in vaccine development and an explanation of motives behind the vaccination-strategies might form a mutual trust that allows to inform the population and the customers of the necessity and advantages of vaccination.

## 2.1.3. Outlook

Although in the last century some deadly diseases could be eradicated or restrained by vaccination, others could not be fought. One explanation for the small number of available vaccines was the success of antibiotics that made many pathogens less threatening. Others were technological restrictions. Just lately it became possible to produce promising virus like particles, such as those used for HPV-vaccination. In addition, improved methods of DNA sequencing and protein prediction enable the design of new antigens and to test them for induction of immunity. In combination with novel vector systems, vaccination is not restricted anymore to communicable diseases. Every year millions of people dye from new epidemics like Alzheimer´s disease, obesity, high blood pressure or smoking (Zimmet and Alberti, 2006). The call for "new imaginative strategies" of the WHO to fight these non communicable diseases might be answered by a "second vaccine revolution" (Dyer et al., 2006). Here, the immunisation is directed against self-molecules like angiotensin II which is connected to hypertension. The new strategies face unique technical challenges as long-lived antibodies against self-molecules raise safety issues resulting from the potentially irreversible depletion of molecules targeted by vaccination. Further, the public opinion towards this progress might not be unproblematic. Comparable to the development of drugs against lifestyle diseases, vaccination against smoking or eating habits could endanger the mentioned trust needed for every immunisation-strategy.

Due to new technologies, the future of vaccination is promising, but if we do not face the problems today we will reduce every possible success of the coming years.

# 2.2. A short overview of adjuvants

## 2.2.1. Introduction

The development of new generation subunit vaccines increases the safety of immunization. In 1989, Janeway called adjuvants "the Immunologist´s dirty little secret", as a great deal of ignorance existed that these subunit vaccines or killed whole organism require the addition of a helper ("adjuvare" in latin means "to help") to be effective. Adjuvants stimulate the immune system and increase the response to a vaccine without having any antigenic effect itself. They are a heterogeneous group of compounds that can be composed of different constituents with different functions and activities, including carrier-, depot- or targeting functions (Guy, 2007). The current challenge facing adjuvant research is to find the "perfect mix" (Guy, 2007). It should be safe, the compounds should work synergistically and the adjuvant should drive the immune response into the desired direction and to the right cells. Generally, antigen presenting cells are the desired targets and here especially the dendritic cells (Gamvrellis et al., 2004).

The first to work with adjuvant-like material was Dr. William B. Coley in 1891, who injected streptococcal organisms into a patient with a malignant bone sarcoma. The treatment stimulated the immune system of the patient and the tumor disappeared (for review see Espinoza-Delgado, 2002; McCarthy, 2006). The so called Coley´s toxins can be regarded as pathogen associated molecular patterns (PAMPs) which activate toll like receptors (see below). In vaccines, adjuvants are used since the early 1920s (for review see Cox and Coulter, 1997). Glenny et al. tested the immunostimulatory properties of various precipitated diphtheria-toxoids. Among these were toxoids precipitated by addition of potassium alum ($KAl(SO_4)_2$ x $12H_2O$). These led to a significant increase in the immune response against toxins (Glenny et al., 1926). The various forms of aluminium-based compounds became the first adjuvants for human application and are up to date the most widely used adjuvants.

Until recently, the mode of action of alum was poorly understood. People suggested the depot formation and the related sustained release of the antigen as the major function of an antigen. In 2008 it was demonstrated that the NALP3 inflammosome is involved in the immuno-stimulatory function of aluminium salts (see below) (Hornung et al., 2008; Núñez, 2008). Today, adjuvant candidates can be found rather easily. Every protein, toxin, peptide, salt, lipid, sugar etc. stimulating the immune system might be suitable. The restriction hampering

the application is the safety in humans. In the following section, the currently used adjuvants as well as the most promising approaches are described.

## 2.2.2. Aluminium compounds

Amoung the various aluminium salts, aluminium hydroxide and aluminium phosphate are most commonly used as adjuvants. The term alum restricted to potassium alum, $KAl(SO_4)_2$ (for review see Lindblad, 2004). Precipitation of diphtheria toxin revealed the immuno-stimulatory effects of Alum in 1926, and later of aluminium phosphate (Ericsson, 1946). In general, aluminium salts form a depot at the site of injection and are proposed to induce antibodies and $T_H2$ responses via activation of the NALP3 inflammasome. The inflammosomes are multi-protein complexes in the cell cytoplasm. The complex is composed of an nucleotide domain leucine-rich repeat containing receptor (NLR), a cysteine protease caspase-1 and the adaptor molecule ASC that connects the NLR and the caspase (Agostini et al., 2004) and important parts of the innate immune system. Best studied is the NALP3 inflammosome that is activated by multiple pathogen-associated molecular patterns (PAMPs) like degradation products of bacterial peptidoglycans. Recently, it has been demonstrated that crystalline structures like Amyloid-β, silica and asbestos and alum activate the NALP3 inflammosome (Ennio De Gregorio, 2008; Hornung et al., 2008; Kool et al., 2008; Cassel et al., 2009). This leads to the cleavage of proIL-1β, IL-18 and IL-33 by caspase-1 into its active form and a subsequent inflammation due to the release of the active interleukins. The general ability of aluminium adjuvants to stimulate the production of IgE as part of the overall $T_H2$ profile is well-established (Hamaoka et al., 1973). This has been mentioned as a disadvantage. Anyhow, it has been difficult to demonstrate cases where vaccination with aluminium adjuvants has led to allergy towards the antigen (Lindblad, 2004).

## 2.2.3. Emulsions

One may discriminate between two prototypes of emulsions, water-in-oil inducing $T_H1$ and oil-in-water inducing $T_H2$ responses. The mechanism of action of adjuvant emulsions includes the formation of a depot at the injection site, allowing slow release of the antigen, and the stimulation of antigen specific B-cells (for review see Aguilar and Rodríguez, 2007).

MF59, licensed by Novartis for a flu vaccine (Fluad®) in 1997, is an oil-in-water emulsion which induces like aluminium compounds a $T_H2$ response (Podda and Del Giudice, 2003).

Montanide 720, is a water-in-oil emulsion (for review see Qiu et al., 2008) that has been used in trial vaccines agains HIV, malaria and breast cancer (Jones et al., 1990). The combination of Montanide 720 and CpG-DNA has recently been demonstrated to induce a mixed $T_H1/T_H2$ response (Roohvand et al., 2007) which would be interesting for further applications.

## 2.2.4. Saponins

Saponins are steroid or triterpenoid glycosides found in wild or cultivated plants, lower marine animals and some bacteria (for review see Rajput et al., 2007). The triterpenoid saponins of the bark extract of the tree *Quillaja saponaria* was demonstrated to induce a $T_H1$ response and to increase immune cell proliferation in vitro (Chavali et al., 1987). But due to their toxicity they could not be use in human application. The development of semi-synthetic saponin derivatives that induce a $T_H1/T_H2$ response might open new possibilities for adjuvant applications (Marciani et al., 2003; Skene and Sutton, 2006). Anyhow, further studies are needed to prove efficacy and safety.

## 2.2.5. Virus-like particles and virosomes

Virus-like particles (VLPs) are based on viral capsid proteins which self-assembly into particulate structures closely resembling immature virus particles (Gheysen et al., 1989; Hagensee et al., 1993). The first step to virosome development was the generation of lipid vesicles containing viral spike proteins (Almeida et al., 1975). Today, virosomes are produced by detergent solubilization and reconstitution of enveloped viruses (Bron et al., 1993). All established VLPs proved to be strong stimulators of the innate immune system. The potential of VLPs to activate and mature DCs has been extensively investigated (Sailaja et al., 2007). Antigen specific stimulation of the immune system is achieved by expressing the antigens at the surface of VLPs (Huckriede et al., 2005).

This method allows new approaches to the field of immunization as vaccines can now be directed against self-antigens. Various attempts using VLPs have already been made to prevent different non communicable diseases like obesity, smoking and high blood pressure with antigens against ghrelin, nicotine and angiotensin, respectively (Dyer et al., 2006).

Further, VLPs can function directly as vaccines. Lately, they have been introduced in HPV-vaccination (for review see Cutts et al., 2007) and might in the future play a role in immunization against HIV (Young et al., 2006 Buonaguro et al., 2006).

## 2.2.6. TLR-agonists

Toll like receptors (TLRs) are critical for the innate immune response and will be described in more detail later. The various natural and synthetic TLR-agonists all exert immune-stimulatory effects and are thus potentially applicable as adjuvants (for review see Pulendran Bali 2004; Lahiri et al., 2008). Different attempts are made to target TLR2 with OspA (Yoder et al., 2003), TLR4 with lipid A mimetics (Cluff et al., 2005), TLR5 with flagellin (Huleatt et al., 2007) and TLR3, TLR7, TLR8 and TLR9 with different nucleotides to induce an immune-stimulation.

### 2.2.6.1. RNA and DNA

One approach to stimulate the immune system is the *in vivo*-transfection of cells with RNA or DNA which would lead to an expression of the antigens encoded in the nucleotide sequence (Fynan et al., 1993). In this regard, the nucleotide would be used as vaccine. But the method is limited by a multitude of hurdles like their low transfection-potency in humans and the lack of suitable vector systems (Donnelly et al. 2003).

In addition to the application of DNA and RNA as vaccines their potential role as adjuvants attracts a great deal of attention. TLR3, TLR7/8 and TLR9 recognize dsRNA, ssRNA and unmethylated CpG-DNA, respectively. Various synthetic substitutes of the nucleotides have also been implicated, like polyinosine-polycytidylic acid (poly(I:C)) for TLR3 activation (Matsumoto and Seya, 2008; Salaun et al., 2009), the imidazoquinoline compounds imiquimod and R-848 for TLR7/8 (Hemmi et al., 2002) and synthetic oligodeoxynucleotides containing unmethylated CpG motifs or poly(dIdC) for TLR9 stimulation.

Due to stability reasons the phosphodiester-backbone of the nucleotides is often replaced by phosphorothioate. These modifications confer advantages like an enhanced binding of the DNA to the cell surface and protection from nuclease activity and are therefore thought suitable for clinical applications (Krieg et al., 1999). Unfortunately various side effects are published for the treatment with modified and unmodified CpG-DNA. In the murine system development of arthritis (Deng et al., 1999) and splenomegaly (Zhao et al., 1996) have been reported which would clearly limit the application in humans.

The need for new adjuvants which are not restricted in regard to their application in humans is obvious. The availability of a broad spectrum of well understood adjuvants that stimulate the immune system in different ways allowing vaccine makers to choose the most suitable for

each vaccine would be beneficial. But though many immunostimulatory compounds are known, today only three adjuvans are licenced for humans in Europe (Alum, MF59 and virosomes in Fluad®) and only Alum is licensed in the United States. None of these is a good general inducer of a $T_H1$ response which would be preferable for many diseases.

## 2.2.7. IC31

IC31®, developed and licensed by Intercell™, represents a very promising adjuvant. At the beginning of the development Intercell™ experimented with DNA and RNA, as the immune-stimulatory effect of these were already known. But the clinical application of nucleotides is limitated as, the material is quickly degraded administration of certain DNA can be harmful (Lipford et al., 1997; Sparwasser et al., 1997). Therefore, it was important to use an adequate nucleotide-sequence combined with a vector system for efficient delivery and stability. In this regard, cationic peptides have long been considered as useful tools to deliver DNA into cells and are still today interesting for gene-therapy (for review see Mann et al., 2008).

Intercell demonstrated that a combination of CpG-DNA and the cationic peptide poly-L-arginine, which is immuno-stimulatory itself, leads to a potent adjuvant with reduced side effects of the CpG-DNA (Buschle et al., 1997; Schmidt et al., 1997; Mattner et al., 2002). They considered that a combination of two immuno-stimulatory compounds represents a more potent adjuvant compared to one compound alone.

After further experiments, the most promising combination, named IC31, was the nucleotide ODN1a (oligo-$(dIdC)_{13}$), a single stranded DNA with a phosphodiester backbone and the short synthetic, cationic peptide KLK ($NH_2$-KLKLLLLLKLK-COOH).

Initially, KLK was found in a systematic screen for synthetic antimicrobial peptides (AMPs) of the active core of sapecin B from *Sarcophaga peregringa* (flesh fly) by Alvarez-Bravo et al. in 1994 and tested later for its antimicrobial activity (Nakajima et al., 1997). Initial experiments proved that KLK somehow interacts with membrane systems (Alvarez-Bravo et al., 1994) and exhibits immuno-stimulatory effects and induces a $T_H2$-type immune response against co-injected antigens (Cho et al., 1999; Fritz et al., 2004). Interestingly, surface clareticulin was shown to be involved KLK uptake and stimulation of neutrophils (Cho et al., 1999). The signalling of ODN1a is dependent on TLR9 and induces an antigen-specific cellular type 1 response and a mixed type 1/2 humoral response. In any case, the presence of KLK was required for an immune response (Schellack et al., 2006). If IC31 is injected into mice, KLK is necessary to form a stable depot with a co-injected antigen at the site of

injection (Schellack et al., 2006). Interestingly, a control peptide of KLK with a proline substitution of the middle leucine named KPK (KLKLLPLLKLK) did not induce depot formation or immune-stimulation (Schellack et al., 2006). How the cationic antimicrobial peptide, KLK, contributes to the adjuvant activity, had to be demonstrated.

# 2.3. Antimicrobial peptides

## 2.3.1. General properties of antimicrobial peptides

All higher organisms need protection against bacteria, viruses and fungi. Beside the adaptive immune response, membrane active peptides and proteins play a crucial role in first line against microorganisms. Gene-encoded AMPs are conserved components of the innate immune response and widespread in nature, as they are synthesized by microorganisms and multicellular vegetal and animal organisms (for review see Bulet et al., 2004). The first AMPs were isolated by electrophoresis of a lysosomal fraction of guinea pig leukocytes (Zeya and Spitznagel, 1966) and named defensins. Many AMPs possess besides their antibacterial and antifungal activities, antiviral or anticanceral properties and can influence inflammation, proliferation, wound healing, release of cytokines, homeostasis and chemotaxis (for review see Kolls et al., 2008). AMPs are regarded as potential agents against antibiotic resistant pathogens (Zaiou, 2007).

Today, more than 1000 antimicrobial peptides are known and collected in various data-bases (e.g. http://aps.unmc.edu/AP/main.php). To improve the effects of natural occurring peptides, a constantly increasing number of AMPs is generated synthetically that mimic sequences found in natural peptides (Isogai et al., 2008; Kitani et al., 2009; Yu et al., 2009). Although AMPs are chemically and structurally heterogeneous, all share three characteristics:

1) They are small molecules with a molecular mass between 1 and 5 kDa.
2) They are cationic or contain positively charged elements of 10-25 amino acids and therefore often named cationic antimicrobial peptides (CAMPs).
3) They have a tendency to form amphipathic structures in non-polar solvents.

According to their size, molecular composition, conformational or predominant amino acid structure they are devided into groups that might differ from one publication to the other (Andreu and Rivas, 1998; Hof et al., 2001; Bulet et al., 2004). The following classification is representative and implies most of the characteristics (Hof et al., 2001):

1) linear peptides with an α-helical structure
2) linear peptides with an extended structure characterised by overrepresentation of one or more amino acids
3) peptides containing a looped structure
4) conformationally more restrained peptides, predominantly consisting of β-strands connected by intramolecular disulfide bridges

## 2.3.2. Interaction of AMPs with membranes

Because of the above mentioned characteristics, AMPs have a strong affinity to phospholipids and it is generally assumed that their antimicrobial activity involves binding to the membrane bilayer of the target cell and thereby perturbing the membrane permeability or changing its ultrastructure. Upon their interaction with lipid membranes AMPs follow the same thermodynamic rules as other proteins and peptides (e.g. β-amyloid peptide (1-40)). Therefore interaction can be devided into three steps (for review see Seelig, 2004):
First, an electrostatic attraction of the positively charged peptide to the negatively charged membrane occurs. Second, adsorption to the membrane structures and third, conformational changes and thus adoption of amphipathic structures can be observed (for review see Hof et al., 2001).
A general feature is the conformational change upon interaction with the membrane. Many proteins and peptides like the AMP melittin (Vogel, 1981) have a random coil conformation in solution and an α-helical structure when associated with a lipid membrane. The Alzheimer β-amyloid peptide (1-40) undergoes conformational transitions in the presence of negatively charged peptides. First from random-coil to β-sheet, and then, at a high lipid to peptide ratio into an α-helix. (Terzi et al., 1997).
In general AMPs kill microbes by causing membrane leakage. Here, direct measurements of the peptide/membrane interaction are not possible and artificial liposomes are used to study the effects of AMPs. Thereby depending on the peptide (Bechinger, 1997) several models have been proposed to explain the molecular events taking place during the process that induce this leakage (for review see Oren and Shai, 1998; Bechinger, 1999; Shai, 1999; Hof et al., 2001).

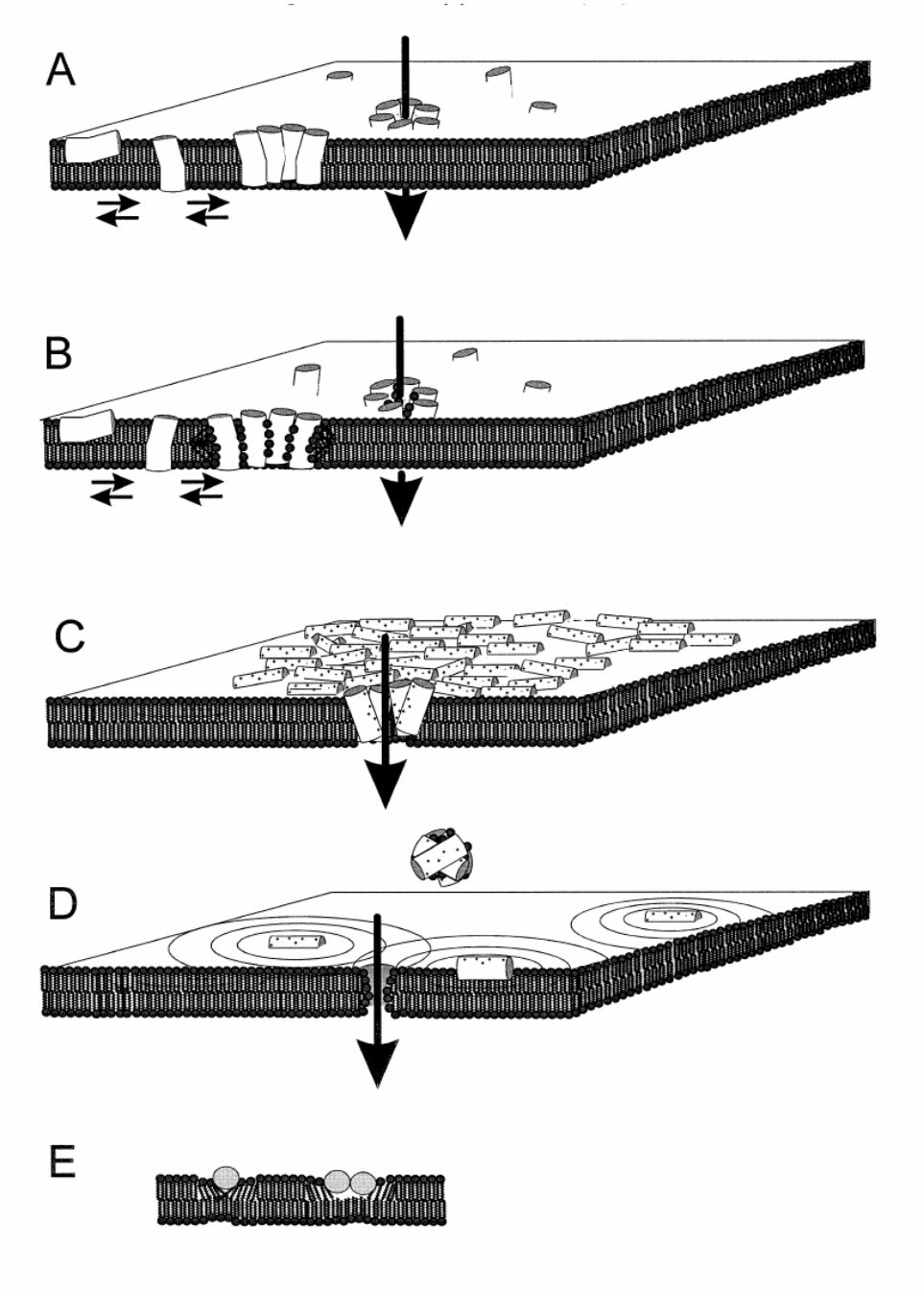


**Figure 2. Models of interaction of AMPs with phospholipid membranes**

(A) Transmembrane helical bundle of mostly hydrophobic polypeptides.

(B) Wormhole model.

(C) Carpet model.

(D) In-plane diffusion model.

(E) The disruption of the lipid bilayer packing due to in-plane inserted peptides is schematically illustrated for monomers and side-to-side dimers. (Bechinger, 1999)

### 2.3.2.1. The barrel-stave model

The barrel-stave model or helical bundle model is the classical picture where α-helical peptides insert into the membrane in a transbilayer orientation, and aggregate to form a pore (Mueller, 1975). The hydrophobic faces line the water filled lumen of the channel and the apolar residues point towards the membrane (Figure 2A). Even though this model was proposed 30 years ago, a conclusive demonstration of its validity was obtained only for alamethicin (Tieleman et al., 2002; Stella et al., 2007; Qian et al., 2008). The barrel-stave model has been questioned and as an alternative, the wormhole model was proposed.

The wormhole model (Ludtke et al., 1996) is a modification of the barrel-stave model, where peptides form together with lipids the walls of the openings. Due to interaction of the peptide and the membrane, the lipid bilayer bends back and the outer and inner layer get in contact and form a pore (Figure 2B). This model was suggested for an antimicrobial peptide from *Xenopus laevis*, magainin (Ludtke et al., 1996). More recently, another mechanism, the "carpet" model was proposed. Therefore, the formation of wormholes possibly just reflects an intermediate state between the membrane micellisation and the peptide activity (for review see Bechinger, 1999).

### 2.3.2.2. The carpet model

The carpet model was first used to describe the mode of action of dermaseptin S (Pouny et al., 1992). Later it was applied to various other AMPs like cecropins and LL-37 (for review see Shai, 1999). In this model, the membrane is fully covered by a carpet-like cluster of peptides (Figure 2C). Membrane permeation occurs, when a critical concentration of membrane-bound peptide is reached. In contrary to the barrel-stave model, the peptides are not inserted into the hydrophobic core of the membrane and the peptide does not need to adopt a specific structure upon its binding to the membrane. The AMP associates with the membrane surface, parallel to it, with the hydrophilic face oriented towards the water phase (Gazit et al., 1996). Finally, the membrane is disintegrated by the disruption of the bilayer curvature. On the molecular level the intercalation of peptides between the phospholipid head groups corresponds to insertion of a cone-shaped molecule into the membrane (Figure 2E). The formation of wormholes might be an intermediate state of the subsequent lysis process (for review see Shai, 1999; Hof et al., 2001).

### 2.3.2.3. Detergent-like effects

Because peptides have earlier been observed to act as detergents (Schafmeister et al., 1993; Bechinger, 1997) the authors referred to it as detergent-like effect. The model is based on the intercalation of the peptides into the bilayer (Bechinger and Lohner, 2006). During the disruption of the membrane micellar structures can bud from the membrane of high local peptide concentration (Oren and Shai, 1998; Bechinger, 1999; Bechinger and Lohner, 2006).

### 2.3.2.4 In-plane diffusion model

In contrast to the carpet- and detergent-like model, the in-plane diffusion model applies to low peptide-to-lipid ratios (Figure 2E). The model is independent of cationic peptide aggregation. Insertion of a peptide into the lipid bilayer leads to a disturbance in the bilayer packing, leading to reduction of its thickness and finally to transient openenings (for review see Bechinger, 1999).

Many artificial antimicrobial peptides used in clinical trials are derived from or mimic structures of natural antimicrobial peptides expressed in various organisms (see below). Natural, gene encoded AMP have limitations in the clinical application as they might act as signalling molecules of the immune system or cause other unintended effects. Thus, to generate the optimal active AMP, a large number of artificial peptides are designed and tested.

## 2.3.3. Gen encoded and synthetic AMPs

### 2.3.3.1. Gene encoded AMPs

Gene encoded AMPs have been found in amoeboid protoczoa (Leippe, 1999), in prokaryotes (for review: Garneau et al., 2002; Nagao et al., 2006), in plants (for review see García-Olmedo et al., 1998) and in many other organisms (for review see Andreu and Rivas, 1998; Bulet et al., 2004). The expression of the proteins and peptides can be constitutively as demonstrated for human β-defensin-1 (Krisanaprakornkit et al., 1998) or upregulated by acute infections like the the human LL-37 (Frohm et al., 1997). It has further been observed, that some peptides act specifically on different microorganisms. Insect defensins for example kill preferentially Gram-positive bacteria. As the steadily growing number of known AMPs would

go beyond the scope of this thesis, the following section turns the attention to a small selection of human antimicrobial peptides.

#### 2.3.3.1.1. Human antimicrobial proteins

Here, three important groups of human antimicrobial peptides, the histatins, the defensins and the cathelecidin LL-37 will be discussed (for review see Smet and Contreras, 2005) while others like C-type lectins, S100 proteins or elastase inhibitors and their regulation (for review see Kolls et al., 2008) will not be mentioned.

**Histatins**

Histatins are a family of 24 small, cationic, histidine-rich peptides present in human saliva that have been reported to exhibit antibacterial and antifungal properties (Holbrook and Molan, 1973; MacKay et al., 1984; Pollock et al., 1984; Castagnola et al., 2004). These peptides are secreted from the submandibular, sublingual and parotid glands. As a part of the innate immune system they play an important role in maintaining oral health by limiting infections in the oral cavity. Histatin 5, which is formed by further processing histatin 3, has the strongest antimicrobial activity. As many other AMPs it shows a random coil structure in aqueous and an α-helix in non-aqueous solvents (Raj et al., 1998) but in contrast to other peptides, histatin 5 targets the mitochondria of fungi (Helmerhorst et al., 1999) or protozoa (Luque-Ortega et al., 2008) and not the cell membrane.

**Defensins**

Defensins are endogenous AMPs acting against bacteria, fungi, viruses and parasites. Ten human defensins have been identified yet that are differenciated according to their structure into α-defensins and β-defensins. Both groups are non-glycosylated, cystein-rich peptides with arginine as their primary cationic residue. α-defensins are smaller (29-35 amino acids) than the β-defensins (38-42 amino acids). Little primary sequence-homology between the two classes can be found but the tertiary structure is due to the presence of three disulfide bonds very similar. Defensins have a β-sheet structure (for review see White et al., 1995; Smet and Contreras, 2005) and can interact because of their amphiphilicity with membranes where they form ion-permeable channels (Lehrer et al., 1989, Kagan et al., 1990) to destroy the pathogen. Beside their antimicrobial activity, defenins have direct immuno-modulatory effects as they are for example able to influence the IL-1β secretion (Shi et al., 2007) or to activate monocyte-derived dendritic cells (Presicce et al., 2009).

The α-defensins can be found in B cells (HNP-1 to 3), natural killer cells (HNP-1 to 3) and in neutrophils (HNP-1 to 4), where they play a role in the oxygen-independent killing of phagocytosed micro-organisms. Two α-defensins (HD-5 and 6) are found in the Paneth cells of the smll intestine and in the epithelial cells of the female urogenital tract (Jones and Bevins, 1992; Jones and Bevins, 1993).

The β-defensins are expressed in various epithelia (hBD-1, hBD-2), in leukocytes and the bone marrow (hBD-2), keratinocytes (hBD-3) and human epididymis (hBD-4 to 6) (for review see Smet and Contreras, 2005).

**Cathelicidins**

The cathelicidin proteins are characterized by a highly conserved N-terminal domain – the cathelin-like domain. This is flanked at the N-terminus by a signal peptide and at the C-terminus by the antimicrobial peptides. All cathelicidins are expressed and stored in cell granules and can be split on demand to produce release the AMP (Zanetti et al., 1995; for review see Dürr et al., 2006). While the uncleaved protein exhibits β-sheet conformations, the released AMP turns into an α-helical in membrane environments. Cathelicidins permeabilize the membranes (for review see Gennaro and Zanetti, 2000) and kill gram-positive and gram-negative bacteria. Some cathelicidins like the human hCAP18/LL-37 have even toxic effects on eukaryotic cells and target also tumor cells.

The 37 amino acid long LL-37 is the only cathelicidin found in humans. The short sequence represents the antimicrobial moiety of the precursor hCAP18. Beside the function as AMP, LL-37 has a role as signalling molecule and is thus found in a large variety of cells, tissues and body fluids (for review see Dürr et al., 2006). Further in mice it was demonstrated that human LL-37 binds and neutralizes LPS and therefore protects against an endotoxic shock (Larrick et al., 1995; Bals et al., 1999).

### 2.3.3.2. Synthetic AMPs

The significant effects of natural AMPs against micro-organisms are promising regarding clinical applications. However, some natural AMPs have to be administered in high doses, some act as signalling molecules and cause unintentional side effects. But the mature barrier to the use of AMPs as antibiotics is their toxicity or ability to lyse eukaryotic cells (Chen et al., 2005). Therefore, there are many attempts to design the optimal active AMP against bacteria (Scott et al., 2008), fungal infections (Ajesh and Sreejith, 2009), protozoan parasites

(Kitani et al., 2009) and additional infectious agends (Isogai et al., 2008; Kitani et al., 2009; Yu et al., 2009).

Different approaches for the synthesis of a functional, artificial AMP exist (for review see Hof et al., 2001). Most promising is the design according to known natural antimicrobial peptides. Here, research in general concentrates on the peptide α-helices. These are regarded to confer the desired biocidal function. By truncation or mutation of the various regions, different synthetic peptides are designed and tested. KLK is an example of this approach. It was found in a systematic screen for synthetic AMPs of the active α-helical core of sapecin B from *Sarcophaga peregringa* (Alvarez-Bravo et al., 1994).

A further method of AMP-design is the random synthesis of peptides and a combination of the designed peptides. The maximum applicable length of such peptides is 5 to 6 amino acids which strongly limits the possibilities of this approach. Both presented methods base on trial and error.

But, as helicity, amphiphaticity, hydrophobicity and charge can be calculated, a rational design is possible (Frecer et al., 2004). The method is limited as the antimicrobial effects of a peptide are not easy to predict and structures are strongly interrelated. Therefore, the examination of peptide properties and the effects of AMP-mutation will lead to a broader understanding of the connections. This will allow advanced design of suitable antimicrobial peptides.

# 2.4. Dendritic cells

## 2.4.1. Introduction

Foreign antigens commonly invade the host through the skin or the epithelia of the gastrointestinal and respiratory system. Pathogens are therefore primarily captured in peripheral tissues that are distinct from the primary lymphoid organs (for review see Moser and Murphy, 2000). These pathogens and also injected vaccine-antigens are recognized by a group of immune cells that are key constituents of innate and later adapted immunity. Dendritic cells (DCs) represent the major class of antigen presenting cells (APCs) of the immune system (for review see Banchereau et al., 2000) and sentinel pathogens and antigens in peripheral tissues. DCs interact with T, B, natural killer (NK) and natural killer T (NKT) cells to guide the development of the immune response (for review see Creusot and Mitchison, 2004).

Multiple subclasses of DCs with distinct life span, immune functions and surface markers have been identified (Shortman and Naik, 2007). The DC subtypes found in steady-state mouse and in human include type-1 interferon-producing plasmacytoid DCs (pDCs) and the nonlymphoid tissue migratory and lymphoid tissue-resident conventional DCs (cDCs) (for review see Wu and Liu, 2007; Merad and Manz, 2009). The monocyte-derived DCs (mDCs) are the best example for a DC-type produced not in steady-state but upon inflammation (for review see Shortman and Naik, 2007).

The main function of pDCs is to secrete type 1 interferon in response to viral infections and to prime T cells against viral antigens (for review see Liu, 2005). The pDCs are derived from lymphoid progenitor cells and can be characterized by specific surface markers. Human pDC express CD4, CD45RA, high levels of CD123 and very low level of CD11c. The neuronal receptor, BDCA4, on the surface is often used to isolate pDCs. In contrast to cDCs they do not efficiently migrate to peripheral tissue.

cDCs have two main functions: the maintenance of self-tolerance and the induction of specific immune responses against invading pathogens (for review see Banchereau and Steinman, 1998). In general, myeloid precursors are the main source of cDCs (for review see Shortman and Naik, 2007). They can be divided according to their tissue localization (for review see Wu and Liu, 2007; Merad and Manz, 2009). The best studied subtype of cDCs are the skin resident Langerhans cells (LCs) that were already described in 1868 (Langerhans, 1868).

Epidermal LCs are derived from haematopoietic precursor cells but can renew locally. They express high levels of CD11c, CD1c, CD1a and can easily identified based on the expression of CD45. Typical for LCs is the expression of the lectin langerin that forms the intracytoplasmic birbeck granule (for review see Merad and Manz, 2009).

The major function of mDCs is the immune response against invading pathogens. mDCs are developed during inflammation. There are two monocyte subsets that vary in chemokine receptor and adhesion molecule expression, in migratory and differentiation properties. "Classical" $CD14^{+}CD16^{+}$ monocytes in humans express CCR2, CD64 and CD62L. "Nonclassical" human $CD14^{low}CD16^{+}$ monocytes lack CCR2 (for review see Wu and Liu, 2007). Monocytes are recruited to the site of inflammation where they can react upon danger signals due to the expression of toll like receptors (TLRs). The subsequent signalling deflects the normal pathway of differentiation towards increase DC development (Nagai et al., 2006).

Beside the differences of the subtypes, all DCs share common features. All take up antigens via different routes, the process the antigens and present them to T cells. These common features will be discussed in the following chapters.

## 2.4.2. Dendritic cell surface, membrane and membrane turnover

The diverse uptake routes of dendritic cells are well studied (Steinman et al., 1976; Steinman et al., 1983; Sallusto et al., 1995; Norbury, 2006), but interestingly, publications concerning specificities of the dendritic cell-membrane are scarce. The importance of the membrane composition is often underestimated as the lipid composition is in many regards a driving force of important functions like phagocytosis (Yeung and Grinstein, 2007) or the formation of the immunological synapse (IS).

DCs interact with T cells by forming the IS - a specialized contact between membranes of two different cell types (Figure 3). Beside multiple receptors that are involved in the synapse-formation, glycosphingolipid-enriched membrane microdomains play an important role in helping to form the structure of the IS (Janes et al., 1999; Ilangumaran et al., 2000; Burack et al., 2002). Such lipid rafts are also linked to various endocytic pathways (Hanzal-Bayer and Hancock, 2007). Recently, it has been shown that endocytosis of major histocompatibility complex (MHC) I and MHC II is dependent on different lipid rafts (Knorr et al., 2009). Therefore, examining the membrane composition of various cells may also lead to an advanced understanding of many AMP-functions.

Today it is well known that the surface of the dendritic cell exhibits negative charges due to for example negatively charged surface-proteins or anionic lipids containing phosphatidylserine (Henson et al., 2001; Foged et al., 2004) and attraction of positive material to the cell has been shown to potentiate its uptake into the cell. This might explain the significant uptake capacity of positively charged PLL-coated polystyrene particles compared to negative particles (Thiele et al., 2001). Further, preferred interaction of positively charged liposomes compared to the negatively charged counterparts (Foged et al., 2004) has been demonstrated. Specific interactions with positively charged peptides as suggested from in-silico-experiments have also been studied in dendritic cells (Seelig, 2004). Recently, it has been shown, that removing of surface sialic acid of immature monocyte derived DCs decreases endocytic activity (Videira et al., 2008).

It is obvious that the effect of the positively charged KLK is closely related to the surface of the target cells. Thus, it would be of importance to gain knowledge regarding the composition of the target DC membrane. Data on the lipid composition of dendritic cells are scarce. The most convincing data were published by Laulagnier and co-workers who described a molar percentage of total phospholipids, which was 43:23:12:9 Phosphatidylcholin (PC) / Phosphatidylethanolamine (PE) / Phospatidylserine-Phosphatidylinositol (PS-PI) / Sphingomyelin (SM) for dendritic cells (Laulagnier et al., 2004).

The uptake of a membrane-bound substance is linked to membrane turnover (Betz et al., 1996). This is generally regulated by the exocytosis-endocytosis cycle (Molecular Biology of the Cell; 4$^{th}$ edition; Alberts et al.; page 762). Therefore a dendritic cell with a high endocytosis rate (Sallusto et al., 1995; Steinman et al., 1999; Norbury, 2006) is supposed to have superior membrane turnover and a high uptake of membrane bound materials (Steinman et al., 1976; Steinman et al., 1983).

## 2.4.3. From antigen uptake to presentation

Immature DCs reside in peripheral tissues where they sense antigens or danger signals via various receptors (e.g. TLRs, mannose-receptor, etc.). External antigens are taken up via distinct mechanisms. Although, DCs are not involved in direct clearance of pathogens they express a large array of phagocytic receptors and effectively phagocyte pathogens (Ariel Savina, 2007). Large quantities of fluid-phase solute are taken up via macropinocytosis (Sallusto et al., 1995; Norbury, 2006). The majority of exogenous ligands bind to receptors at

the surface that are endocytosed via clathrin coated pits (Khan et al., 2007) and some via clathrin independent pathways (Steinman et al., 1999; Khan et al., 2007; Barral et al., 2008).

As mentioned above, DCs can also recognize pathogen associated molecular patterns (PAMPs), such as unmethylated DNA, single stranded RNA, Lipopolysaccarides (LPS, (Iwasaki and Medzhitov, 2004) and damage associated molecular patterns (DAMPs), such as uric acid (M. A. M. Willart, 2009) via different receptors. Some of these danger signals also have to be taken up into the cell to interact with their receptors. Unmethylated CpG-DNA has for example been demonstrated to interact with TLR9 in distinct vesicles within DCs (Latz et al., 2004). These signals and patterns stimulate immature DCs and lead to expression of various cytokines but unlike antigens, they are not presented to T- or B-cells.

Following exposure to the antigen or other stimuli, DCs undergo maturation that converts the primarily antigen sensing immature DCs to specialized antigen presenting cells and T-cell activators in the lymphoid organs. The maturation includes the presentation of an antigen via major histocompatibility complex (MHC), the migration of the dendritic cells to the lympoid organs, the reduction of endocytic activity and the change of expression patterns of various cytokines and chemokines (for review see Granucci et al., 1999).

External antigens taken up by APCs are processed by proteases into peptides while travelling the endocytic route (Bryant et al., 2002). In late endosomal vesicles these peptides are acquired by newly synthesized MHC class II molecules (Bryant and Ploegh, 2004). Immature DCs are not capable to creat class II-peptide complexes. Here MHC II is stored in MHC II-enriched compartments (MIICs). In these compartments the peptide binding groove of the MHC II molecule is occupied by a polypeptide, the CLIP fragment. Only upon stimulation of DCs for example by LPS, the CLIP fragment is replaced by an antigen (Alfonso and Karlsson, 2000) and the loaded class II-peptide complexes are transported via tubular organelles to the plasma membrane (Kleijmeer et al., 2001).

Cytoplasmic antigens like viral proteins but also external antigens that where exported into the cytosol (Savina and Amigorena, 2007) can be processed by proteasomes into eight to nine amino acid peptides. These are transported into the endoplasmic reticulum (ER) by the transporter associated with antigen processing (TAP, Wright et al., 2004), if necessary trimmed by the ER aminopeptidase associated with antigen processing (ERAAP, Serwold et al., 2002) and loaded onto MHC I molecules. The loaded MHC I molecule then travels via the Golgi apparatus to the cell membrane, exposed to the cell surface where it is accessible for $CD8^+$ T cell (Peter Cresswell, 2005).

The turnover of dendritic cells in the tissue is very slow ($t_{1/2}$ ~ 14-30 days in the skin, for review see Alvarez et al., 2008). During migration dendritic cells detach from the peripheral tissues and migrate to the local draining lymph node (LN) where they interact with homing T cells. Besides PAMPs and DAMPs, TNFα and IL-1β play a critical role as initial mobilization signals which seem also to be involved in detachment by reducing for example the E-cadherin expression of Langerhans-cells (LCs) in the skin (for review see Alvarez et al., 2008). The DCs pass the barriers of the extracellular matrix (ECM) and travel to the LN whereat chemokine (C-C motif) receptor 7 (CCR7) and its ligands, chemokine (C-C motif) ligand 19 (CCL19) and CCL21, are the primary chemokines responsible for the migration. Stimulation with TNFα increases the expression of CCL21 by lymphatic endothelial cells and making them more attractive to migrating DCs (for review see Martin-Fontecha et al., 2003).

In the lymph node antigen specific naïve T cells recognize via their T cell receptor (TCR) the antigen presented via the MHC. Depending on the MHC class the antigens are loaded at different types of T cells that are then activated. Peptides presented by the class I molecules are recognized by $CD8^+$ cytolytic (or cytotoxic) T lymphocytes (CTLs) whereas $CD4^+$ helper T cells interact with MHC II and are polarized towards Th1, Th2 responses or to Th17 cells (Infante-Duarte et al., 2000). The activation of antigen specific T cells is dependent on the formation of a prolonged but dynamic interaction named immunological synapse between the DC and the T cells (Figure 3). This specific synapse departs from the concentric bull´s eye pattern for the T cell-B cell and T cell-planar bilayer interactions (Brossard et al., 2005). Leucocyte function associated antigen 1 (LFA-1) of the T cell and intercellular adhesion molecule 1 (ICAM-1) of the dendritic cell form narrow interactions whereat the distance of the resulting cleft is still under debate (for review see Brossard et al., 2005; Dustin et al., 2006; Figure 3B). The formation of this tight apposition is essential for the activation of T cells but interestingly, it seems not to depend on the formation of one stable interaction of an antigen specific TCR with an antigen loaded MHC but the serial engagement and triggering of the TCR by peptide-MHC (for review see Lanzavecchia and Sallusto, 2001). Besides LFA-1 and ICAM-1 that form the synapse, a set of co-stimulatory molecules like CD80 and CD86 expressed by the dendritic and CD28 and CD2 expressed by the T cell cell is involved in the signalling and activation the latter.

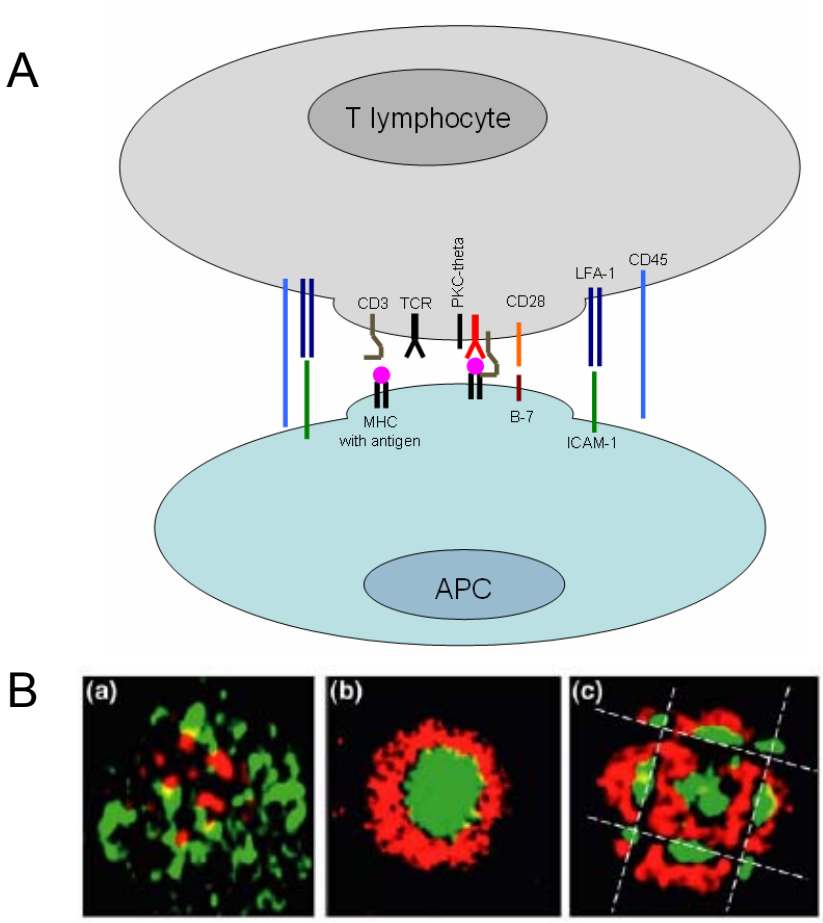


**Figure 3. The immunological synapse**

A) Mechanisms that sustain and amplify signaling at the immunological synapse.

At the synapse, membrane molecules are organized in supramolecular clusters with short molecules, such as the TCR–CD3-ζ complex and CD28 (T cell), peptide-MHC and B-7 (APC), in a central region. Large molecules, such as LFA-1, and CD45, are found in the peripheral region. TCRs (in black) are continuously internalized and recycled. Those that are engaged by peptide-MHC (red) are tethered into raft microdomains containing PKC-theta, initiate the signaling cascade and are subsequently degraded. The number of rafts is developmentally regulated in naïve and primed T cells and can be increased by costimulation. (Figure according to Lanzavecchia and Sallusto, 2001)

B) Immunological synapse patterns in T cell–DC interface and model systems.

(a) Fluorescence view of fixed T cell–DC immunological synapse (TCR is labeled green and protein kinase C-θ is labeled red). A multifocal TCR cluster pattern is visualized. The TCR clusters each contain in the order of 100 TCRs. (b) IS formed by T cells and supported planar bilayers that lack any diffusion barriers (TCR is labeled green and ICAM-1 is labeled red). (c) IS formed on by a T cell on a patterned planar bilayer in which chrome lines (dashed lines) disrupt diffusion of agonist MHCp and ICAM-1 in the bilayer (TCR is green and ICAM-1 is red). (Dustin et al., 2006)

## 2.4.4. Stimulation of the Th1, Th2 and Th17 responses

The existence of two different effector T-helper type (Th) populations, the Th1 and the Th2 cells, was demonstrated more than 20 years ago (Mosmann et al., 1986). A third independent type, Th17, was described 14 years later (Infante-Duarte et al., 2000). The development of these different populations from naïve T cells is orchestrated by the costimulatory signals and the appropriate cytokine environment (Figure 4). These diverse populations are characterized by their differential cytokine production profiles and immune regulatory functions. The development of Th1 cells is potentiated by IL-12, which is released by APCs via a positive feedback loop. Th1 cells produce IFN-γ as well as IL-2 and lymphotoxin-β. The cells mediate defense against intracellular microbes and modulate isotype switching to immunoglobulin G2a (IgG2a) of B cells. Mast cells, basophils and natural killer cells produce IL-4 that drives the development of Th2 cells. These cells produce IL-4, IL-5 and IL-13, mediate isotype switching to IgG1 and IgE and thus help clearing extracellular organisms like helminths. Further, via induction of IgE, Th2 cells play a role in allergic reactions (Kerri A. Mowen, 2004; H. Bowen, 2008; Martinez et al., 2008). IL-6 and transforming growth factor-β induce the differenciation of Th17 (Bettelli et al., 2006) which produce IL-17, IL-17F, IL-21 and IL-22. These cells indirectly induce the recruitment of neutrophils and macrophages to tissues by regulating the secretion of granulopoietic factors (G-CSF and SCF), CXCL and CCL chemokines, matrix metalloproteases, pro-inflammatory cytokines and antimicrobial peptides, depending on the target cells (for review see Dong, 2008) and play a role in various diseases (for review see Martinez et al., 2008; Figure 4).

## 2.4.5. Toll like receptors – TLR9 function and expression

Toll like receptors (TLRs) are a family of conserved pattern recognition receptors (PRRs). TLRs are critical for the innate immune response as they recognize pathogen associated molecular patterns (PAMPS). TLRs are expressed in antigen presenting cells such as macrophages (Henning et al., 2008), dendritic cells, B-cells and monocytes (Kokkinopoulos et al., 2005), lymphatic endothelial cells (Kang et al., 2009), ovary and ovary-tumor cells (Zhou et al., 2009) and more.

The expression profile of the different TLRs varies between distinct cell types (Figure 5) – as shown for the TLR9 below. Further, it has been demonstrated that TLR4-expression is lower

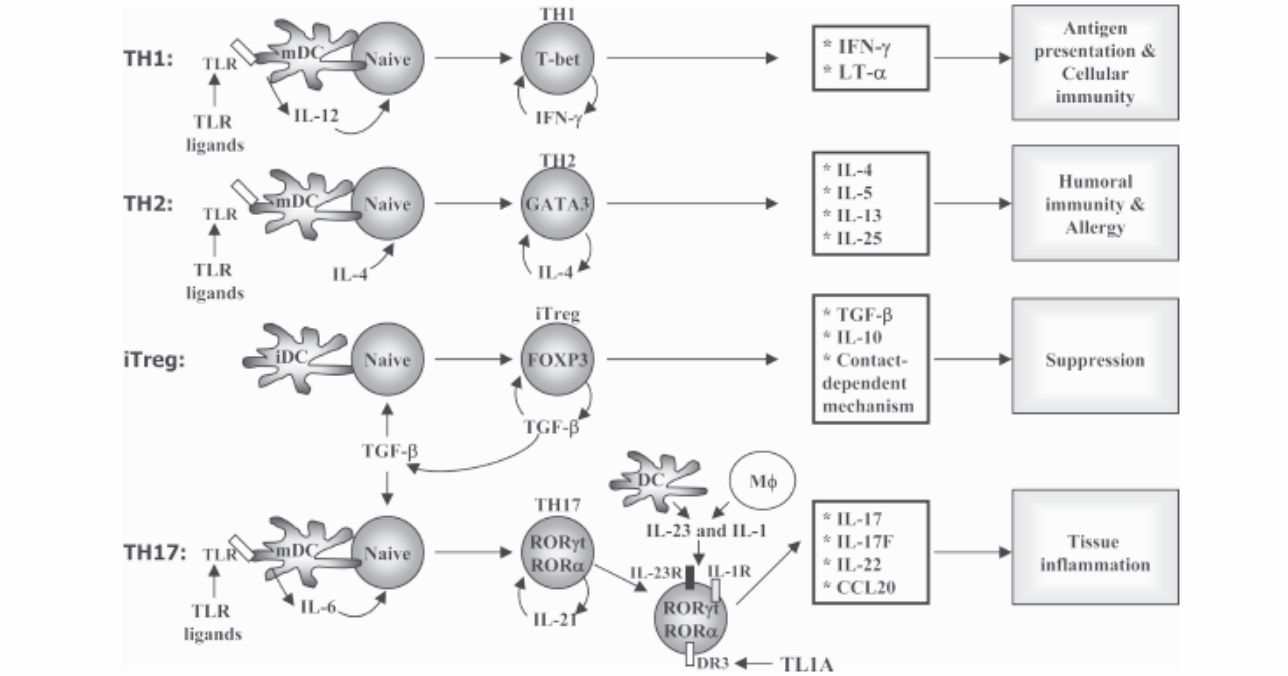


**Figure 4. Differentiation of T helper cell subsets**

Naive CD4+ T cells, upon encountering their cognate antigens presented by professional antigen-presenting cells (APC), differentiate into effector cells (TH1, TH2, TH17, iTreg) that are characterized by their cytokine production profiles and immune regulatory functions. TH1 cells produce IFN-γ and regulate antigen presentation and immunity against intracellular pathogens, whereas TH2 cells, which produce IL-4, IL-5, and IL-13, mediate humoral responses and immunity against parasites, and are important mediators of allergic diseases. TH17 cells express IL-17, IL-17F, IL-21, and IL-22 (and IL-26 in humans) and participate in inflammation and autoimmunity processes. iTregs express Foxp3 transcription factor and mediate immune suppression by secretion of TGF-β and IL-10 and by contact-dependent mechanisms. (Martinez, 2008)

in older adults but that the cytokine production as a response to LPS stimulation is comparable to young adults (David van Duin, 2007). The first human toll like receptor was described in 1991 as the orthologe of *Drosophila* toll (Gay and Keith 1991) known today as TLR4. Up to the date, 13 mammalian toll like receptors have been identified, 10 in human and 12 in mice (Beutler, 2004). Their extracellular domain contains 19-25 tandem copies of leucine rich repeat (LRR) motive (Galiana-Arnoux and Imler, 2006). The LRR domains of TLRs form a horseshoe structure, and it is thought that the concave surface of the LRR domains is involved directly in the recognition of various pathogens (for review see Akira and Takeda, 2004; Jin and Lee, 2008). TLRs have a conserved region of about 200 amino-acid that shows striking homologies to the IL-receptor and therefore named Toll/IL-1R (TIR) domain (Akira and Hemmi, 2003; Akira and Takeda, 2004). The binding of a ligand induces dimerization of the TIRs and a conformational change of these domains that is required for recruitment of downstream signalling molecules TLRs.

The ligand specificity of the different TLRs is well studied. TLR1 and TLR6 interact with TLR2 at the plasma membrane to recognize bacterial lipid and mycoplasmal lipid, respectively, while TLR2 itself binds peptidoglycan, lipoteichoic acid and lipoproteins. The main ligand for TLR4 is bacterial lipopolysaccharide and for TLR5 it is flagellin (for review see Akira and Hemmi, 2003). All mentioned receptors are present at the membrane surface of the cells and recognize DAMPs in the environment. TLR3, TLR7, TLR8 and TLR9 on the other hand reside in the lysosomal compartments or are directed to this compartments as demonstrated for TLR9 (Latz et al., 2004). TLR3 recognizes double stranded RNA (Alexopoulou et al., 2001), TLR7 and TLR8 sense single-stranded RNA (Diebold et al., 2004; Heil et al., 2004), and TLR9 was primarily demonstrated to signal upon binding bacterial DNA (Hemmi et al., 2000) and synthetic oligonucleotides containing CpG-motives (Hartmann G., 2003).

The recognition of DNA by TLR9 is not completely understood yet. It has been shown that several classes of small oligodeoxynucleotides (ODNs) bind to and stimulate TLR9 transfected HEK cells in distinct dose-dependent relationships. B-class ODNs induce NFκB activation at lower doses than C- or A-class ODNs (Jörg Vollmer, 2004). Further, the different types of ODNs have been demonstrated to induce variable immune responses in vivo (for review see Marc S. Lamphier, 2006). Why these differences occur remains elusive. Recent data suggest, that it is not exclusively the bacterial CpG-sequence which is recognized, but that the detection of the DNA sugar backbone 2′ deoxyribose plays a pivotal role in the activation of the TLR9 (Wagner, 2008). The interaction between DNA and TLR9 occurs in

specific compartments. The group of Eike Latz has shown that TLR9 first resides in the endoplasmic reticulum and signals after translocating from the ER to tubular lysosomal compartments were it senses the CpG DNA (Latz et al., 2004). The localization of TLR9 within this compartment plays a pivotal role in the prevention of self DNA recognition (Barton et al., 2006) and the cathepsin-cleavage of the receptor that seems to be critical for the subsequent signal transduction (Park et al., 2008) via MyD88.

The expression of TLR9 in the various cell types is still a matter of debate. While the current dogma states that in humans this receptor is exclusively expressed in plasmacytoid dendritic cells (Iwasaki and Medzhitov, 2004; Wagner, 2004; Krieg, 2006; Figure 5) and not in Langerhans cells (Flacher et al., 2006) various other publications show that human monocyte derived and immature DCs also transcribe and express TLR9 (Kokkinopoulos et al., 2005; Hoene et al., 2006). Murine dendritic cells differ in this regard from their human counterparts and it is possible to obtain TLR9 positive cells by in vitro stimulation (for review see Iwasaki and Medzhitov, 2004).

A

| | Freshly isolated DCs | | | In vitro differenciated DCs |
|---|---|---|---|---|
| | Monocyte | mDC | pDC | GM-CSF + IL4 |
| TLR1 | ++ | ++ | + | ++ |
| TLR2 | ++ | ++ | - | ++ |
| TLR3 | - | ++ | - | ++ |
| TLR4 | ++ | - | - | ++ |
| TLR5 | ++ | + | - | +/- |
| TLR6 | ++ | ++ | ++ | ++ |
| TLR7 | +/- | +/- | ++ | - |
| TLR8 | ++ | + | - | ++ |
| TLR9 | - | - | ++ | - |
| TLR10 | - | + | + | |

B

| | Freshly isolated DCs | | | | In vitro differenciated DCs |
|---|---|---|---|---|---|
| | CD4+ | CD8+ | DN | pDC | GM-CSF+ IL4 |
| TLR1 | ++ | ++ | ++ | ++ | |
| TLR2 | ++ | ++ | ++ | ++ | |
| TLR3 | - | ++ | ++ | - | |
| TLR4 | ++ | ++/- | ++/- | ++/- | ++ |
| TLR5 | ++ | - | ++ | + | |
| TLR6 | ++ | ++ | ++ | + | |
| TLR7 | ++ | - | ++ | ++ | |
| TLR8 | ++ | ++ | ++ | ++ | |
| TLR9 | ++ | ++ | ++ | ++ | ++ |

**Figure 5. Expression of Toll like receptors.**

A) TLR expression of different human DC subsets and monocytes. B) TLR expression of different murine DC subsets. +, ++ and – indicate relative mRNA expression levels of each TLR by the DC subsets. When both + and – are indicated, ambiguous expression patterns are published. (Iwasaki and Medzhitov, 2004)

# 2.5. Endocytosis – coated and uncoated

## 2.5.1. Introduction

Cellular uptake mechanisms are essential for every cell. While the uptake of ions can be regulated by membrane transporters, in eukaryotic cells the uptake of receptor ligands, lipids, large particles or soluble molecules needs the formation of membrane-based pits and vesicles. The subsequent engulfment mechanism is called endocytosis. Endocytic systems are important for cells to get information about their immediate environment. Here, the different molecules and membrane proteins can be taken up by distinct and specific pathways.

These pathways include phagocytosis, caveolae- and RhoA-mediated uptake, macropinocytosis and clathrin- and caveolin independent pathways (Figure 6). Best-studied is the clathrin mediated pathway, but clathrin-indipendent (CI) pathways are also in the focus of intensive research. An additional distinction between the uptake routes can be made by the involvement or absence of dynamin which mediates the fission mechanism.

The mechanism of cargo selection for the different pathways is still a matter of debate. In clathrin-dependent endocytosis various adaptor molecules exist that recruit cargo to coated pits. One favours the involvement of micro-domains, another ubiquitination (Sigismund et al., 2005) or lipid-based mechanisms (Mayor and Rao, 2004; Satyajit Mayor, 2004). If and how these different models interact stays elusive, but it becomes more and more obvious that all endocytic pathways except phagocytosis converge into transferrin receptor (TfR) positive early endosomes (EEs) (for review see Mayor and Pagano, 2007; Figure 6).

After the vesicle has formed and pinched off the plasma membrane in a dynamin-dependent or independent way, the fate of the intraluminal cargo is still not predetermined as recycling back to the plasma membrane can occur at various stages of the endocytic pathway (for review see Johannes and Goud, 1998).

At the level of early endosomes, housekeeping receptors are uncoupled from their ligands at the pH ~ 6.2 milieu. The subsequent distribution is depending on the presence of different GTPases of the Rab-family. Domains containing Rab4 are thought to bud off and move to the plasma membrane. The Rab7 domains contribute to the biogenesis of late endosomes and transport of cargo to the lysosome (for review see Spang, 2009).

Further, as counterbalance of membrane and protein transport to the plasma membrane, retrograde transport exists. Using partly endocytic pathways, cargo is transported back to the

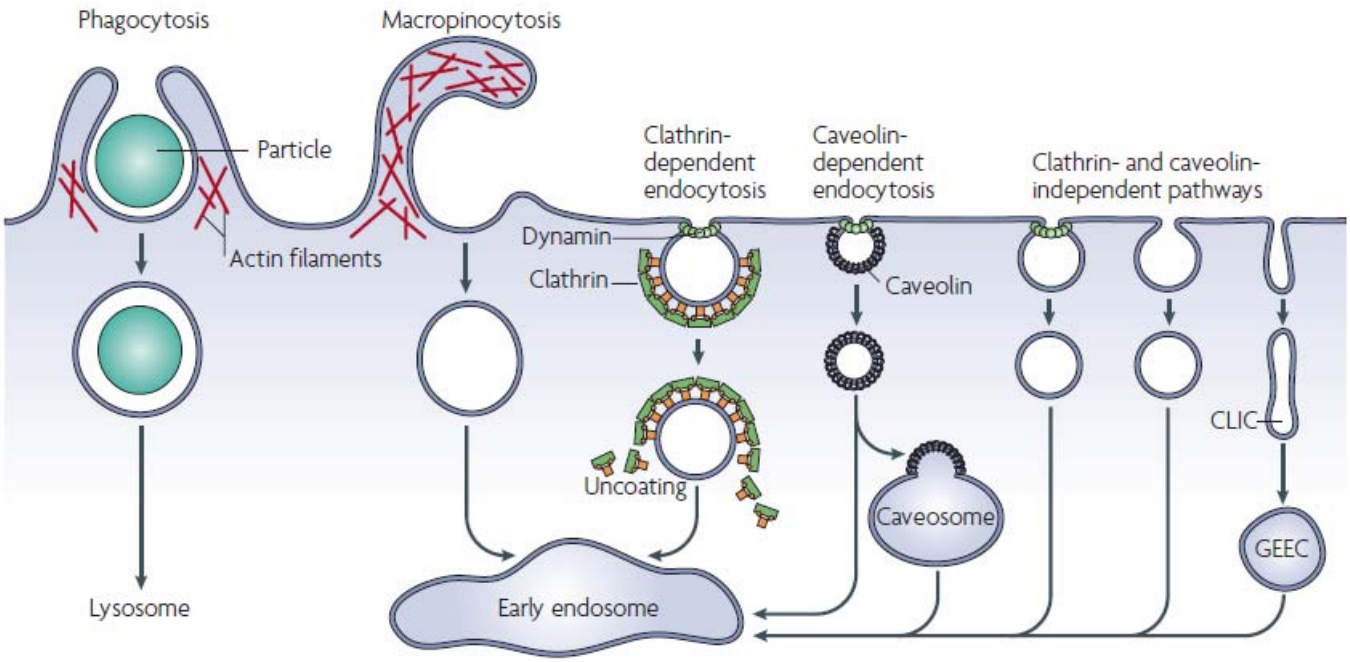


**Figure 6. Cellular internalization pathways**

Large particles are internalized by phagocytosis. The uptake of fluid occurs by macropinocytosis. Both processes are dependent on actin-mediated remodelling of the plasma membrane. Additional major internalization pathways include the clathrin- and caveolin-dependent endocytotic processes. The vesicles formed by phagocytosis and macropinocytosis are considerably larger than the vesicles of the other pathways.

Numerous cargoes can be internalized via clathrin and dynamin indipendent pathways. Here, most internalized cargoes are delivered to the early endosome via vesicular (clathrin- or caveolin-coated vesicles) or tubular intermediates (known as clathrin- and dynamin independent carriers (CLICs)) that are derived from the plasma membrane. (Mayor and Pagano, 2007)

Golgi apparatus and to the endoplasmic reticulum. From the early endosome to the trans Golgi network (TGN) at least two independent retrograde routes have been observed (for review see Pavelka et al., 2008). One leads to the TGN via late endosomes (Barbero et al., 2002) while the other one is a direct route from early and/or recycling endosomes to the TGN, thus bypassing late endosomes (Mallard et al., 1998).

The presence of various proteins drives the selection for the retrograde transport of different cargoes within the early endosome. Transport of Shiga toxin from the EE to the TGN is dependent on epsinR (Mallard et al., 1998). Retrograde transport of the yeast *S. cerevisiae* carboxypeptidase Y receptors involves the vacuolar protein sorting (VPS)-subcomplex (Seaman et al., 1998). SNX1 (sorting nexin1), a homologue of the VPS5 protein has been found in mammals (Horazdovsky et al., 1997). In both pathways the involved proteins are supposed to polymerize on the endosome, deform the membrane into a tubular structure and allow a transfer of material to the TGN (Spang, 2009).

## 2.5.2. Dynamin dependent pathways

The large molecular weight GTPase, dynamin, has been linked to the late stages of endosomal vesicle-budding. The first hint for the function of dynamin came from the study using a temperature sensitive mutant of the gene shibire in *Drosophila melanogaster* (Kosaka and Ikeda, 1983). It was observed, that the formation of coated vesicles from coated pits was inhibited at high temperature. Morphological analysis revealed an accumulation of membrane invaginations and coated pits at the neuromuscular junction suggestive of a defect in the scission of coated pits to form coated vesicles (Kosaka and Ikeda, 1983). Later, dynamin has been identified as the mammalian homologue of shibire (van der Bliek and Meyerowrtz, 1991). Dynamine participates in both the late stages of invagination and scission. It is recruited to the neck of a coated vesicle where GTP binding and hydrolysis by dynamine is required to form a deeple invaginated coated pit. During invagination and scission, dynamine might interact with binding partners like endophilin or amphiphysin (Hill et al., 2001).

### 2.5.2.1. Clathrin mediated endocytosis

Clathrin-mediated endocytosis is the major pathway for the uptake of nutrients and signalling molecules in higher eurkaryotic cells (for review see Ungewickell and Hinrichsen, 2007).

Clathrin-coated pits (CCPs) have a diameter from 10 to more than 500 nm and were first characterized in oocytes of the mosquito *Aedes aegypty* by electron microscopy (Roth and

Porter, 1964). The formation of such coated pits starts with internalization signals located in the cytoplasmic tails of transmembrane proteins such as ubiquitin (Traub and Lukacs, 2007). These signals are recognized by the tetrameric adaptor protein AP-2 or monomeric adaptors like ARH, Dab2 and Eps15 (Rapoport et al., 1998; Matthew J. Hawryluk, 2006; Chaudhuri et al., 2007; Doray et al., 2007). All of these adaptor molecules except Eps15 can bind clathrin and contain phosphoinositide-binding modules that target them to the plasma membrane. Eps15 is important to recruit several proteins of the clathrin mediated pathway.

Clathrin is recruited to these adaptor proteins and forms polyhedrical structures around the pits (Heuser, 1980). The invagination of the membrane was demonstrated to be clathrin-dependent (Hinrichsen et al., 2006) but the presence of clathrin is not sufficient for membrane curvature to take place (Ralph Nossal, 2001). The nascent CCP is pulled back by myosin motor proteins that move alongside actin filaments (Girao et al., 2008; Idrissi et al., 2008) and scission involving dynamin releases the pit from the plasma membrane (Kosaka and Ikeda, 1983; Hill et al., 2001). In addition it was shown, that invagination and scission are a highly dynamic and temporally coordinated process (Merrifield et al., 2005).

### 2.5.2.2. Caveolin dependent endocytosis

Caveolae are 50-80 nm flask shaped, non-coated plasma membrane invaginations present in many cell types, but mainly characteristic to endothelial cells (for review see Mineo and Anderson, 2001; Parton, 2003; Parton and Simons, 2007). These structures were first described in the early 60´s by electron microscopical analysis by George E. Palade and Eichi Yamada (Palade, 1953; Yamada, 1955). The caveolar membrane has shown to be enriched in cholesterol (Rothberg et al., 1990) Caveolae-mediated endocytosis is dynamin-dependent and associated with the turnover of lipid-rafts (for review see Simons and Ikonen, 1997) and glycosyl phosphatidylinositol-anchored proteins (GPI-APs; for review see Mayor and Pagano, 2007).

Various cargoes like cholera toxin B (Torgersen et al., 2001) are also known to be taken up not only by this pathway but also via a dynamine independent route. Further, cell type specific differences exist, as for example albumin is internalized in some cell types via caveolae (Schnitzer and Oh, 1994), whereas others use RhoA-dependent pathway (Cheng et al., 2006).

The expression of caveolin 1 is sufficient to generate caveolae in cells that lack these structures initially (Lipardi et al., 1998) and caveolin knock out mice do not have obvious caveolae (Drab et al., 2001; Razani et al., 2002). Therefore, it became a commonplace to equate caveolar functions with that of caveolin (for review see Nichols, 2003). Interestingly, a

subpopulation of caveolin-1-positive caveolae was identified which is not actively involved in budding and trafficking but static at the plasmamembrane. It is still a matter of debate, how the switch between the dynamic and the static caveolae is regulated (for review see Nichols, 2003).

Beside the already described early and the recycling endosome the existence of a so called caveosome is claimed. This would function as a transport intermediate between the caveolae and the endosomes. It has initially been studied during the vesicular transport of the simian virus 40 to the ER (Pelkmans et al., 2001) and has later been regarded important for the entry of human papillomavirus type 31 (Smith et al., 2008). Whether recycling back to the plasma membrane is possible at the level of the caveosome has to be demonstrated (for review see Spang, 2009).

#### 2.5.2.3. RhoA-dependent pathway

As previously described, Eps15 is an important adaptor molecule for the formation of clathrin-coated pits. A dominant negative mutation of the protein-recognition domain of Eps15 leads to a selective and efficient blockage of both constitutive and ligand-induced clathrin dependent uptake. Using this system, IL2 has been demonstrated to be taken up via a dynamin dependent, Rho-GTPase regulated pathway that is distinct from the caveolae-mediated uptake route (Lamaze et al., 2001). Although little is yet published, recent data suggest that RhoA-dependent uptake is involved in the trafficking of a voltage-sensitive potassium channel (Stirling et al., 2009) and has been implicated in the Oligophrenin1 mouse model of mental retardation (Khelfaoui et al., 2009).

### 2.5.3. Dynamine independent pathways

Expressing a temperature sensitive dynamin-mutant in HeLa-cells, Damke et al. demonstrated that the receptor mediated uptake of transferrin is inhibited, while the fluid-phase uptake recovers within 30 min to the wild-type level (Damke et al., 1995). They suggested an additional pathway that can compensate for the loss of clathrin- and caveolin-mediated endocytosis (Damke et al., 1995). The small GTPases CDC42 of the Rho family (Guha et al., 2003) or ARF6 from the Arf family seem to be key proteins in the formation of these vesicles, whereas the exact role of the latter is not yet clear (for review see Mayor and Pagano, 2007).

Inhibition of CDC42 was demonstrated to reduce the fluid-phase uptake of CHO cells and redistributing GPI-APs to the clathrin-mediated pathway (Sabharanjak et al., 2002). These

shifts concerning uptake of cargoe by alternative routes is well described. As mentioned, beside internalization via the caveolin-independent route, Cholera toxin B and GPI-anchored proteins (GPI-APs) have also been shown to be taken up into the cell via caveolin-dependent pathways.

Thus it seems obvious, that a blocked uptake route can be replaced by the activity of another.

The current theory suggests the dynamine-independent pathway as the main route for the non-clathrin, non caveolar uptake of cholera toxin B (Torgersen et al., 2001), the plant protein ricin (Simpson et al., 1998, the *Helicobacter pylori* vacuolating toxin VacA (Gauthier et al., 2005) and GPI-APs (Sabharanjak et al., 2002). There cargos can be detected in clatrhin- and dynamine-independent carriers (CLICs) (Kirkham et al., 2005) GPI-APs are directed into GPI-AP enriched early endosomal compartments (GEECs) which may form from CLICs (Sabharanjak et al., 2002).

The specific uptake pathway for GPI-APs was first suggested after using GPI- and transmembrane-anchored isoforms of the same protein (Keller et al., 1992). Today, GPI-APs represent the best studied cargo of the dynamin-independent pathway. Their association with detergent-resistant membranes (DRM) marks them as valuable markers for lipid-raft turnover (Sharma et al., 2002). It is important to note, that the location in DRMs does not implicate a specific uptake route, as for example the already mentioned IL2-receptor (Lamaze et al., 2001) or anthrax toxin (Abrami et al., 2003), which are associated to DRMs but endocytosed via a RhoA- and clathrin-dependent pathways, respectively.

# 3. Materials and Methods

## 3.1. Materials

### 3.1.1. IC31 components

| | |
|---|---|
| KLKLLLLLKLK (KLK) | (10 mg/ml in water, Intercell[AG]) |
| KLKLLLLLKLK-FITC (KLK-FITC) | (10 mg/ml in water, Intercell[AG]) |
| KLKLLPLLKLK (KPK) | (10 mg/ml in water, Intercell[AG]) |
| ODN1a | (6705.1 µg/ml in water, Transgenomic, Inc.) |
| ODN1a-Cy5 | (1000 nmole/ml in water, Purimex) |

### 3.1.2. Dyes and Antibodies

| | |
|---|---|
| FM1-43, FM® Lipophilic Styryl Dyes | (Invitrogen) |
| ER-Tracker™ Green | (Invitrogen) |
| DAPI | (Roche) |
| Anti-human/mouse TLR9-FITC | (Eubio, Alexis) |
| Anti-human CD71 (TfR)-FITC | (BD Pharmingen) |
| Anti-human CD107a (Lamp-1)-PE | (BD Pharmingen) |

### 3.1.3. Media

| | |
|---|---|
| RPMI 1640 | (PAA-Laboratories) |
| DMEM-GlutaMAX | (PAA-Laboratories) |
| L-Glutamine | (PAA-Laboratories) |
| Sodium-pyruvate | (PAA-Laboratories) |
| Non-essential amino acids | (PAA-Laboratories) |
| Gentamycin | (PAA-Laboratories) |
| β-mercaptoethanol | (PAA-Laboratories) |
| Fetal bovine serum (FBS) | (PAA-Laboratories) |

| | |
|---|---|
| Penicillin/Streptomycin | (PAA-Laboratories) |
| IL-4 | (Peprotech, Eubio; Cat.Nr.: 200-04) |
| GM-CSF (human) | (Cell-Genix; Cat.Nr.: 1412-050) |
| GM-CSF (mouse) | (X6310 cell supernatants; Reutterer et al., 2008) |
| Yeast extract | (Formedium$^{TM}$) |
| Peptone | (BD Pharmingen) |
| Dextrose | (AppliChem) |

**YPD medium**

1% yeast extract, 2% peptone, 2% dextrose

**DC-medium (human)**

RPMI 1640,10% FBS, 1 % L-Glutamine, 1 % Sodium-Pyruvate, 0.1% β-mercaptoethanol, 1x Pen/Strep, 500 U/ml IL-4 and 0.1 μg/ml GM-CSF

**DC-medium (mouse)**

DMEM-GlutaMAX, 10% FBS, 1x Pen/Strep, 5% X6310 cell supernatant (Reutterer et al., 2008).

**ECV-medium**

RPMI 1640, 10% FBS, 1x Pen/Strep

**HEK, C2C12, HELA, CaCO cell medium**

DMEM-GlutaMAX, 10% FBS, 1x Pen/Strep

# 3.2. Methods

## 3.2.1. Studying membrane interactions of KLK

### 3.2.1.1. Isolation of mitochondria

DBY747 wild type cells (ATCC cat. No. 204659) and DBY747 *mkh1Δ* mutant cells (MKH1 gene disrupted) (Froschauer et al., 2005) were grown overnight in YPD medium and harvested at stationary phase. Mitochondria were isolated as described elsewhere (Zinser and Daum, 1995) and resuspended in breaking buffer (250 mM Sucrose, 10 mM Tris-HCl pH 7,4). Mitochondria were either processed immediately or stored at –80 $^0$C until use.

### 3.2.1.2. Preparation of yeast submitochondrial particles (SMPs)

5 mg (about 0,5 ml in a typical yield) mitochondria were diluted to 1 ml in breaking buffer and further diluted 5-fold with low osmolarity buffer (10 mM Tris pH 7.4, 0.1 M sorbitol) and incubated on ice for 20 min in thick wall polycarbonate tubes (Beckman). The resulting mitoplasts were essentially without outer mitochondrial membrane as shown earlier (Nowikovsky et al., 2004). Particles were collected (40000 *g´*, 10 min at 4°C, Beckmann TL-100 Ultracentrifuge), resuspended in 1 ml breaking buffer and tip-sonicated for 3 min at 80 % intensity on ice (Bandelin Sonoplus GM70 sonicator equipped with a UW 70 head, Berlin, Germany). Suspensions were pelleted (10000 *g´*, 10 min at 4°C), supernatants transferred into new tubes and SMPs collected by centrifugation (100000 *g´*, 1h at 4°C). Pellets were resuspended in 250 mM Sucrose buffer and stored at –80 $^0$C until use.

### 3.2.1.3. Loading SMPs with ion-sensitive fluorescent dyes

SMP pellets (1 mg total protein) were resuspended in 1 ml sucrose buffer and 75 μM tetraammonium salt of the $K^+$-sensitive fluorescent dye, benzofuran isopthalate, PBFI (Molecular Probes, The Netherlands), was added. Reactions were tip-sonicated on ice as described above to entrap the ion-sensitive fluorescent dyes within SMPs. Particles were collected by ultracentrifugation (100000 *g´*, 10 min), washed in buffer and resuspended in the same buffer at 0.05 mg protein per ml.

### 3.2.1.4. Fluorescence measurements

Excitation wavelengths were set at 340 and 380 nm for PBFI, while the emission wavelength was set to 500 nm. Fluorescence emitted by both free and ion-bound dyes was recorded with a Perkin-Elmer LS-55 spectrofluorometer with Fast Filter Accessory mode. Measurements were performed in quartz cuvettes with a total volume of 2 ml while slow stirring at 25 $^0$C. KLK or KPK and KCl, were added directly to the cuvettes at the indicated time points.

### 3.2.1.5. Generation and loading with PBFI of large unilamellar asolectin vesicles

100 mg of soybean asolectin phospholipids (Sigma-Aldrich, USA) were emulgeated in 1ml of dd$H_2O$ by sonication. The suspension was diluted 9-fold with HEPES-NaOH, 100 mM NaCl and 1 % CHAPS, pH 7.4 (Sigma-Aldrich, USA). Vesicles were formed by removing CHAPS by extensive dialysis against the above buffer without CHAPS for 48 h at 4 $^0$C and collected by centrifugation at 100 000 x g for 30 min at 4 $^0$C. Vesicles were washed once in CHAPS-free buffer and vesicle pellet resuspended again in 200 µl of CHAPS-free buffer. Asolectin liposomes were loaded with PBFI as described for SMPs.

### 3.2.1.6. Blood samples and osmotic resistance tests

Heparinized human blood samples (100 IU/ml) were drawn from young healthy volunteers. Samples were centrifuged at 4000 *g´* at room temperature for 10 min, the plasma and buffy coat were carefully removed, and the erythrocyte pellet re-suspended in physiological saline at 50% hematocrit. Samples (20 µl) of erythrocyte suspension were added to 8 ml of various osmolarity NaCl solution (50-300 mosmol in 25 mosmol increments). Samples were incubated at room temperature for 30 min, and centrifuged at 5000 *g´* for 5 min. The 540 nm absorption of the supernatant was measured with a Perkin-Elmer Lambda 2 (USA) spectrophotometer. Complete hemolysis of the samples was induced by the addition of 0.1% Triton X-100 detergent, and the 540 nm absorption measured again.

### 3.2.1.7. Erythrocyte ghost preparation and fluorescence emission anisotropy measurements

Erythrocyte ghosts were prepared as described elsewhere (Dodge et al., 1962). Isolated ghosts were labeled with DPH or TMA-DPH as previously described (Miseta et al., 1995). Measurements were carried out with a Hitachi F-4500 fluorescence spectrophotometer

(Japan), equipped with polarization accessories, at 25 °C using wavelengths of 360 nm and 425 nm for excitation and detection, respectively. Fluorescence anisotropy was calculated according to the equation $r=(I_{vv}-GI_{vh})/(I_{vv}+2GI_{vh})$, where $I_{vv}$ and $I_{vh}$ are the fluorescence intensities measured with a vertical polarizer, and a vertically or horizontally mounted analyzer, respectively ($G=I_{hv}/I_{hh}$) (Donner and Stoltz, 1985). For each sample the fluorescence was corrected for the scattering effect of unlabeled ghosts.

### 3.2.1.8. Preparation of small unilamellar vesicles and circular dichroism measurements

Small unilamellar vesicles (SUVs) were prepared using 1-palmitoyl-2-oleoyl-sn-glycero-3-phosphocholine (POPC) and 1-palmitoyl-2-oleoyl-sn-glycero-3-phosphoglycerol (POPG) lipid components (Sigma-Aldrich, USA). POPC and/or POPG at a molar ratio of 3:1 were diluted in chloroform and vacuum-dried. SUVs of 100 nm diameter were generated by extruding the water-reconstituted lipids through the membrane of the device Avestin-Extruder (LiposoFast). Circular dichroism measurements were performed on aqueous or NaP-buffered (20mM) of the peptides KLK and KPK in the absence or presence of POPC/POPG-SUVs using 10 mm path length quartz cuvette in a PiStar-180 CD spectrometer (Applied Photophysics). 20-80% 2,2,2-trifluoroethanol (TFE, Sigma-Aldrich, USA) were administered to KLK or KPK in water or phosphate buffer where indicated.

### 3.2.1.9. Electron microscopy

#### 3.2.1.9.1. SMPs

Submitochondrial particles (2 x 500 µl aliquots/sample) were placed on ice and treated with 10 nmole/ml of KPK or KLK for 30 min. To the control sample, equal volume of sucrose buffer was added. SMPs were pelleted by centrifugation (40000 *g´*, 10 min at 4°C). Pellets of SMPs attached to the bottom of Eppendorf tubes were washed in Sorensen`s buffer (Hayat, 1989). Subsequently, they were fixed with 3% glutaraldehyde in 0.15 M Sorensen`s buffer, pH 7.4, for 30 min. The pellets were detached by using a small spatula and glutaraldehyde fixation continued for further 30 min. After washing, the pellets were postfixed with 1% $OsO_4$ in Sorensen´s for 1 h and dehydrated with increasing concentrations of ethanol. Finally, samples were embedded in epoxy resin Agar 100 (Agar Scientific Ltd, UK). Thin section of 60-80 nm were cut with LEICA Ultracut S ultramicrotome, mounted on copper grids, contrasted by uranyl acetate and lead citrate, and examined at 80 kV in a JEOL JEM-1210

electron microscope (Jeol Ltd., Japan). Images were acquired using a Morada digital camera for the wide-angle port of the TEM and analySIS FIVE software (Soft Image System).

#### 3.2.1.9.2. Cell culture

Human monocyte derived dendritic cells were treated with 100 nmole/ml KLK or KPK diluted in fresh medium. To the control sample an equal volume of fresh medium was administered. After 15 minutes the cells were pelleted by centrifugation (300 g´, 10 min at room temperature) and fixed with 3% glutaraldehyde n 0.15 M Sorensen´s buffer. Samples were subjected to postfixation and sectioning as described for SMPs.

ECV endothelial cells were grown on ACLA-slides to a cell density of 80%. 100nmole/ml KLK in fresh medium was administered. To the control sample an equal volume of medium was added. After 5 minutes cells were fixed in 0.5 % glutaraldehyde using an EMS microwave (15 seconds and 50 % power). Postfixation was performed in 3 % glutaraldehyde for 30 minutes. Samples were processed as described elsewhere (Reipert et al., 2008).

## 3.2.2. KLK distribution in SMPs

### 3.2.2.1. MALDI-TOF mass spectrometry analysis of vesicular sub-fractions

SMPs were ultracentrifuged and supernatants were saved (supernatant 1). Pellets were washed extensively, resuspended in reaction buffer and tip-sonicated to disrupt vesicles. Sonicated SMPs were again ultracentrifuged and supernatants (supernatant 2) and pellets (pellet) were separated. Samples were acidified by the addition of 1% trifluoroacetic acid (TFA)/water (20% v/v final) and extracted with diethylether to remove lipids. The samples were then purified via Ziptips C18 (Millipore, USA) for matrix assisted laser desorption/ionisation – time of flight (MALDI TOF) mass spectrometry analysis. Ziptips were wetted by aspirating and dispensing (cycling) pure acetonitrile and then equilibrated by cycling 0,1% TFA/water several times. Peptides were bound to Ziptips by cycling the sample solution through the tips several times. The tips were then washed by cycling 0,1% TFA/water through the tip. The purified peptides were eluted directly onto the target plate by aspirating approximately 2 µl of matrix solution [10 mg/ml alpha-cyanohydroxycinnamic acid (CHCA) in TFA/water/acetonitrile (0,1:50:50; v/v/v)] into the tip and cycling the solution a few times onto the target plate. Samples were analyzed on a Voyager DE-STR (Applied Biosystems, Darmstadt, Germany) in the positive ion reflection mode. External calibration was performed with the known masses of a synthetic peptide mixture.

### 3.2.2.2. Distribution of KLK-FITC within SMPs

10 nmole/ml FITC-labelled KLK was administered to SMPs. These were ultracentrifuged and supernatants were saved (supernatant 1). Pellets were washed extensively, resuspended in reaction buffer and tip-sonicated to disrupt vesicles. Sonicated SMPs were again ultracentrifuged and supernatants (supernatant 2) and pellets (pellet) were separated. Samples were analysed using a Zeiss Axioplan 2 Fluorescent microscope**.**

## 3.2.3. Aggregate formation

### 3.2.3.1. Gel retardation and particle size

10 µg ODN1a was mixed with 40 µg KLK or KPK and loaded on a 2% agarose gel. Binding of KLK to the nucleotide was analyzed via gel-retardation of ODN1a.

For the measurement of particle size distribution 0.4 nmole/ml ODN1a were mixed with 10 nmole/ml KLK/KPK in water. 1ml of the mixture was analyzed using a Malvern Mastersizer 2000.

## 3.2.4. Cell culture experiments

### 3.2.4.1. Preparation of human immature dendritic cells

Whole human heparinized blood was obtained from the Red Cross and 500 ml of blood was diluted 1:1 in PBS. Diluted blood was placed on LSM 1077 lymphocyte separation medium (PAA, Austria) gradient and centrifuged for 20 minutes at 350 g. Monocytes were harvested and $CD14^+$ cells were selected by MACS purification (MiltenyiBiotech) and incubated in DC-medium (human) at 37 °C in 5% $CO_2$ for 7 days. At day 6 of culture, CD83 (below 10%), CD1a (50-70%) and MHCII (70-90%) were assured by FACS analysis. At day 7 non-adherent cells were collected and used in subsequent experiments.

### 3.2.4.2. Preparation of mouse bone marrow derived dendritic cells and macrophages

C57Bl/6 were housed under pathogen free condition according to FELASA guidelines (Nicklas et al., 2002) Bone marrow-derived DCs and macrophages were isolated and maintained according to (Reutterer et al., 2008).

### 3.2.4.3. Cultivation of HEK, C2C12, HELA and CaCo-cells

Cells were cultivated in appropriate medium. At 80% density cells were splitted using 1x Trypsin for 5 minutes at 37°C. The cells were diluted to reach a density of 80% after incubation for 24 hours at 37°C in 5% $CO_2$ and placed in an 8 well Lab-Tek II Chamber Slide (LAB-TEK®, Nunc).

### 3.2.4.4. ODN1a-Cy5 uptake experiments

Cells were placed in an 8 well Lab-Tek II Chamber Slide (LAB-TEK®, Nunc) at a density of 1.5-3 x $10^5$ cells per well and incubated over night at 37°C in 5% $CO_2$ in appropriate medium. Fresh medium was added to the wells with ODN1a-Cy5 and KLK/KPK added to a final concentration of 0.4 nmole/ml (low dose) or 1.2 nmole/ml (high dose) and 10 nmole/ml, respectively. Where indicated 6 nM FM1-43 or 1 μM ER-tracker was added to the mixture. Cells were incubated for various lengths of time, washed once with PBS and then fixed for 30 minutes at 37°C with 4% PFA (Sigma-Aldrich). Cells were washed twice with 0.5% Tween in PBS for 1 minute, rinsed once with PBS and then incubated with 2% BSA (Sigma-Aldrich) or 2% goat serum (Vector Laboratories). In case of subsequent DAPI or antibody staining cells were exposed to 2μg DAPI diluted in 200μl PBS or anti-human CD71-FITC and anti-human CD107a-FITC diluted 1:33 in 2% BSA, or to anti-human/mouse TLR9-FITC dilutet 1:100 in 2% goat serum for 1 hour at 37°C in a humid chamber. Cells were then washed two times with 2% BSA or 2% goat serum and once with PBS and examined using Zeiss Axioplan 2 LSM510 Meta laser scanning fluorescence microscope. Images were subsequently analyzed using the Zeiss LSM ImageBrowser software.

### 3.2.4.5. Localization of KLK experiments

Cells were placed in an 8 well Lab-Tek II Chamber Slide (LAB-TEK®, Nunc) at a density of 1.5-3 x $10^5$ cells per well and incubated over night at 37°C in 5% $CO_2$ in appropriate medium. 10 nmole/ml FITC-labelled KLK in fresh medium was added. Cells were incubated for 1 hour, washed once with PBS and then fixed with PFA as described before.

### 3.2.4.6. Live cell laser confocal imaging

At day 7 dendritic cells were collected and transferred to new dishes containing sterile glass cover-slides. Cells were incubated at 37°C in 5% $CO_2$ over night. ODN1a-Cy5, KLK/KPK and dyes were mixed as described above. The medium was removed carefully from the cover-slide and a few micro-liters of the mixture were placed on the slide. The glass slide was put on

an object slide and sealed before the sample was observed using a Zeiss Axioplan 2 laser scanning fluorescence microscope equipped with a LSM510 Meta camera. Images were processed using the Laser Scanning Microscope Version 3.2 SP program.

### 3.2.4.7. FRET measurements

FRET experiments were performed using FRET-pair forming fluorochrome-labeled components; KLK-TAMRA and ODN1a-Cy5. FRET efficiency was calculated with the acceptor-bleaching technique (acceptor: Cy5; Donor: Tamra) according to the formula $FRET_{eff}$= ($Intensity_{post}$-$Intensity_{pre}$)/$Intensity_{post}$ with photo-bleaching corrections. For fluorescent imaging in FRET experiments, a modified epi-fluorescence microscope was used (Axiovert 200, Zeiss, Germany), which was equipped with a temperature control system (POCmini, Zeiss, Germany). Samples were illuminated through a 100x NA=1.45 Plan-Apochromat objective (Zeiss) using the 514 nm line (excitation of TAMRA) of an Ar+-ion laser (Innova, Coherent, USA) and 647 nm (excitation of Cy5) of a Kr+-ion laser at excitation intensities of up to 10kW/$cm^2$ by using epi-configuration. An acousto-optic modulator (Isomet, 1205C) was used to achieve exact timing of the laser illumination. After filtering (custom-made dichroic and emission filters, Chroma, USA), images were recorded on a back-illuminated liquid nitrogen cooled CCD camera (Micro Max 1300-PB, Roper Scientific). Each CCD pixel corresponds to 200 nm x 200 nm in the sample plane. All live cell experiments were performed in Hank`s balanced salt solution (HBSS; PAA) at 37 °C.

# 4. Results

## 4.1. Molecular properties of KLK

The cationic antimicrobial peptide KLK (KLKLLLLLKLK) was originally found in a systematic screen of synthetic AMPs (Alvarez-Bravo et al., 1994) and tested later for its antimicrobial activity (Nakajima et al., 1997). KLK itself induces a predominantly $T_H2$ immune responses against co-injected antigens *in vivo* by stimulating the expression of high levels of antigen-specific antibodies against the model antigen ovalbumin (OVA) or a commercial influenza vaccine (Fritz et al., 2004). KLK was efficient in enhancing association of antigen to antigen-presenting cells (APCs, including dendritic cells). Intercell™ combined KLK with the TLR9 agonist ODN1a. This two-component adjuvant was termed IC31®. Co-injection of IC31® with appropriate immunogenic peptides or proteins induces a potent antigen-specific, predominantly type 1 T cell response and elicits antigen-specific cytotoxic T cell activity (Schellack et al., 2006). The protein-based vaccines are further capable of inducing antigen-specific mixed type 1 and type 2 humoral responses. It has also been demonstrated that IC31® efficiently stimulated the maturation and activation of dendritic cells (DCs) that in turn enabled the induction and proliferation of naïve T cells (Schellack et al., 2006).

Interestingly, a substitution of the middle leucine to proline results in a peptide with complete loss of its immuno-stimulatory properties. This peptide, KPK (KLKLLPLLKLK) exhibits the same amount of charged residues as KLK but behaves differently. While KLK forms a stable depot at the injection site, KPK does not (Intercell personal communication). Therefore, the first attempt to clarify the mode of action of IC31® was to examine the properties of KLK. Thus far, no studies had been published that aimed to resolve the structure of KLK and KPK. Such information would provide deeper understanding of biological functions of these peptides.

## 4.1.1. Conformational properties of KLK

Our first experiments were performed using circular dichroism (CD) measurements. CD analysis allows a fast determination of the secondary structure of a given protein or peptide. The conformational properties of the protein or peptide can be monitored under various buffer conditions, in different pH, in presence of various ions but also in membrane mimicking environments like detergents or small unilammelar vesicles (SUVs).

### 4.1.1.1. KLK undergoes various conformational transitions in presence of SUVs

In water both KLK and KPK showed a typical random coil conformation (Figure 7A). To mimic a membranous environment, we added small unilammelar vesicles (SUVs) to the peptides. The SUVs contained the uncharged 1-palmitoyl-2-oleoyl-sn-glycero-3-phosphocholine (POPC), the positively charged 1-palmitoyl-2-oleoyl-sn-glycero-3-phosphoglycerol (POPG) or a 3:1 molar mixture of POPC and POPG. Addition of this mixture or of the uncharged POPC alone led to a prompt random coil to beta sheet conformational transition of KLK (Figure 7B).

Because of the size of the peptide we consider this β-sheet structure as an intermolecular aggregation. The same amount of lipids administered to the control peptide KPK did not lead to conformational transitions even at higher lipid to peptide ratios.

Positively charged proteins are attracted by negatively charged membranes, the proteins get in contact with the membrane and a conformational transition into an alpha helix can be observed (Seelig, 2004). Thus, in the following experiment increasing amounts of the negative charged POPG were administered to KLK and the conformational transitions were monitored. As demonstrated before, KLK exhibited random coil conformation in water. Addition of POPG led to a beta-sheet conformation. With increasing lipid to peptide ratios KLK showed a further transition from intermolecular beta-sheet to alpha helix (Figure 7C).

Comparable to other peptides (Seelig, 2004) KLK is also capable of responding to the lipid environment with conformational transitions at the vicinity of membranes. These transitions could not be demonstrated for KPK.

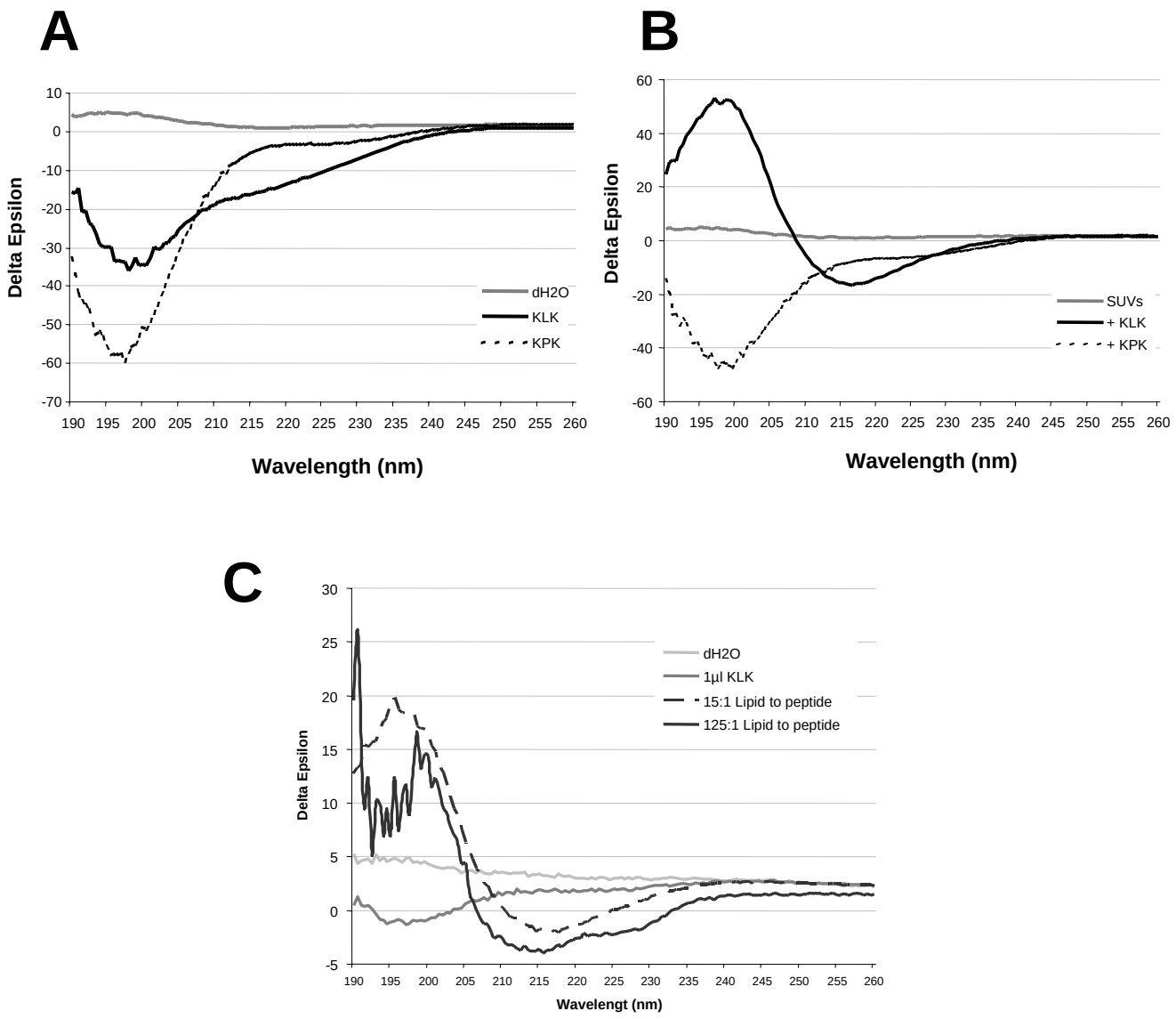


**Figure 7. Conformation of KLK and KPK in presence of lipids**

(A) Both KLK (black line) and KPK (dotted line) show typical random coil conformation in dH2O. (B) Conformational transition into β-sheet of KLK (black line) but not KPK (doted line) in the presence of POPG:POPC (1:3 molar ratio) SUVs at a lipid-to-peptite ratio of about 30. (C) Conformational transition of KLK at increasing lipid to peptide ratios. KLK exhibits random coil conformation in water (grey line). POPG triggers conformational transitions into β-sheet at low lipid to peptide ratio (15:1 molar ratio; black dashed line) and α-helix at high lipid to peptide ratio (125:1 molar ratio; black line).

#### 4.1.1.2. Beta-sheet and alpha-helical propensity of KLK and KPK

To further examine the conformational propensities of KLK and KPK, sodium dodecyl sulphate (SDS) and 2,2,2-trifluoroethanol (TFE) were included in the CD measurements.

SDS was added to a buffer to create a hydrophobic environment that mimics membrane hydrophobicity (Moraes et al., 2007). As seen in Figure 8A, addition of 1% SDS led to a transition of KLK from random coil to beta-sheeted conformation. As demonstrated with uncharged SUVs, KLK readily formed a beta-sheet that was not dependent on available charges but seems to be induced by the hydrophobic environment. It can be argued that, in this situation, intermolecular interactions covering the positively charged lysines are energetically preferable. The presence of SDS did not affect the random-coil conformation of KPK (Figure 8A).

2,2,2-trifluoroethanol (TFE) stabilizes alpha helical structures in proteins and peptides (Goodman et al., 1969) and can be used to determine the alpha-helical propensity of proteins (Segawa et al., 1991; Henrik et al., 1997).

20% TFE was added to KLK in water. This prompted the formation of a clear alpha-helix (Figure 8B). The same amount of TFE administered to KPK did not change the conformation of this peptide (Figure 8B).

#### 4.1.1.3. Phosphate buffer stabilizes the beta-sheet conformation of KLK

In a subsequent experiment we changed the buffer system and used 20 mM sodium-phosphate buffer instead of water. Phosphate strongly stabilized the beta-sheet of KLK in all our experiments (Figure 8C), whereas the random coil conformation of KPK was not affected by phosphate (Figure 8D). In contrast to our previous findings it was not possible to induce an alpha-helix by addition of TFE (Figure 8E). Up to 60% TFE were administered without apparent conformational transition from beta-sheet to alpha-helix (Figure 8F).

### 4.1.2. Interaction of KLK with various membrane systems

Cationic peptides in general elicit their antimicrobial activity by binding to membranes and changing the membrane stability and permeability. One possible mechanism is the formation of pores through which certain constituens are released. Alvarez-Bravo et al. showed that administration of 5 µg/ml KLK leads to release of glucose from artificial lipid vesicles (Alvarez-Bravo et al., 1994). The latter experiment is rather artificial as natural membranes

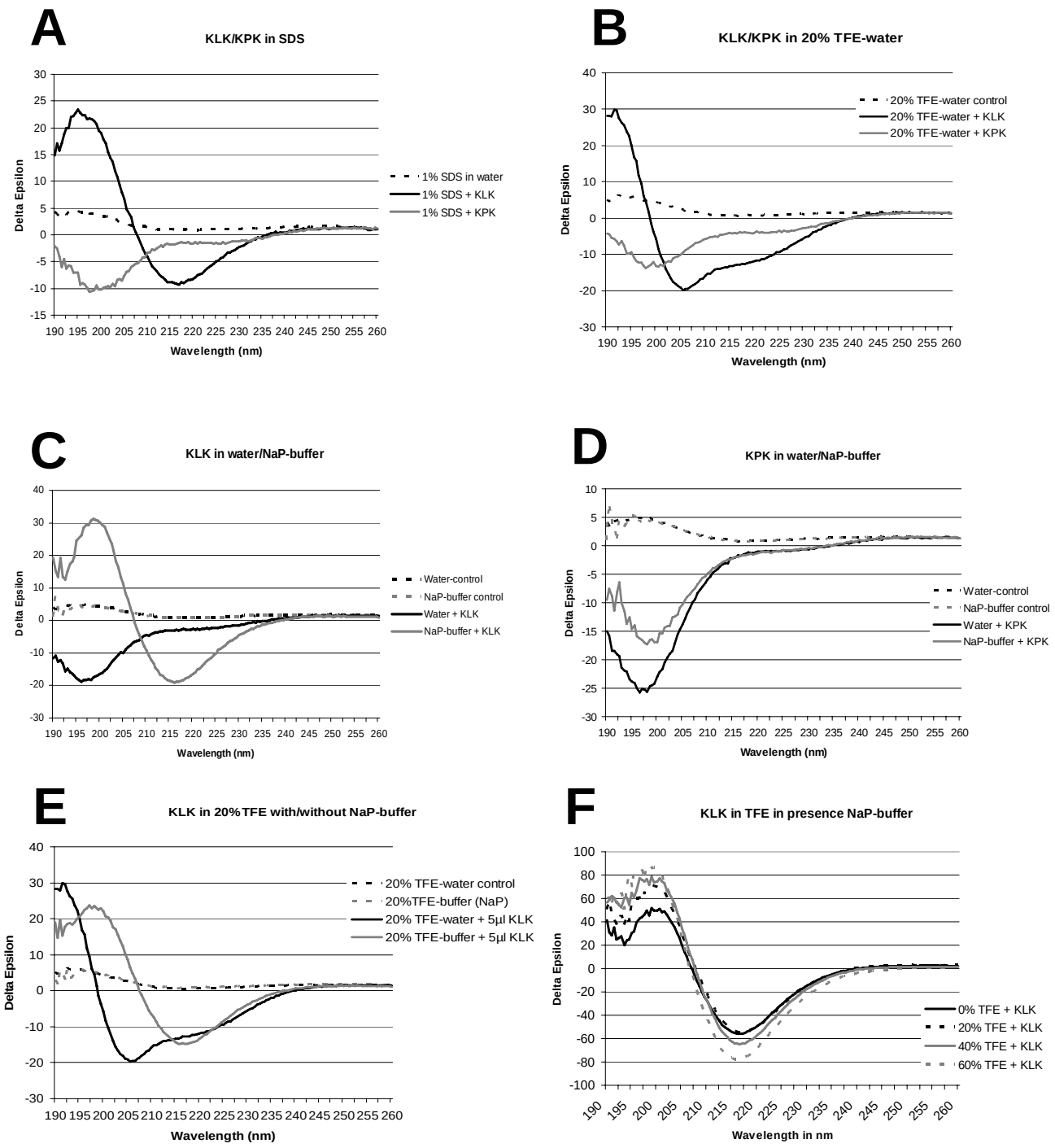


**Figure 8. Conformational propensities and stabilization**

(A) In the presence of 1 % SDS KLK (black) but not KPK (grey) demonstrates typical β-sheet conformation on a Circular dichroism spectrum. (B) KLK (black) but not KPK (grey) has α-helical propensity in presence of 20% TFE. (C) Phosphate buffer stabilizes β-sheet structure of KLK (grey). (D) KPK is not affected by presence of phosphate buffer. (E) Phosphate buffer prevents TFE-induced alpha-helix formation of KLK even at higher amounts of TFE (F).

have integral proteins that could affect KLK activity. Therefore, we tested the standard concentration of 10 nmole/ml (16 µg/ml) KLK in a more natural system.

### 4.1.2.1. Interaction of KLK with SMPs

To test whether KLK and KPK alter membrane stability or permeability, we used the established system of yeast sub-mitochondrial particles (SMPs) previously established in our laboratory (Nowikovsky et al., 2004; Froschauer et al., 2005). SMPs are derived from the inner mitochondrial membrane of the yeast *Saccharomyces cerevisiae* by sonication. Membrane proteins are present but directed inside out. Various ion selective dyes such as PBFI can be enclosed into these vesicles. The basal fluorescence emmission profile of PBFI is altered in the presence of potassium. When SMPs derived from wild type mitochondria are loaded with PBFI and potassium is administered to the outside, the $K^+/H^+$ exchanger protein Mkh1p leads to antiport of potassium through the membrane and a subsequent change in the fluorescence of PBFI. Knock out of Mkh1p (*mkh1Δ*) completely abolishes potassium-flux through the tight membrane. Only the disruption of the membrane by detergents or pore-forming peptides would allow contact between potassium and PBFI. Therefore, this system allowed the observation of KLK and KPK effects on a natural membrane.

#### 4.1.2.1.1. KLK interacts with the potassium-selective dye PBFI

Initial experiments revealed a unique interaction between the ion-selective dye PBFI and KLK. The peptide increases the fluorescent signal-intensities emmitted by both the unbound and the bound fractions (excitation curve at 380 nm and 340 nm, respectively), but the increase of the unbound fraction is considerably larger and therefore leading to a decline in the ratio curve (Figure 9A). A following addition of potassium reverted the effect of KLK suggesting that $K^+$ binds PBFI with higher affinity than KLK. Thus, further administration of KLK to a potassium-saturated system did not induce a comparable shift in fluorescence (Figure 9B). The observed phenomenon is specific for KLK as KPK did not exhibit any effects on the dye (Figure 9C).

#### 4.1.2.1.2. KLK interacts with vesicle enclosed PBFI without pore formation

For the next experiments PBFI was entrapped in SMPs derived from wild type and *mkh1Δ*-strains (Figure 10A and B). In the wild type situation administration of 150 mM potassium led to an immediate Mkh1p driven transport through the SMP-membrane and a subsequent interaction with PBFI enclosed in the vesicles. This interaction results in an increase of the

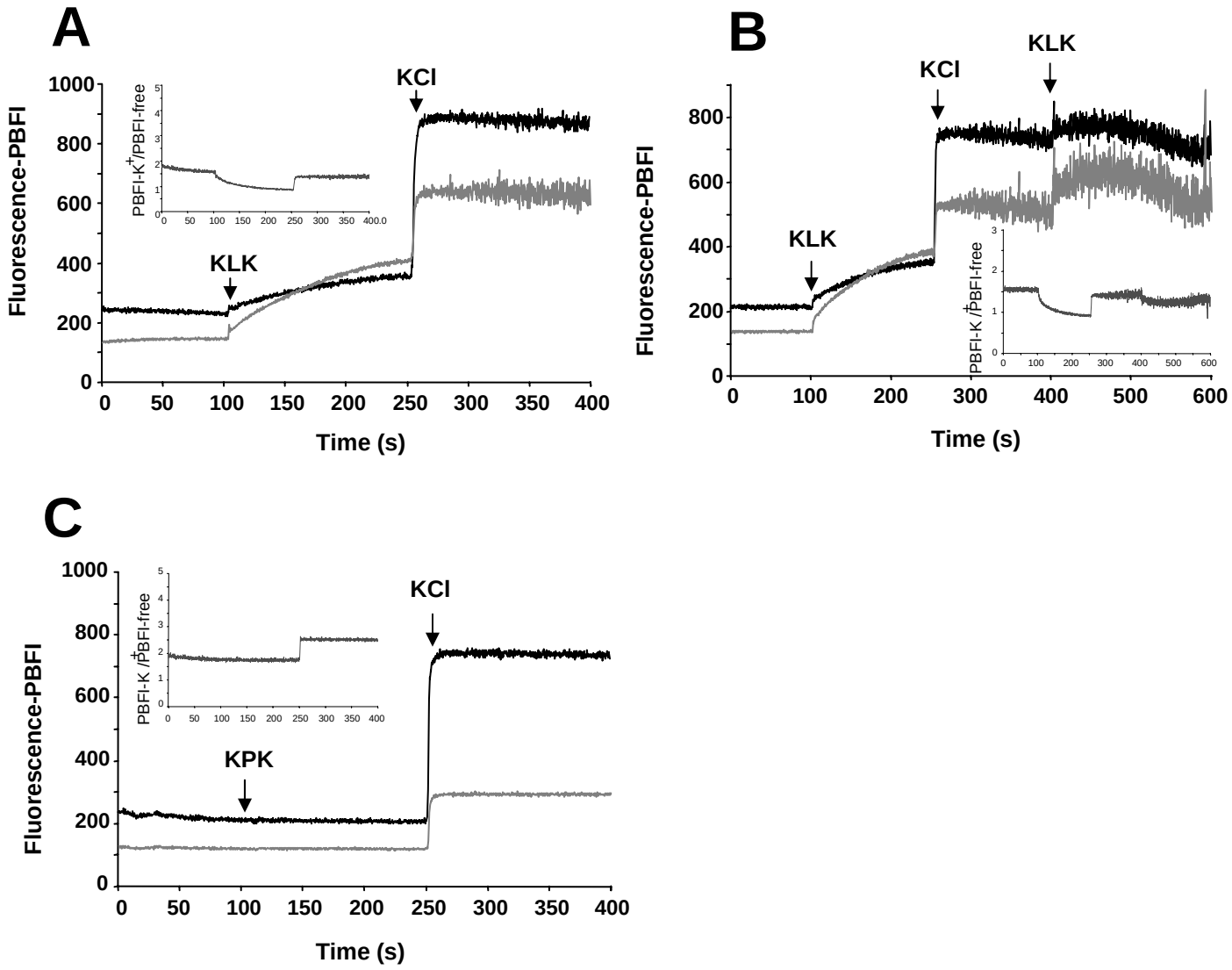


**Figure 9. Interaction of KLK and its derivative KPK with the K+-selective fluorescent dye PBFI**

Fluorescent signal intensities emitted by K+-bound and free PBFI were recorded simultaneously (black and light grey curves, respectively). KLK, KPK and KCl were administered at the indicated time points. (A) Data recorded with KLK. (B) Observations made with administration of KLK, followed by KCl and subsequently by KLK. (C) Results obtained with KPK. Inserts depict the ratio of fluorescence given by K+-bound and free PBFI in the same experiments.

bound fraction of PBFI (Figure 10A). In the SMPs of the *mkh1Δ*-strain transport and interaction are abolished (Figure 10B).

In Figure 10C potassium was first added to the SMPs to demonstrate that the vesicles are tight (Figure 10C). Subsequent administration of KLK led to the described typical effect on the signals demonstrating that KLK gets in contact with the dye enclosed in the vesicle. At the same time it is apparent that no pores are formed which would lead to an interaction of potassium and PBFI and therefore to a reversion of the KLK effect causing a signal as observed in the PBFI control experiment (Figure 9A). As expected, addition of KPK shows no effect (Figure 10D). To clarify whether the observed phenomenon is dependent on proteins, that are still present in the SMP-system, similar experiments were conducted using artificial asolectin vesicles that can also be loaded with PBFI but do not have membrane proteins. The loading efficiency of these vesicles is reduced and thus the signal intensities of the dyes are not as strong as in SMPs. Nevertheless the results clearly demonstrate that the effect of KLK is not dependent on SMP-proteins (Figure 10E).

#### 4.1.2.1.3. Localization of KLK within the SMPs

Two different possibilities can explain the interaction of KLK with the entrapped dye. First, KLK might pass the membrane and accumulate within the vesicules. Second, KLK is attracted by the outer and the inner leaflet of the membrane and stays in close contact with the membrane. In this case, as the peptide is not diffusing freely, only minor portions of KLK would be found within the vesicle. To discriminate between the two possibilities KLK was administerd to SMPs which were centrifuged and the supernatant was collected, the pellet fraction was sonicated by tip-sonication to release the entrapped material and the pellet fraction, the entrapped material and the supernatant were subjected to MALDI-TOF mass spectrometry analysis.

KLK appears as two specific peaks in the MALDI-TOF spectrum (Figure 11A). These peaks are found in the supernatant fraction (Figure 11B) and in the pellet fraction that represents the membrane of the SMPs (Figure 11D) but negligebly within the vesicles (Figure 11C).

FITC-labelled KLK was used to confirm these results microscopically. In the presence of SMPs KLK accumulates in the vicinity of the vesicles and forms large aggregates (Figure 11E). After centrifugation a small portion of SMPs and KLK-FITC can be observed in the microscope (Figure 11F). When the SMPs are sonicated, KLK-FITC predominantly stains the membrane fraction (Figure 11H) and no signal is found in the entrapped material (Figure 11G). Although this method has limited ability for quantification, it is sufficient to estimate

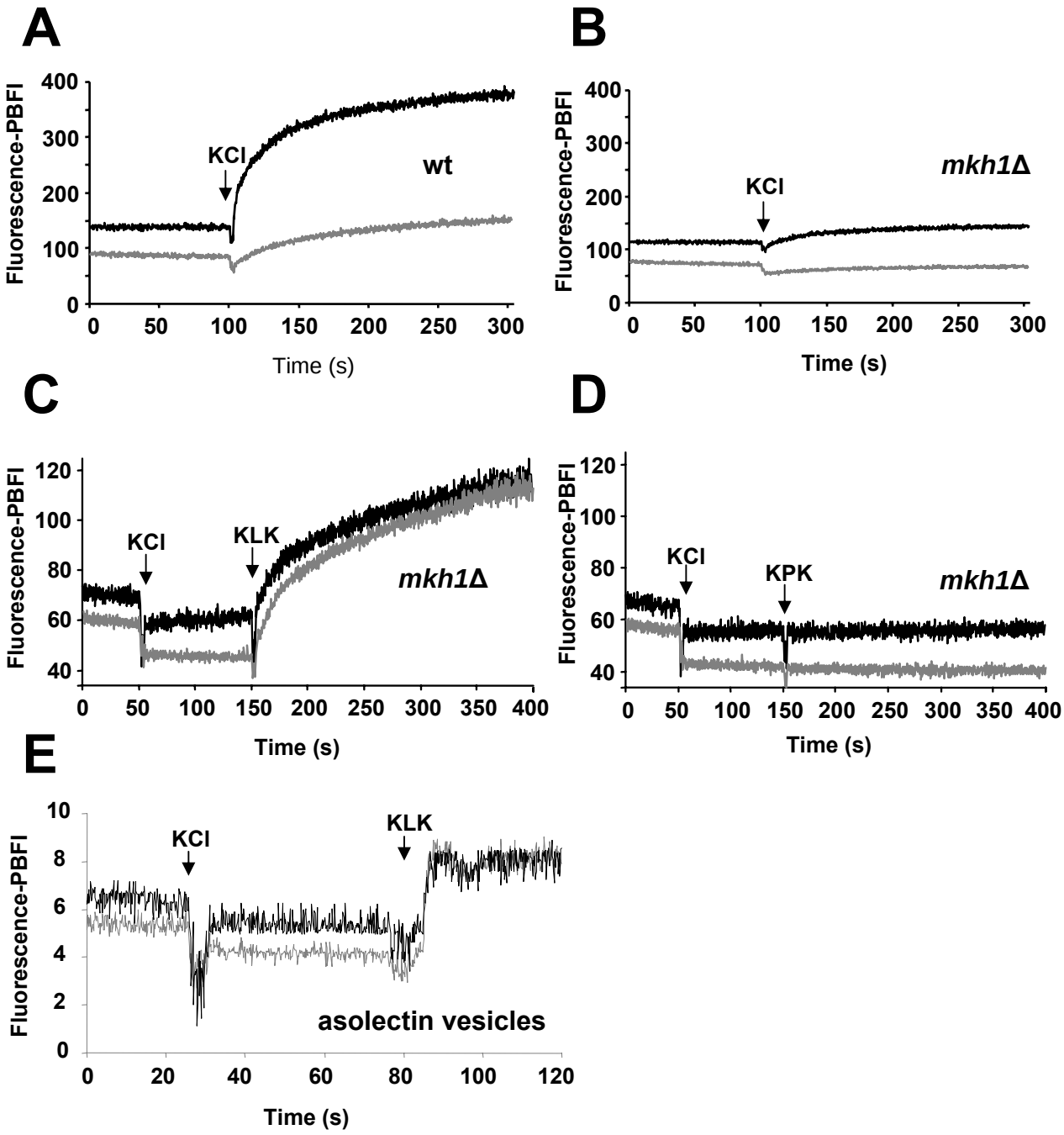


**Figure 10. Effect on KLK and KPK on SMP-vesicles**

Wild type or *mkh1Δ* sub-mitochondrial particles (SMPs) and large unilamellar asolectin vesicles were loaded with the $K^+$-sensitive fluorescent dye PBFI. KCl and KLK/KPK were administered at the indicated time points. Fluorescent signals emitted by K+-bound and free PBFI were recorded (black and light grey curves, respectively). SMPs isolated from wild type DBY747 (A) or DBY747 *mkh1Δ* (B) *S. cerevisiae* strains. Effect of KLK (C) and KPK (D) on PBFI-loaded *mkh1Δ* SMPs. Effect of KLK on PBFI-loaded asolectin vesicles (E).

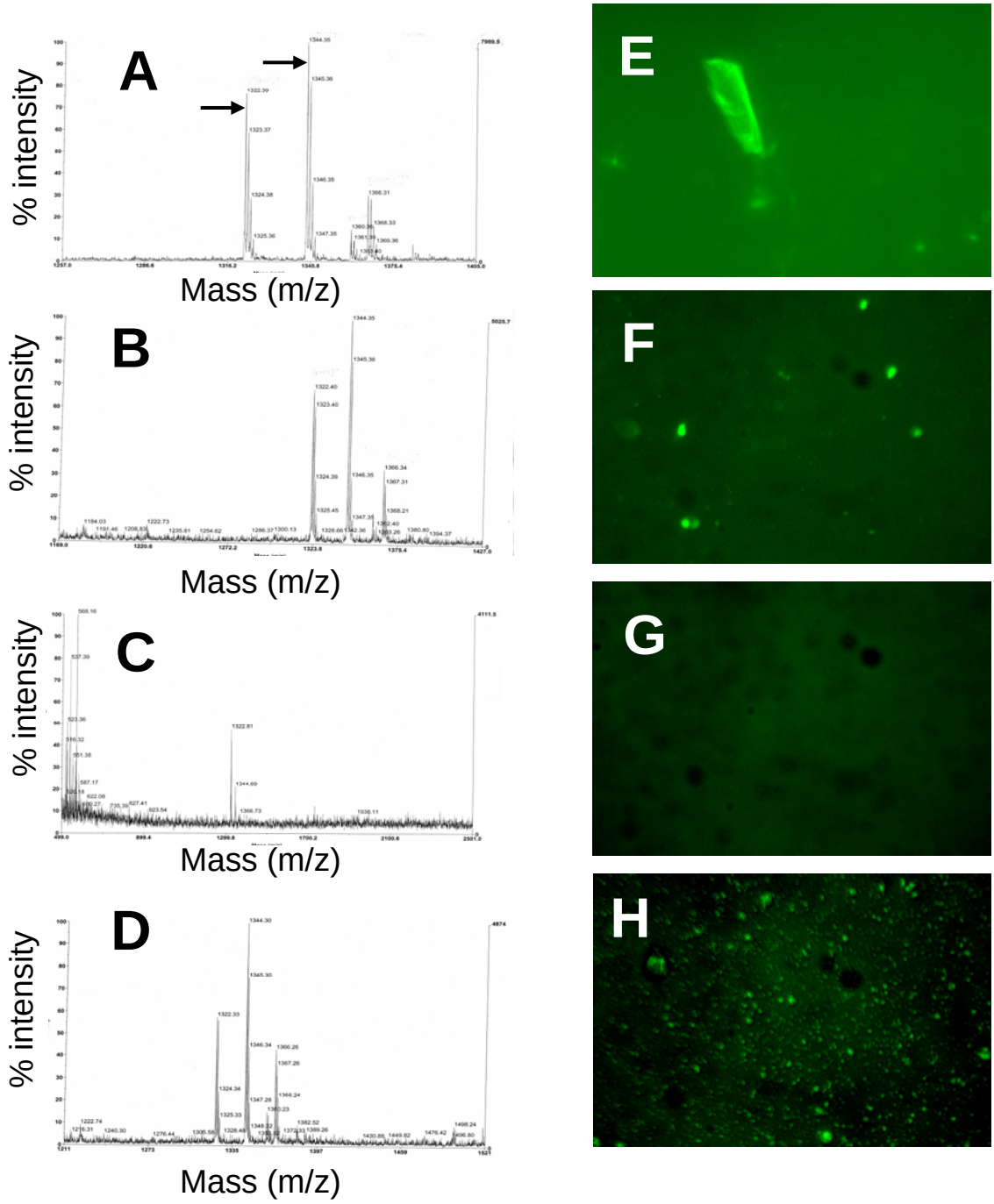


**Figure 11. Localization of KLK within SMPs**

*Mkh1Δ* SMPs were incubated with 20 nmole/ml KLK (A-D) and KLK-FITC (E-H) for 30 min on ice and centrifuged. Supernatant was saved and the vesicles washed extensively with reaction buffer. SMPs were then mechanically disrupted by tip-sonication and centrifuged. Supernatant (C, G) and pellet (D, H) together with the supernatant from the first centrifugation (B, F) and a buffer control with KLK added (A, E) were analysed for KLK and KLK-FITC content by MALDI-TOF mass spectrometry and fluorescence microscopy, respectively.

distribution of the peptide in the examined samples. These results together suggest that the majority of KLK associates with or intercalates into the membrane of the SMPs and is not generally distributed within the vesicles. Our experiments also reveal that the peptide associates with the membrane in a way that it is accessible for reactive material, like the PBFI dye, enclosed in the vesicle.

### 4.1.2.2. KLK affects erythrocyte membrane fluidity

Because of the relatively simple, homogeneous and well described membrane model offered by human erythrocytes and erythrocyte ghosts (Dodge et al., 1962), we tested the effect of KLK and KPK on the osmotic fragility of these cells as well as on fluidity parameters.

Untreated, KLK- or KPK-treated erythrocytes were exposed to increasing hydrophobic environment (Figure 12A). Haemoglobin release was detected by measuring optical density at 540 nm. The osmotic resistance of both KLK and KPK treated samples was identical to the control (Figure 12A).

Diphenylhexatriene (DPH) is a fluorescent probe that incorporates into the hydrophobic core of biological membranes. The fluorescent probe trimethylammonium-DPH (TMA-DPH) is a more hydrophilic derivative and incorporates into the outer parts of lipid bilayers. The incorporation into the plasma membrane is dependent of membrane fluidity or viscosity and leads to detectable fluorescence of the dye at 425 nm. Therefore, DPH- or TMA-DPH-dependent anisotropy measurements represent the state of fluidity of the hydrophobic core and surface compartment of the membrane, respectively (Bogner et al., 2002).

Our experiments revealed that KLK strongly increases both DPH and TMA-DPH dependent anisotropy indicating increased micro-viscosity or decreased membrane-fluidity of both the inner and the outer core of the lipid bilayer (Figure 12B).

None of these microviscosity parameters were affected when the samples were treated with KPK (Figure 12B).

### 4.1.2.3. Ultrastructural effects of KLK on various membranes

One aspect of the biocydal effects of AMPs is the binding to membranes where the induce pore formation or changes of the membrane structure which finally leads to lysis of the pathogen (Hof et al., 2001). The observed effects of KLK on various membranes and the decrease of fluidity in erythrocyte-ghosts let us speculate whether these effects are also associated with ultra-structural changes of the membranes. Therefore, the membrane-structure

of KLK or KPK treated SMPs was compared with untreated samples in the transmission electron microscope (TEM).

#### 4.1.2.3.1. Small mitochondrial particles

Control vesicles are membrane-boarded structures with a constant size of 0.1-0.3 nm in diameter, they lack electron dense content and due to the preparation, the vesicles are occasionally surrounded by membrane fragments resulting in a debris-like background.

KLK induced a striking reduction in vesicle size with simultaneous enrichment of the debris-like background material. The vesicles appeared ragged-edged and often with reduction of osmophilicity in their membranes (Figure 13A). Larger magnifications show generally disordered bilayer structure, a morphology that was characteristic of nearly all vesicles in the field of view (Figure 13B). None of these effects were observed in KPK treated samples (Figure 13A)

#### 4.1.2.3.2. Dendritic and ECV-cells

After revealing these KLK-effects the next important step was to administer the peptide to dendritic cells (DCs). DCs represent professional antigen presenting cells (APCs), the primary target cells of IC31$^{TM}$. 100 nmole/ml KLK were administered to human monocyte derived DCs. After 15 minutes the semi-adherent cells were centrifuged and fixed with glutaraldehyde. In the electron microscope KLK-treated DCs appeared with a changed morphology including protrusion of the dendrites (Figure 14A).

In a co-operation with the group of Gerhard Schütz at the Kepler University of Linz, we further analysed the membrane structure after KLK treatment in a well-established cell system. ECV endothelial-cells were treated with a high dose (100 nmole/ml) KLK for 5 minutes before they were fixed with glutaraldehyde. KLK-treated ECV cells exhibit vesicle-enriched periphery of their cytoplasm as well as yet unidentified filamentous depositions at the cell surface (Figure 14B).

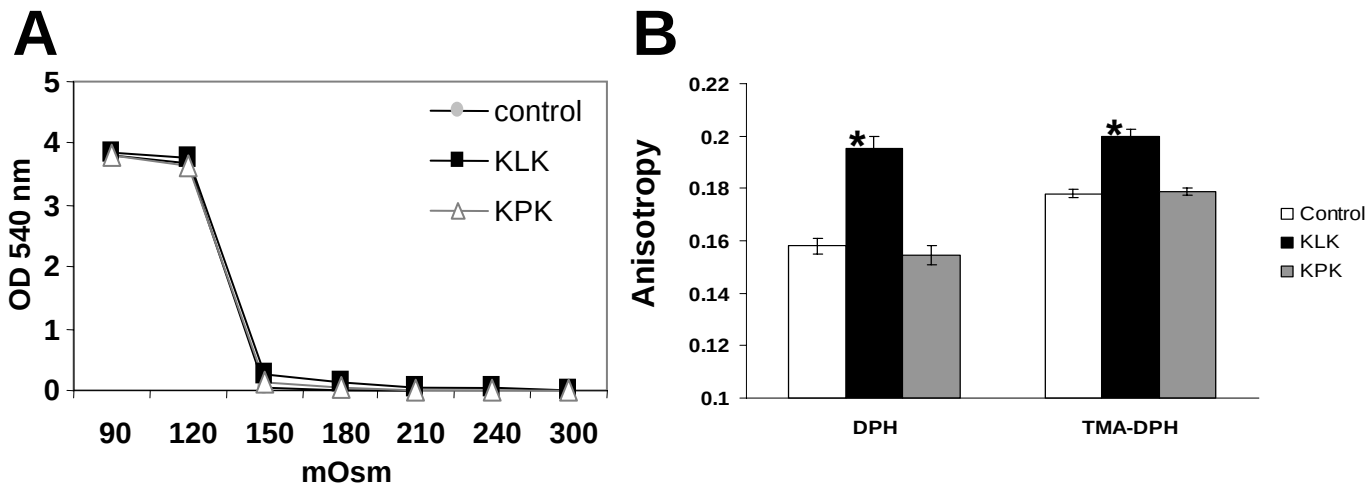


**Figure 12. Effect of KLK and KPK on human erythrocyte membranes**

Human erythrocytes were exposed to media with increasing osmolarity and the effect of KLK and KPK was recorded on the osmotic resistance as measured by haemoglobin release at OD of 540nm (A). Effect of KLK and KPK on the fluorescent anisotropy of DPH- and TMA-DPH-loaded erythrocyte ghosts (B). For each sample the fluorescence was corrected for the scattering effect of unlabeled ghosts. Asterisks represent *p*-values, $p < 0{,}001$.

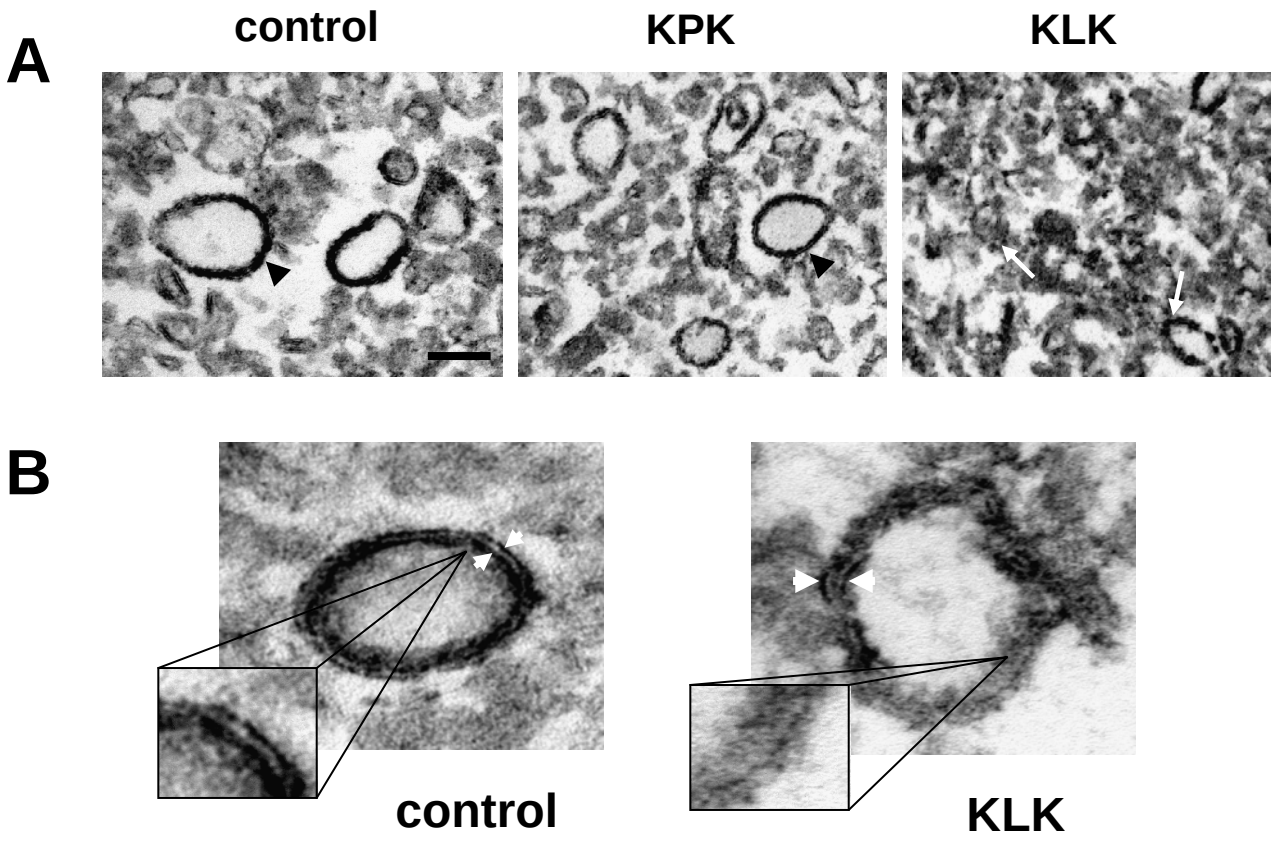


**Figure 13. KLK effects on SMP membrane ultrastructure**

(A) Untreated control and KLK- or KPK-treated *mkh1Δ* SMPs were incubated for 30 min on ice and centrifuged. Pellets were processed for electron microscopic analysis. Black arrowheads indicate larger vesicles with electron dense membranes, while white arrows show smaller, ragged-edged vesicles with less osmiophylic membranes. Bar corresponds to 0.1 µm. (B) Larger view of transmission electron micrographs obtained from control vs. KLK-treated *mkh1Δ* SMPs. White arrowheads indicate widths of control (upper panel) and a KLK-treated (lower panel) SMP membrane-bilayers. Comparison of larger magnifications in the inserts allows judgement of membrane rearrangement caused by KLK.

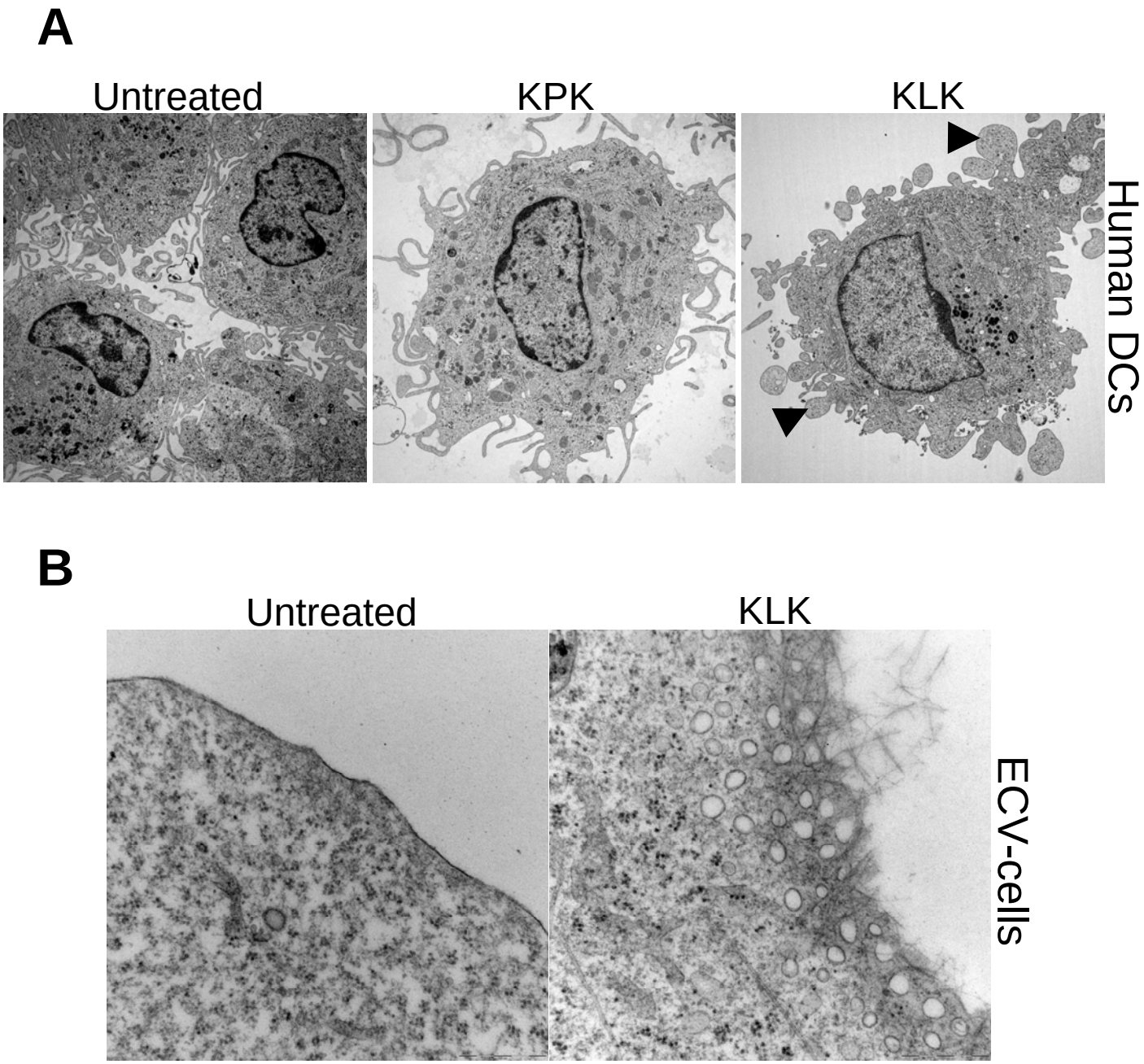


**Figure 14. Ultrastructural effects of KLK on cells**

Transmission electron micrograps of untreated control or KLK/KPK treated dendritic and ECV-cells. Black arrowheads indicate protrusion of dendrites (A). KLK-treated ECV cells exhibit vesicle enriched periphery of their cytoplasm as well as yet unidentified filamentous depositions at the cell surface. (B).

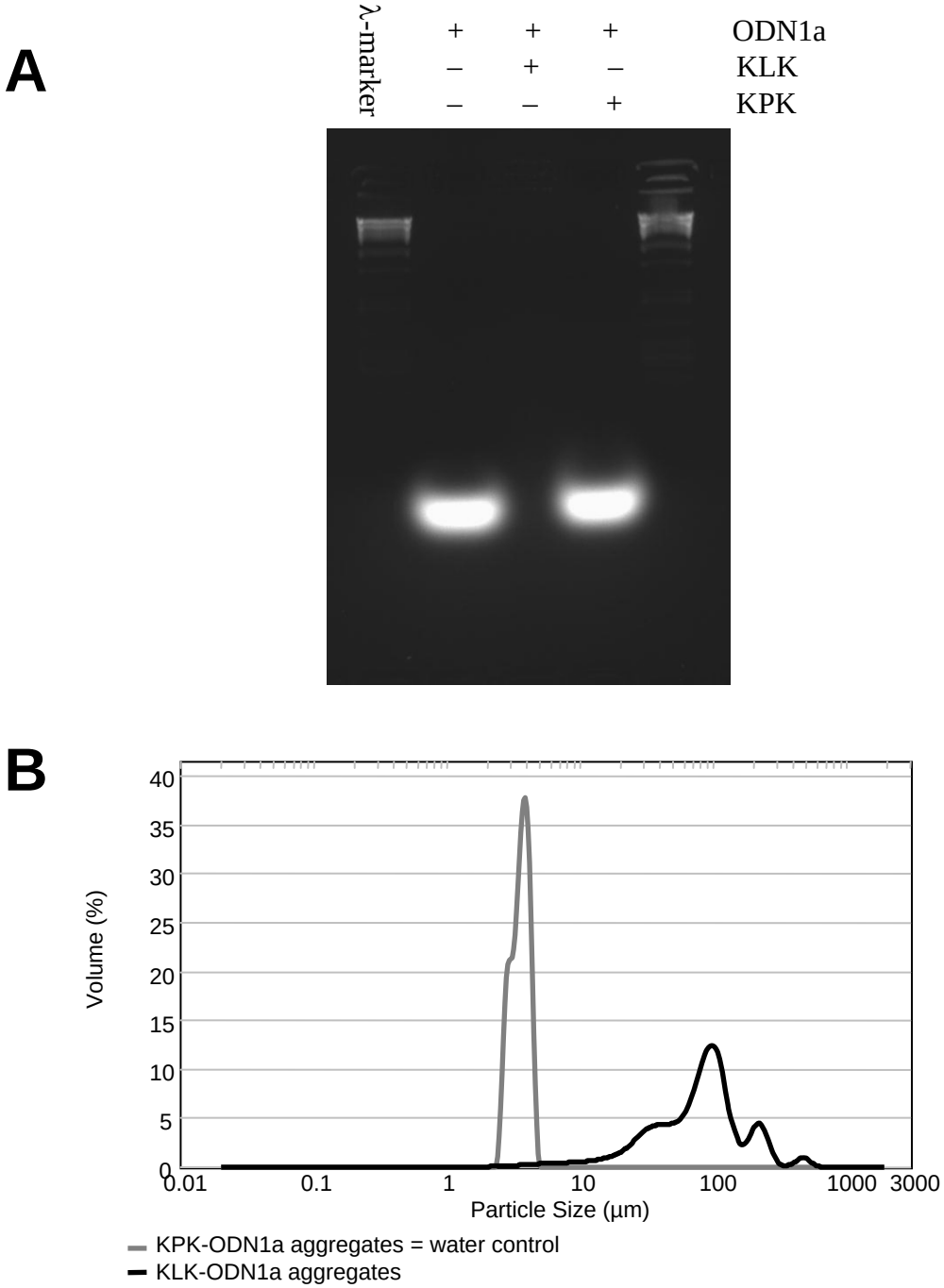


**Figure 15. Aggregate formation of KLK and ODN1a**

(A) Aggregate formation by KLK and ODN1a was confirmed using a gel retardation assay. ODN1a (lane 2), KLK/ODN1a (lane 3) and KPK/ODN1a (lane 4) were loaded on a 2% agarose gel. KLK/ODN1a-aggregates did not migrate into the gel and were washed out of the slot during the run. (B) Particle size distribution measurements of KLK/ODN1a aggregates (black line) and KPK/ODN1a aggregates (grey line) in water using a Malvern Mastersizer 2000.

## 4.1.3. Complex formation of KLK with ODN1a

IC31® was demonstrated to form a stable depot at the injection site (Schellack et al., 2006). Before IC31® is injected the components are mixed and aggregate. We assumed that the different conformational properties of KLK and KPK might be an important factor in these complexes and this could explain why KLK but not KPK is able to form the stable depot at the injection site.

In an initial experiment 10 µg ODN1a were mixed where indicated with 40 µg KLK or KPK and loaded on a 2% agarose-gel. KLK readily aggregated with ODN1a and completely inhibited the movement of ODN1a into the gel. (Figure 15A). In comparison, administration of KPK did not lead to retardation.

To measure the size of the observed aggregates, the Malvern Mastersizer 2000 was used. According to the Mie-theory the scattering of electromagnetic radiation by spherical particles can be used for characterization of particle-sizes (Stebbing et al., 2008).

In Figure 15B, the area below the graph represents the amount of complexes with the indicated size. KPK showed a peak similar to the water control and thus did not form particles or aggregates with ODN1a (Figure 15B). KLK on the other hand exhibited a non-homogenous size distribution. Four distinct groups were observed (Figure 15B). The smaller complexes had a diameter below 70 µm, while considering the area below the graph, only one or two complexes with a size of 500 µm and 800 µm formed the last two fractions. In these measurements the majority of the complexes had sizes between 70 and 250 µm, in agreement with the microscopic examinations showing that most ODN1a-Cy5/KLK aggregates had a diameter below 100 µm (see following chapters, e.g. Figure 17, arrow 1).

# 4.2. Uptake and distribution of the components of IC31® in dendritic cells

The previous experiments revealed strong membrane interacting properties of KLK, which can form aggregates with ODN1a. Therefore we assumed that KLK might elicit additive effects on ODN1a function in vivo. The TLR9 agonist has to be taken up into the target cells, the dendritic cells, and interact in specific compartments with the receptor. TLR9 itself resides in the ER and is relocated to the lysosomal compartments upon stimulation with CpG-DNA (Latz et al., 2004). With the following experiments we aimed to shed more light on the uptake routes of ODN1a and KLK and clarify their roles in interplaying as an adjuvant.

## 4.2.1. The cellular fate of ODN1a

ODN1a is thought to be the main stimulus for the activation of dendritic cells by IC31®. Thus a clear picture of the fate of ODN1a in an in vitro and in vivo situation is essential for the understanding of the adjuvant effects. Therefore we were interested in studying the influence of KLK on ODN1a uptake and the distribution of the nucleotide within the cell.

### 4.2.1.1. KLK enhances ODN1a uptake by dendritic cells

To test whether the described membrane interactive properties of KLK show effects at the cellular level, ODN1a was labelled at the N-terminus with Cy5 as described elsewhere (Schellack et al., 2006), it was pre-mixed with KLK/KPK, diluted in medium and added to various cell types.

We show that KLK but not KPK enhances the uptake of ODN1a in immature human monocyte derived DCs (Figure 16A) and immature mouse bone marrow derived DCs (Figure 16B). The uptake can be blocked by incubation of the cells on ice (Figure 16B). Low temperature affects the cell membrane fluidity and thus the membrane turnover. This indicates that ODN1a has to be taken up via the classical endocytic routes and KLK is not working as a cell penetrating peptide that carries the nucleotide through the membrane into the cytoplasm.

The uptake of ODN1a is rapid as it can be found in dendritic cells already after 5 minutes, but the signal intensity of ODN1a-Cy5 increases over time with a peak at about 60 minutes (Figure 17). Then the staining slowly disappears within the next hour as ODN1a is probably degraded. When both components of IC31® are mixed and added to the cell we can find

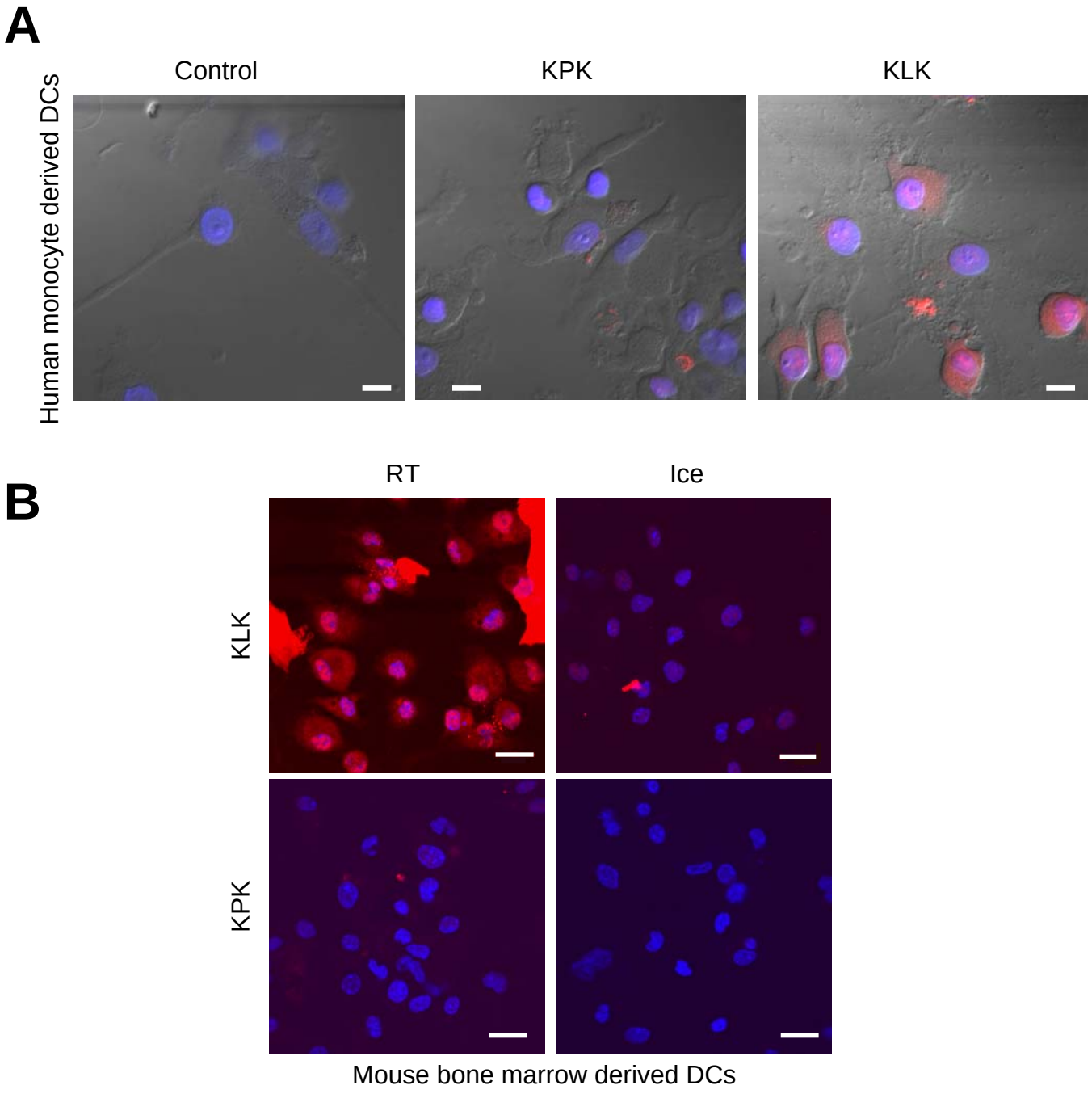


**Figure 16. KLK enhances ODN1a uptake by dendritic cells**

(A) ODN1-Cy5 (red) were mixed with KLK/KPK and administered to immature human monocyte derived DCs. As a control ODN1a was added directly to the cells. Cells were fixed after 60 minutes and nuclei were labelled with DAPI (blue). (B) ODN1a-Cy5 (red) uptake by immature mouse bone marrow derived DCs in the presence of KLK or KPK at room temperature (RT) and 0°C. White bars represent 10 µm.

complexes in the microscope that are comparable in size to the measured particles in the master-sizer (~ 100 µm). The majority of these aggregates associate with one or more DCs in the culture and often one large complex covers many cells (Figure 17, black arrowhead).
In various experiments ODN1a seems to appear in the nucleus. This is a well-known artefact of the fixation procedure. The PFA treatment enables ODN1a to pass through the nuclear membrane where it is attached to DNA-binding proteins like histons. (Lundberg and Johansson, 2002). The nuclear localisation is not seen during live-cell imaging (see below).

#### 4.2.1.2. Dynamics of KLK/ODN1a complex association at the cell surface

We were interested to see, how KLK/ODN1a aggregates interact with the cell surface over time. Therefore we monitored these complexes with live cell fluorescent confocal time-laps imaging. These experiments revealed that the interaction between cell membrane and the KLK/ODN1a-complex is highly dynamic. The complex gets in contact with sites at the membrane. Interestingly not every contact leads to a stable interaction. As shown in Figure 18, a complex approaches the tip of a dendrite where we observe the formation of a stable interaction that lasts for more than 60 minutes (Figure 18, black arrowhead). Alongside of the dendrite another complex gets in contact with the membrane but a stable interaction is not formed and the complex leaves the contact site (Figure 18, white arrowhead). At the tip of the same dendrite another interaction is formed (Figure 18, black arrow).

#### 4.2.1.3. ODN1a is taken up into early and late endosomes

Based on earlier observations we assumed that the uptake of ODN1a is energy dependend and most likely an endocytotic process (Figure 16B). To further proof this, we treated DCs with ODN1a-Cy5 and an antibody against human transferrin receptor (TfR), an early endosomal marker which is known to be internalized via a clathrin-mediated pathway (Duarte C Barral, 2008), and with an antibody against human Lamp1 to visualize late endosomes. The well studied CpG-DNA (Heeg et al., 2008) was used as a positive control as this TLR9 ligand has been shown to locate to these compartments (Latz et al., 2004). Figure 19 shows that ODN1a-Cy5 localizes with both TfR and Lamp1 positive structures, suggesting ODN1a distribution in both early (A) and late endosomes (B), similarly to CpG-DNA.

#### 4.2.1.4. ODN1a is localized in the endoplasmic reticulum

Our studies indicated that besides various endosomal localizations ODN1a is clearly seen in compartments other than the endosomes (Figure 19). One location is perinuclear and we

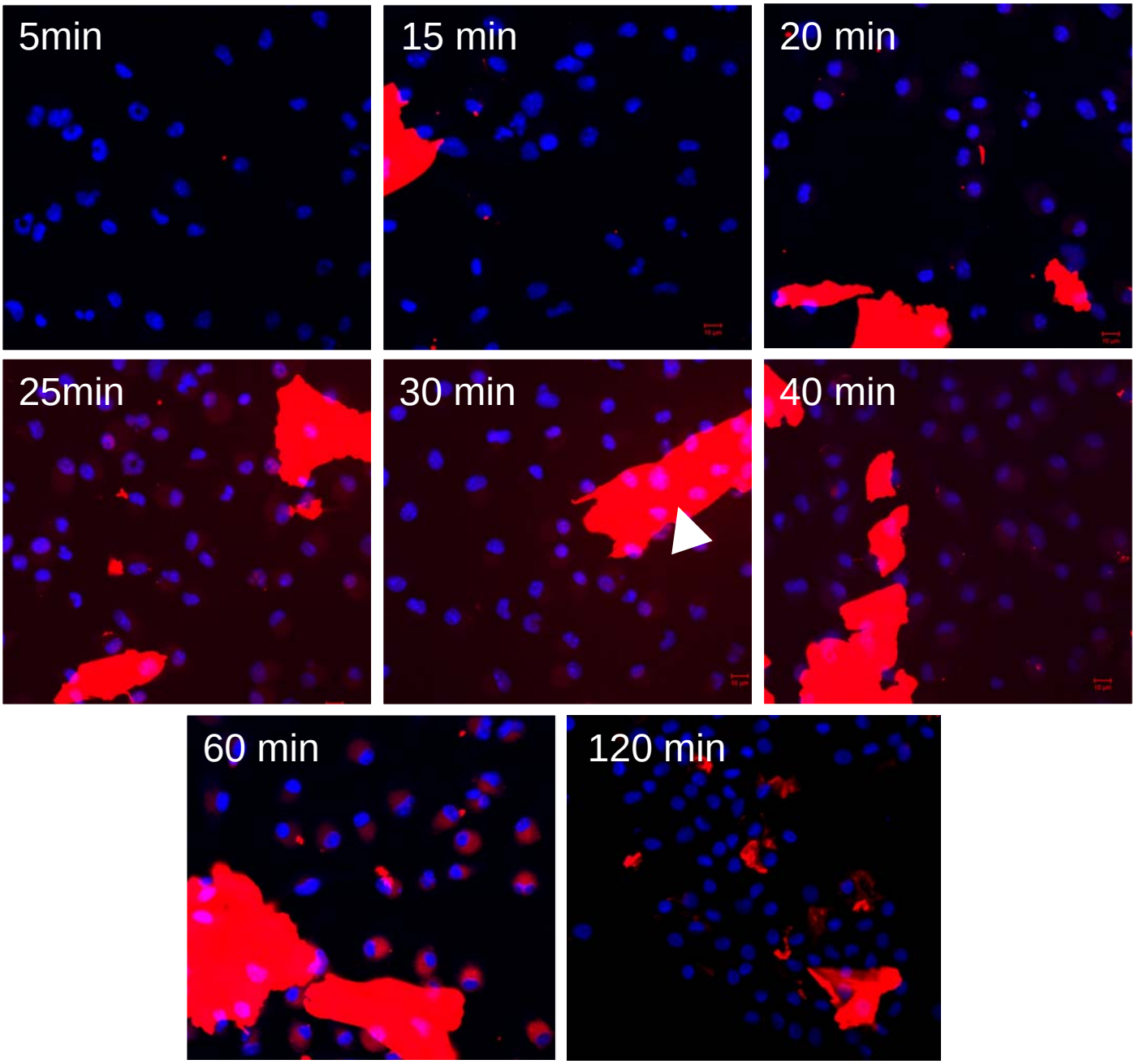


**Figure 17. Time course of ODN1a uptake by dendritic cells**

ODN1a-Cy5 (red) and KLK were administered to immature mouse bone marrow derived DCs. After indicated time points the cells were fixed and the nuclei were stained with DAPI (blue). Cells were monitored by laser confocal imaging. White arrowhead indicates an example of KLK/ODN1a-aggregate covering cells.

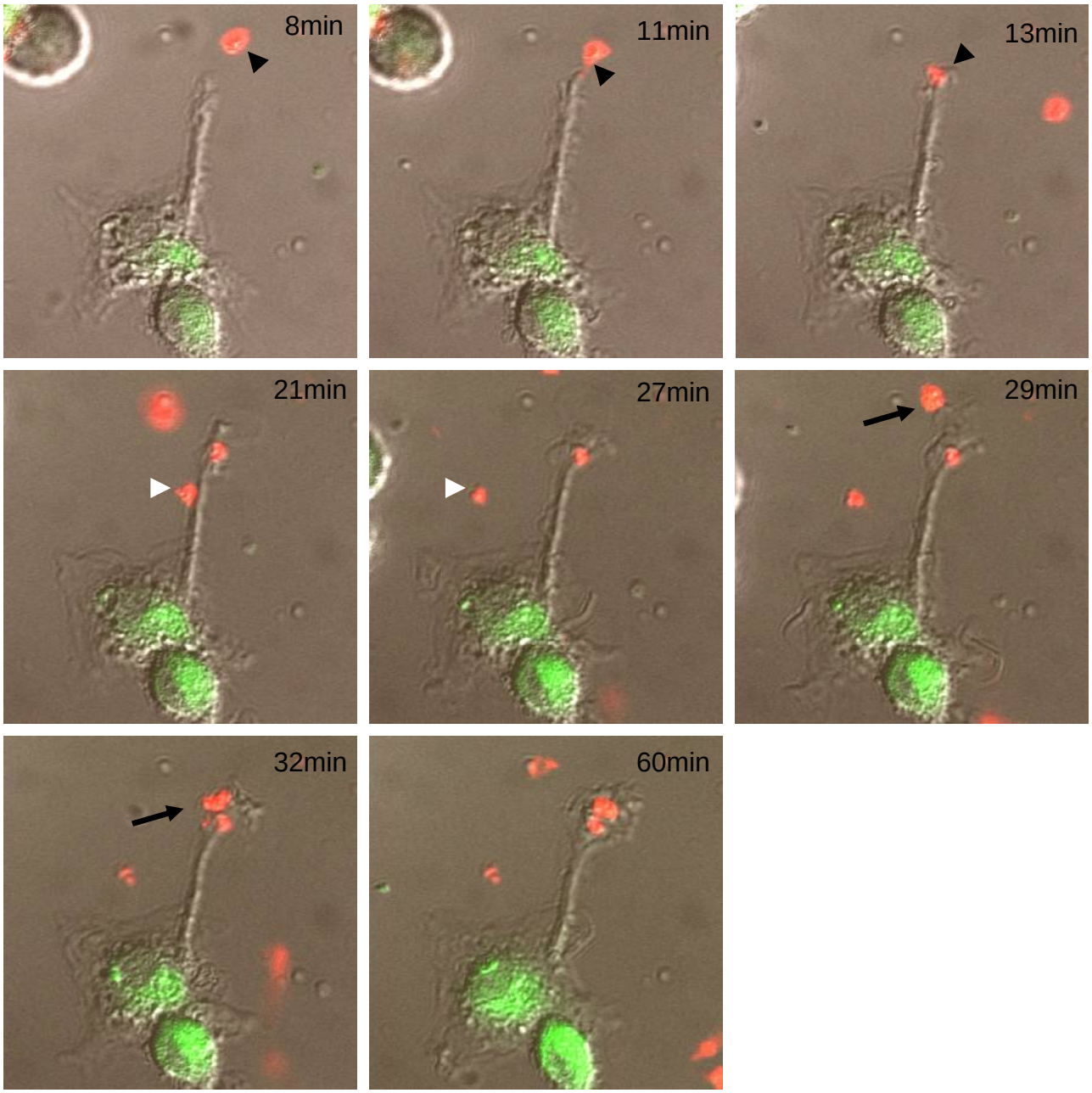


**Figure 18. Interaction dynamics of KLK/ODN1a complex with dendritic cells**

Live cell laser confocal imaging of human monocyte deriveded dendritic cells demonstrating the dynamics of ODN1a/KLK-aggregate interaction. ODN1a-Cy5 (red) was mixed with KLK and administered to the cells. At the tip of a dendrite stable interactions are formed (black arrowhead; black arrow) while alongside of the dendrite a complex leaves the contact side (white arrow). ER-tracker (green) was added to stain the endoplasmic reticulum.

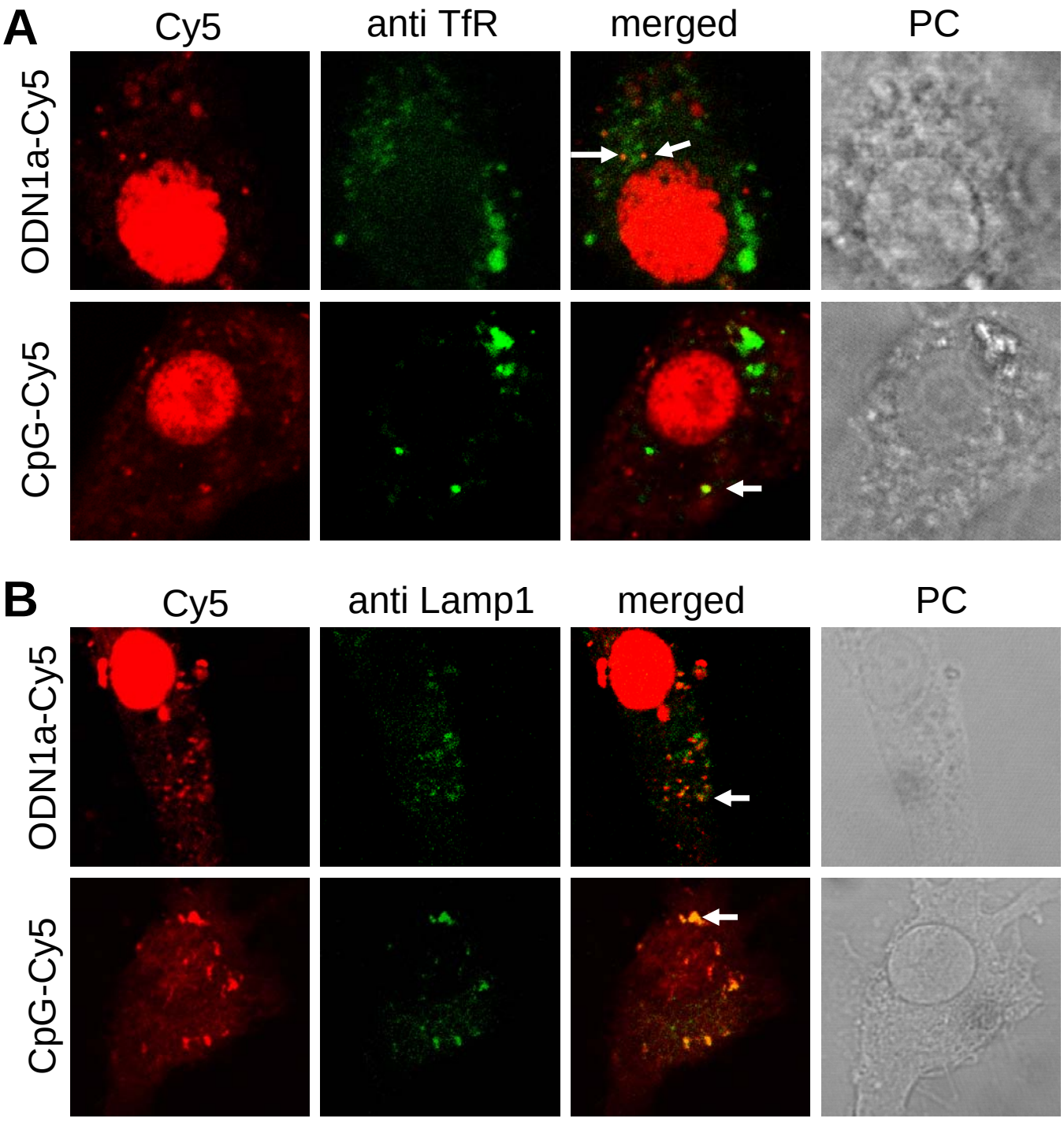


**Figure 19. Detection of ODN1a in early and late endosomes**

Immature human monocyte derived dendritic cells were exposed to ODN1a-Cy5/KLK or CpG-Cy5 for 60 minutes. Cells were fixed and stained with antibodies against (A) the early endosomal marker TfR (green) or (B) the late endosomal marker Lamp1 (green). Co-localization (wite arrows) was revealed by laser confocal imaging.

therefore stained DCs with the drug conjugate glibenclamide BODIPY® FL that binds to the sulphonylurea receptor of ATP-sensitive $K^+$ channels, prominent proteins of the ER. The staining of the ER with this ER-tracker takes up to 30 minutes. Live-cell imaging reveals this delay as the signal intensity of the tracker increases over time. In fixed cells we demonstrated that the residual ODN1a that is found in the dendritic cells is distributed within the ER of human monocyte derived dendritic cells and mouse bone marrow derived dendritic cells, similarly to CpG-DNA (Figure 20). Using live cell laser confocal imaging ODN1a/KLK-complexes could be detected at the cell surface (Figure 21, black arrowheads). We observed that the red ODN1a signal gradually turns yellow as ODN1a was taken up into the cell and co-localizes with the ER (Figure 21, black arrow).

#### 4.2.1.5. ODN1a colocalizes with TLR9 but its uptake does not require TLR9

ODN1a is a TLR9 agonist. Latz et al. have demonstrated that TLR9 resides in the ER but relocates to the so called tubular lysosomal compartments in the presence of CpG-DNA (Latz et al., 2004). We have seen ODN1a in endosomes as well as ER but wanted to have a direct proof for ODN1a/TLR9 colocalization. With newly available antibodies against human and mouse TLR9 we showed that ODN1a clearly colocalizes with TLR9 positive structures (Figure 22A).

Uptake of ODN1a into dendritic cells was independent of the presence of the receptor. Similarly to wild type cells DC from TLR9-/- mice took up comparable amounts of ODN1a within 45-60 minutes (Figure 22B).

#### 4.2.1.6 ODN1a uptake of various cell types

KLK interacts with ODN1a and with the cell membrane. Based on our results that KLK stimulates ODN1a uptake most likely via endocytosis, we assumed that the rate of endocytosis or the membrane turnover is important in the ODN1a uptake process. Immature dendritic cells are known as professional APC and exhibit compared to other cell types an increased uptake of material via endocytosis (Sallusto et al., 1995). In accordance with this, when experiments were performed using Hela-, C2C12- and CaCo-cells we found the typical binding of the ODN1a/KLK-complex to the cell surface but we did not observe an uptake of ODN1a (Figure 23A). The basal endocytosis-rate of these cells did most likely not allow the internalization of enough ODN1a to be visible in our experiments.

Macrophages, however, cells of the immune system that are specialized to take up antigens from the environment, took up ODN1a regardless of the presence or absence of KLK (Figure

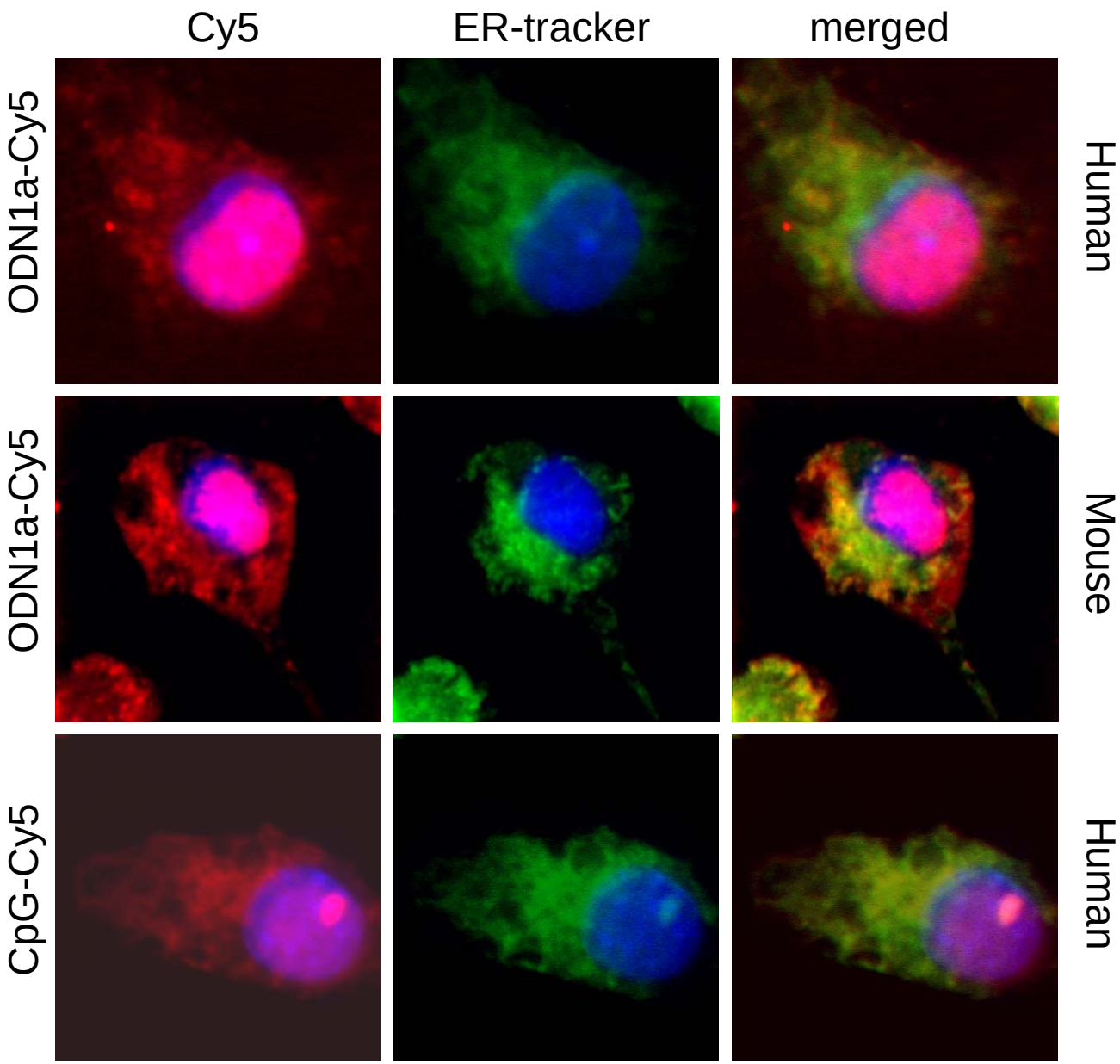


**Figure 20. ODN1a uptake into the endoplasmic reticulum**

Immature human monocyte derived and immature mouse bone marrow derived DCs were stained with ER-tracker (green) and exposed to ODN1a-Cy5 (red) and KLK or CpG-Cy5 in absence of KLK. Cells were fixed and nuclei were stained with DAPI (blue). Co-localisation was revealed using laser confocal imaging.

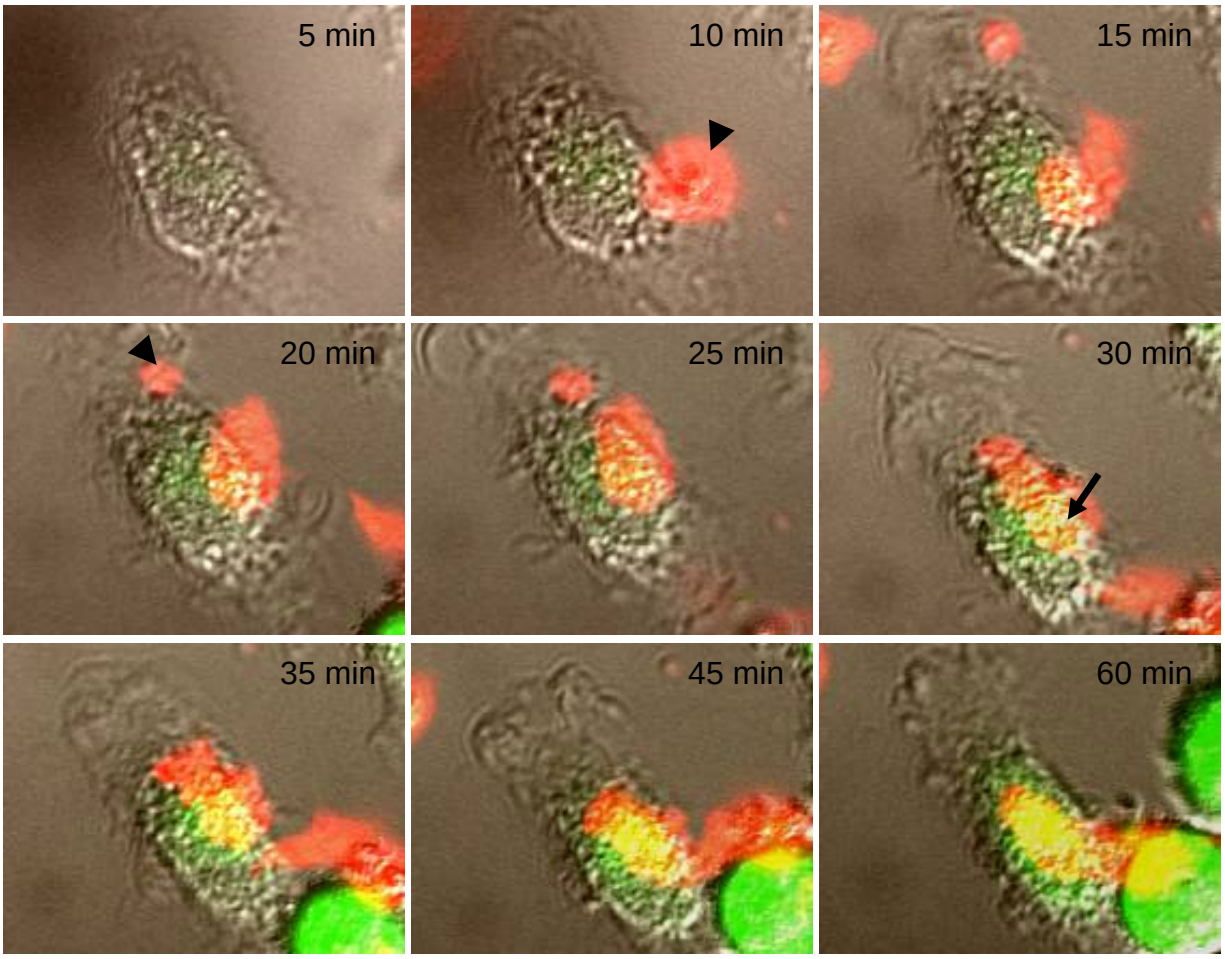


**Figure 21. Live cell confocal imaging of ODN1a uptake into the ER**

Time-lapse fluorescence confocal imaging of immature human monocyte derived DC that encounters ODN1a/KLK-aggregates (black arrowheads) and internalizes ODN1a into the endoplasmic reticulum stained with ER-tracker (green). Arrow indicates the cytoplasmic region of the cell were ODN1a co-localizes with the ER-compartment.

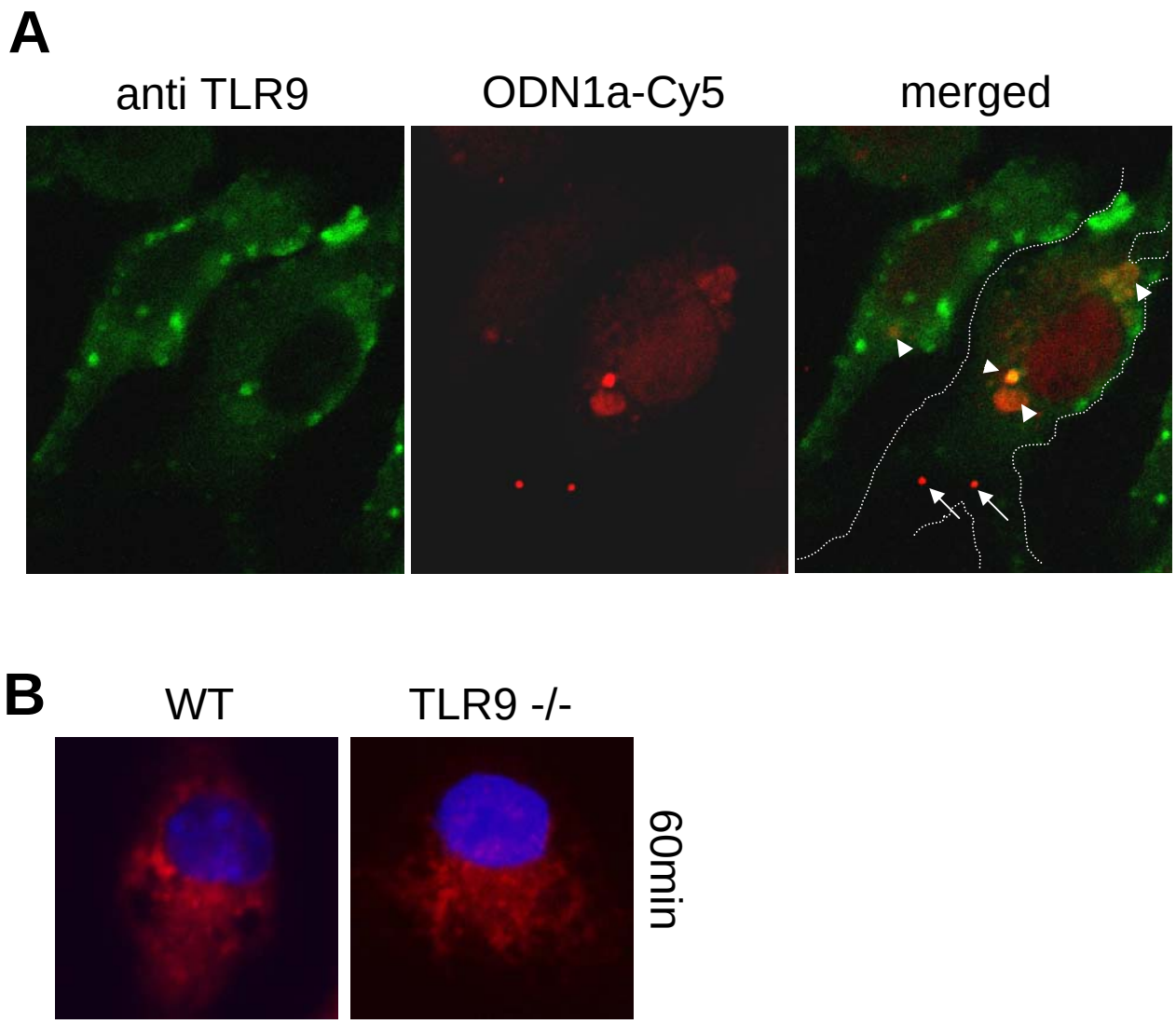


**Figure 22. ODN1a colocalizes with TLR9, but ODN1a uptake is TLR9 indipendent**

(A) Immature mouse bone marrow derived DCs were exposed to ODN1a-Cy5 (red) and KLK and stained with antibodies against TLR9 (green) after fixation. Co-localisation was monitored by laser confocal imaging. On the right panel the contours of a DC are marked with a white dotted line. Arrowheads indicate TLR9 and ODN1a double positive structures, arrows point to ODN1a positive vesicles. (B) Immature mouse bone marrow derived DCs from wild type and from TLR9-/- were exposed to ODN1a-Cy5 (red) and KLK for 60 minutes. After fixation the nuclei were stained with DAPI and samples were analysed by laser confocal imaging.

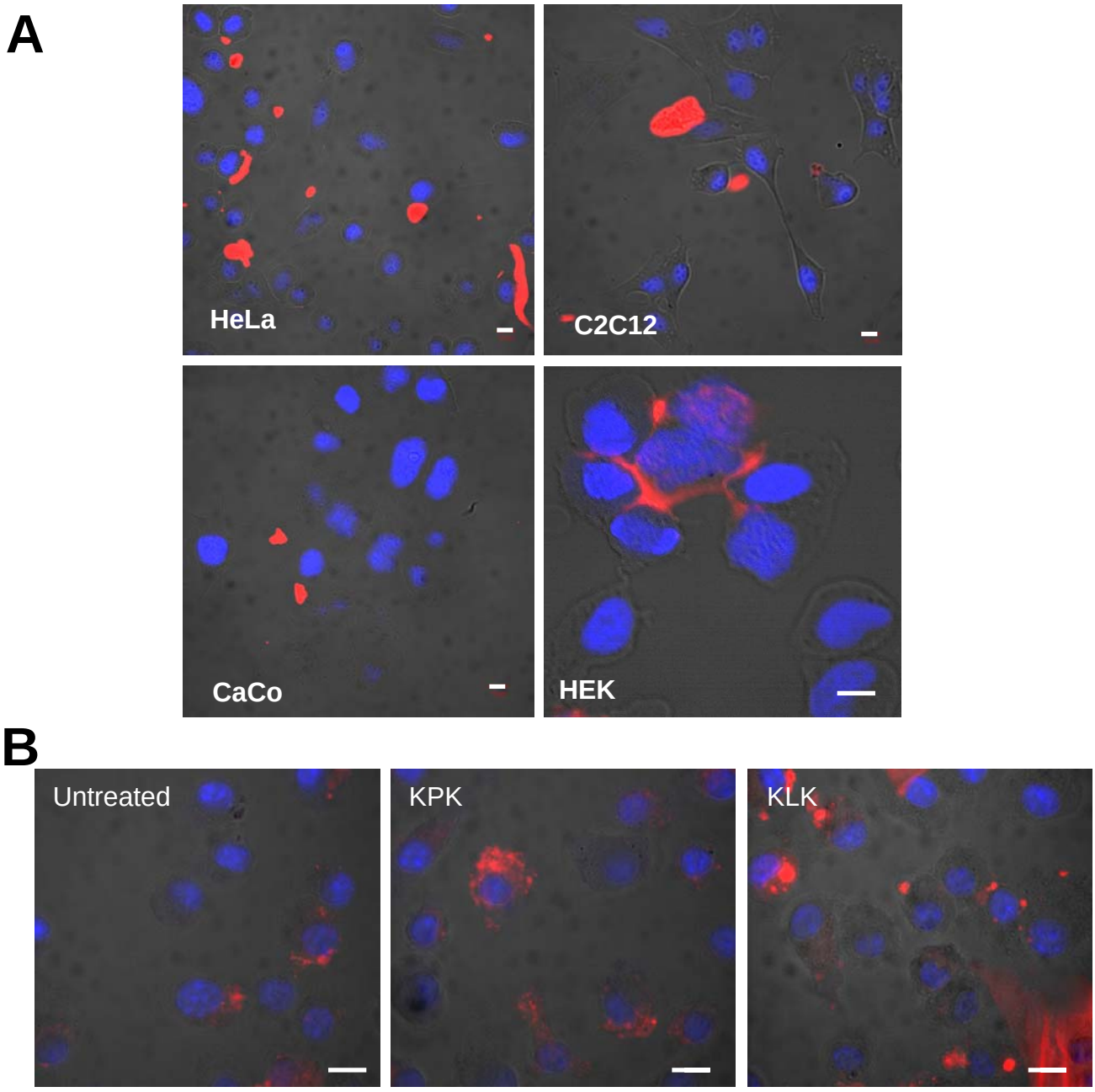


**Figure 23. ODN1a uptake of various cell types**

(A) ODN1a-Cy5 (red) and KLK were administered to HELA-, C2C12-, CaCo- and HEK-cells for 60 minutes before the cells were fixed nuclei were stained with DAPI (blue). Cells were monitored by laser confocal imaging. (B) ODN1a-Cy5 was administered to the mouse bone marrow derived macrophages in presence or absence KLK/KPK. After 60 minutes the cells were fixed and the nuclei were stained with DAPI. Bars represent 10 µm.

23B). Using the endosomal marker FM1-43 we could proof a clear localization of ODN1a endosomal vesicles of macrophages (Figure 24).

## 4.2.2. The cellular fate of KLK

KLK is essential for the formation of a stable complex at the injection site. This depot formation is a key factor in the stimulation of the immune system. Further, as demonstrated above, KLK also increases the endocytic uptake of ODN1a into dendritic cells. We have seen that KLK/ODN1a-complexes interact with the cell membrane and are then taken up and that ODN1a-Cy5 can be found in early and late endosomes as well as in the endoplasmic reticulum. As a next step we examined the fate of KLK during this process by using FITC-labelled peptide.

### 4.2.2.1. KLK is not taken up into DCs

Interestingly when administered to DCs we can microscopically not observe any uptake of KLK into the cells. KLK readily stains the plasma membrane but is not found within endosomes or other cytoplasmic structures (Figure 25A).

In a further experiment we added a mixture of KLK-FITC/ODN1a-Cy5 to the cells. Complexes appear yellow and are found in close contact with the cell membrane (Figure 25B, arrows). During the process of endocytosis the complex dissociates and only ODN1a is taken up into the cell (Figure 25B, arrowheads).

To prove this contact loss between the adjuvant components upon internalization of the nucleotide, fluorescence resonance energy transfer (FRET) experiments were performed using TAMRA-labelled KLK and Cy5-labelled ODN1a. This microscopy technique measures the proximity of two fluorophores and is often used to determine when and where two or more biomolecules interact within their physiological surroundings. As energy transfer occurs over distances of 1-10 nm, a FRET signal corresponds to a particular location of two biomolecules. The measurement offers an additional distance accuracy surpassing the optical resolution (~0.25 mm) of the light microscope. The average FRET value between ODN1a-Cy5 and KLK-TAMRA on a glass slide was 8.8% (Figure 25C, Bar 1). Here, the FRET value was concentration dependent. At a concentration ratio (cr) of ODN1a-Cy5 to KLK-TAMRA of <10 the FRET value was 6.9 %, at cr > 10 10.8 %, (data not shown). No FRET was observed between KLK-TAMRA and Cy5 only (fluorochrome without the nucleotide), suggesting that the FRET shown in Figure 25C was not due to the high concentration of the labelled

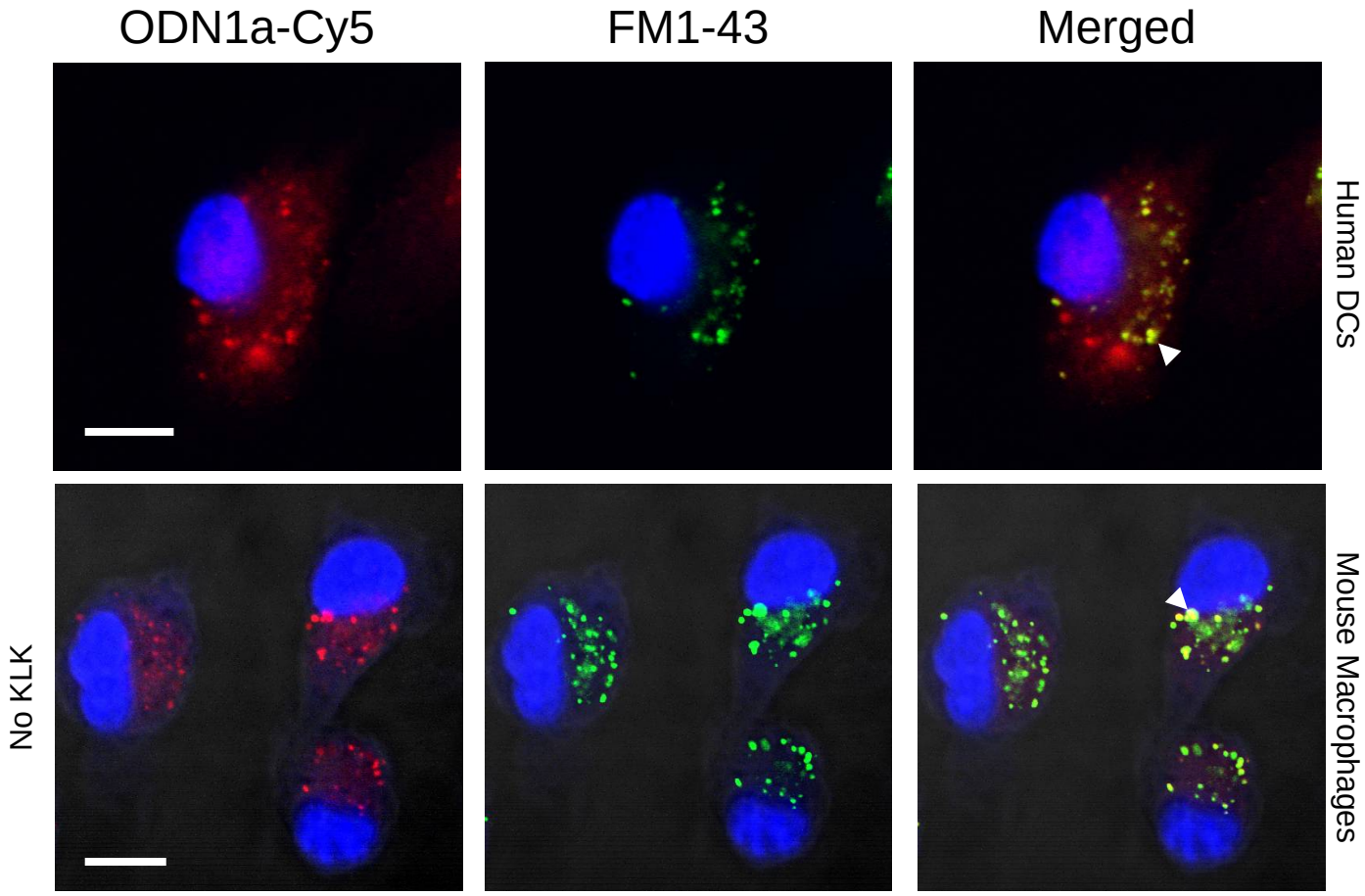


**Figure 24. Comparison of endosomal ODN1a uptake by dendritic cells and macrophages**

Immature human monocyte derived DCs and mouse bone marrow derived macrophages were exposed to ODN1a-Cy5 (red) in presence of KLK (DCs) or ODN1a-Cy5 alone (macrophages). Endosomes were stained using FM1-43 (green). After 60 minutes cells were fixed and nuclei were stained with DAPI (blue). Samples were analysed by laser confocal imaging. White arrowheads indicate ODN1a-Cy5 co-localizing with FM1-43. Bars represent 10 µm.

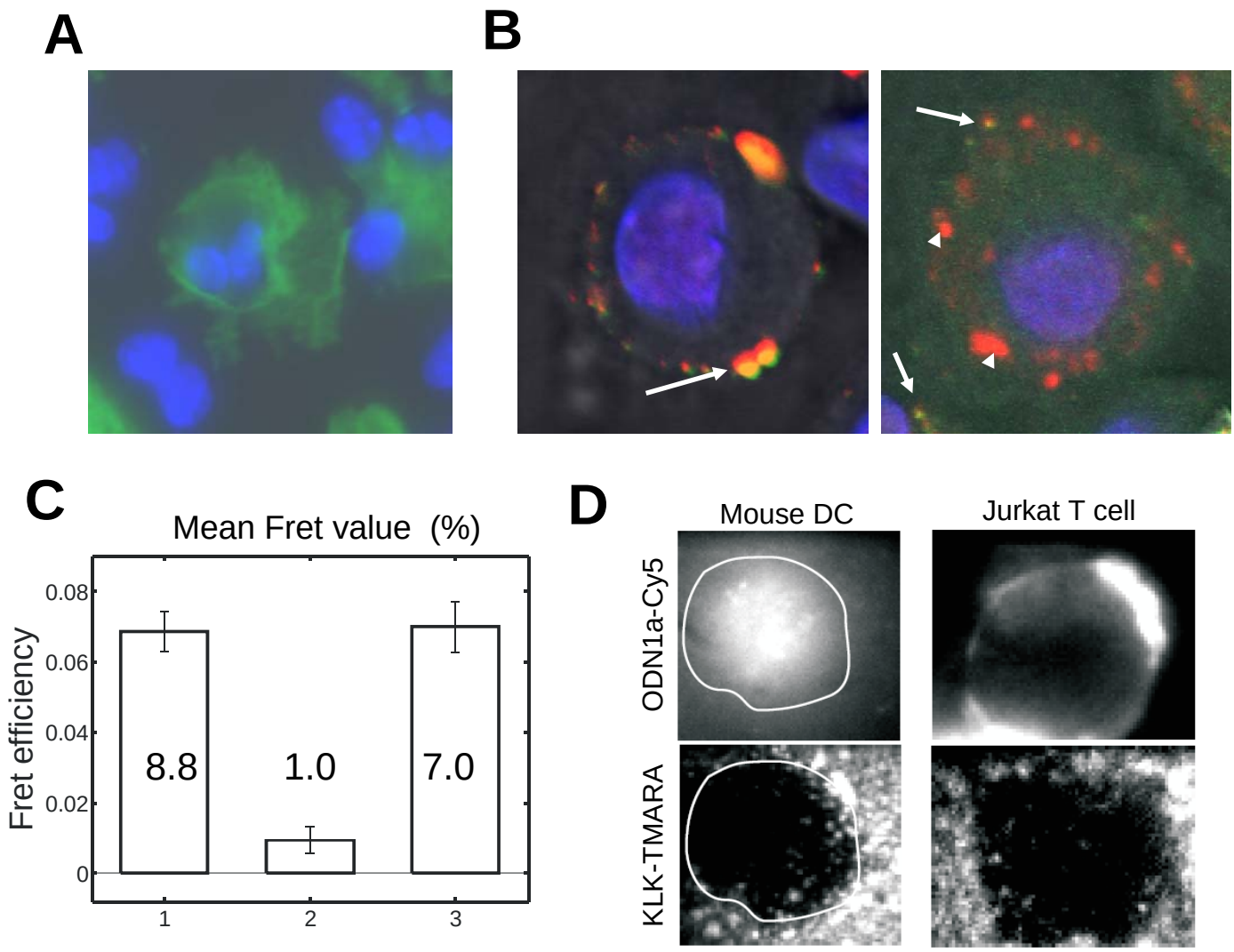


**Figure 25. KLK is not internalized by dendritic cells**

(A) KLK-FITC (green) was administered to immature human monocyte derived DCs and cells were monitored with fluorescence microscopy. (B) ODN1a-Cy5 (red) was mixed with KLK-FITC (green) and administered to immature humane monocyte derived DCs. Cells were fixed and the nuclei were stained with DAPI (blue). Samples were analysed using laser confocal imaging. Arrows point to KLK and ODN1a double positive complexes. Arrowheads indicate ODN1a positive vesicles. (C) Jurkat T cells were exposed to ODN1a-Cy5 and analyzed for FRET as described in Material and Methods. ODN1a-Cy5 and KLK-TAMRA (1), Cy5 and KLK-TAMRA on a glass slide (2), extracellular FRET signal average efficiency (3). (D) Fluorescent images of a Jurkat T cell and a mouse bone marrow derived dendritic cell channeled to detect ODN1a-Cy5 and KLK-TAMRA emission signals. The contour of the mouse DC is outlined in the figure for better orientation.

components. In a next step, the FRET value between nucleotide and peptide was measured in presence of Jurkat T cells. After incubation of the cells with both substances, FRET was calculated in the extracellular space and within the cells. In the extracellular space the average FRET of 7 % was similar to the measurements without cells (6.9 % for cr <10; Figure 25A, Bar 3). Since no intracellular FRET intensity was observed, we attempted to obtain fluorescent images of Jurkat T cells exposed to ODN1a-Cy5 and KLK-TAMRA. As demonstrated for other cells (Figure 23A), no uptake of ODN1a-Cy5 could be shown. This result explained why no FRET signal could be measured within these cells. Despite of multiple attempts, it was not possible to detect FRET using dendritic cells, but fluorescence imaging of these cells clearly revealed ODN1a localization within the cell and – similarly to Jurkat T cells – KLK remained outside (Figure 25D).

Together these data favour the assumption that ODN1a is internalized by DCs while KLK remains localized at the cell periphery.

# 4.3. Antigen uptake

IC31® is used as an adjuvant to stimulate the immune reaction against co-injected antigens and to modulate this response to the desired way. As we have already dissected the fate of the two adjuvant-components, our attention turned to the antigen uptake.

## 4.3.1. OVA-FITC

Fritz et al. presented clear data that KLK entraps the antigen at the injection site and enhances the adaptive immunity to co-injected antigens (Fritz et al., 2004). Our aim was to examine, whether KLK stimulates the uptake of the model antigen OVA-FITC (FITC labelled Ovalbumin) in comparison with ODN1a-Cy5 into DCs. 10 μg/ml OVA-FITC was administered directly or after mixing with 10 nmole/ml KLK to immature mouse bone marrow derived DCs. The aggregation of KLK and OVA-FITC subducts free antigen from the medium and therefore the general staining of the cells with OVA-FITC is higher in KLK-free samples. It is seen that in special proximity to KLK/OVA-FITC aggregates, DCs show increased OVA-FITC uptake (Figure 26A).

To compare the uptake of OVA-FITC and ODN1a-Cy5, both were premixed with KLK and added to the cells. Interestingly, although the antigen and the nucleotide show a vesicular localization after 1 hour and some vesicles contain both fluorescent components, not all are colocalizing (Figure 26B, white and black arrows). This suggests that the uptake of ODN1a and antigen are mediated by identical as well as distinct internalization routes.

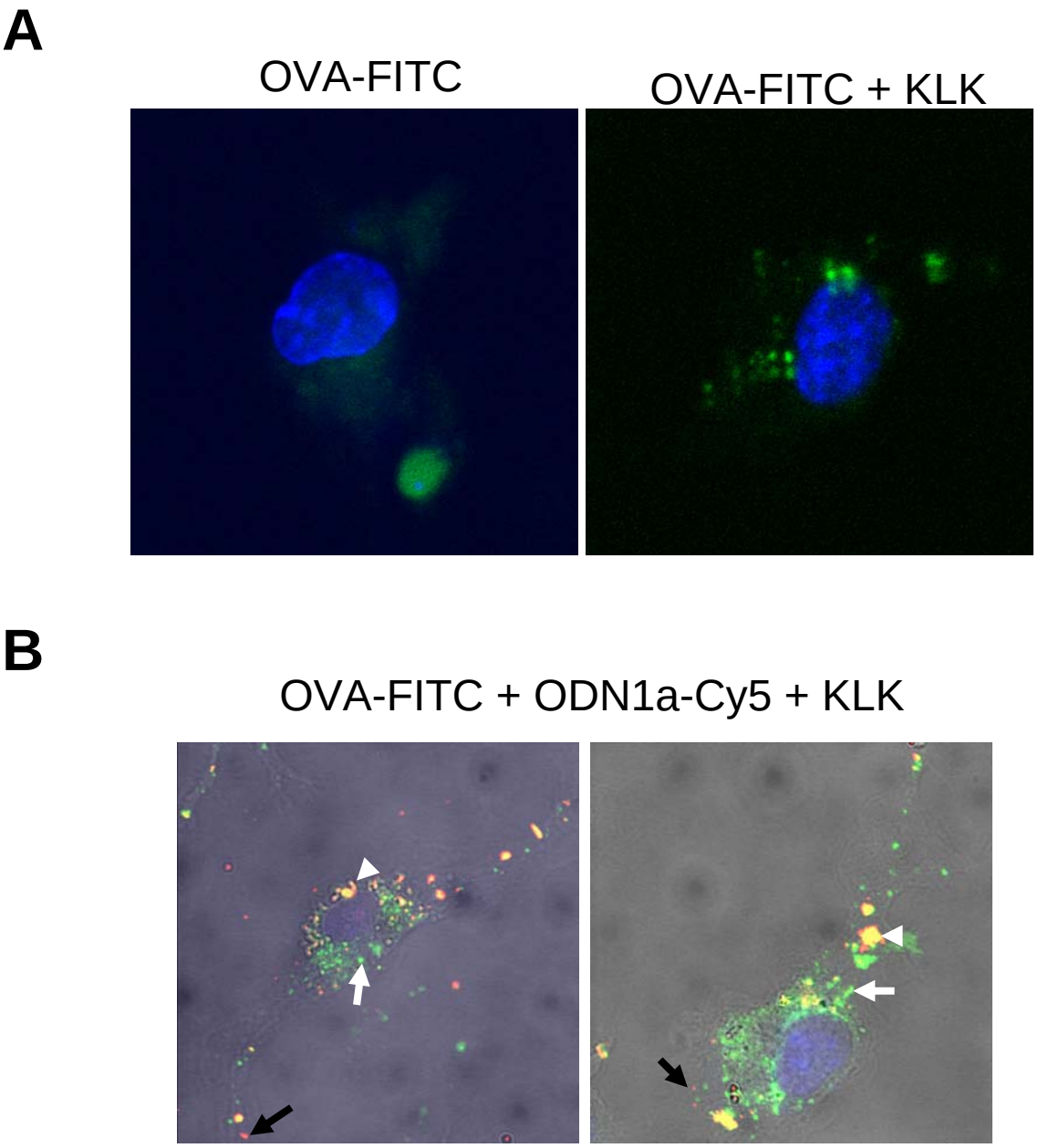


**Figure 26. Simultaneous uptake of antigen and ODN1a by dendritic cells**

Laser confocal images of immature mouse bone marrow derived DCs. OVA-FITC (green) was administered in presence or absence of KLK (A) or in presence of ODN1a-Cy5 (red) and KLK(B). After 60 minutes the cells were fixed and the nuclei were stained with DAPI (blue). White arrowheads point to ODN1a and OVA double positive, white arrows to OVA and black arrows to ODN1a positive structures.

# 5. Discussion

In the recent years numerous studies have been published concerning the profound immuno-stimulatory effect of IC31® (Agger et al., 2006; Schellack et al., 2006; Lingnau et al., 2007; Kamath et al., 2008; Riedl et al., 2008). Although, broader knowledge has become available about the immuno-modulatory mechanisms of the TLR9 agonist ODN1a, our understanding of how the peptide component KLK contributed to the immunological effects of IC31® remained elusive. Therefore, our first aims were to shed light on the physico-chemical parameters of KLK, including membrane interacting properties, conformational propensities as well as its direct effects on various model membrane systems. It has been shown that ODN1a, when it is injected alone dissipates quickly from the site of injection in mice. KLK is necessary and sufficient to form a stable depot with ODN1a at the injection site (Schellack et al., 2006). Although as positively charged as KLK, the immunologically inactive derivative KLKLLPLLKLK (KPK) does not induce this depot formation with ODN1a. It is therefore likely that the different effects are caused by alternative peptide structures which might be linked to the environment-dependent conformational properties of the peptide.

An equally exciting question was to understand how KLK mediated the delivery of ODN1a into the primary target cell of IC31®. Internalization of ODN1a by dendritic cells is considerably up-regulated by KLK, a phenomenon that was cell specific, peptide specific and linked to endocytotic activity. Thus, we have carefully dissected mechanisms linked to interaction of KLK/ODN1a comlex with DCs, to endocytotic uptake routes, cytoplasmic distribution and receptor-ligand binding.

# 5.1. Conformational properties of KLK

Using circular dichroism measurements we observed, that comparable to many other peptides KLK and KPK exhibited a random coil structure in water (Seelig, 2004). Administration of the detergent SDS leads to immediate transition of KLK to a β-sheet conformation (Figure 8A). To create a membrane-mimicking environment, SUVs containing uncharged lipids, were included in the measurement. KLK readily transited to a β-sheet conformation (Figure 7B). Having the length of KLK in mind, we considered this structure as a consequence of intermolecular interactions. This β-sheeted molecular aggregate most probably represents the conformational state in which KLK forms large complexes with ODN1a (see below). Considering the well-known charge attraction of cationic peptides to negatively charged moieties of membranes, increasing amounts of negatively charged SUVs were administered. In this experiment, an additional, β-sheet to α-helical conformational-transition of KLK could be observed (Figure 7C). After administration of the same concentration of uncharged SUVs, KLK did not exhibit an alpha-helical conformation (data not shown). This supports a three-step molecular recognition mechanism similar to that suggested for the main peptide component of Alzheimer plaques, βAP (1-40) (Terzi et al., 1997; Meier and Seelig, 2007). In the absence of lipids the βAP peptide displays a random coil conformation. Administration of unilamellar vesicles composed of neutral POPC and negatively charged POPG (3:1) to βAP (1-40) induces a dramatic spectroscopic shift leading to a CD-spectrum with 70% β-structure. As for KLK, a second transition is observed if increasing amount of negatively charged POPG are added (Terzi et al., 1997). The middle leucine-to-proline substitution in KPK completetly abolished the formation of conformational transitions (Figure 7 and 8). To further analyze alpha-helical propensity of KLK, 2,2,2-trifluoroethanol (TFE) was administered to the peptide. TFE was demonstrated to stabilize alpha helical structures in proteins and peptides (Goodman et al., 1969). After administration of TFE, KLK readily showed a direct transition from random-coil to alpha-helix, indicating a high potential to form a helix, whereas KPK was not affected by the addition of TFE (Figure 8B).

We assume that our CD measurements detect equilibria between the possible conformations at a given condition. Hydrophobic environment or administration of TFE shifts this equilibrium towards β-sheet and α-helix, respectively. Further, we demonstrated that phosphate buffer strongly stabilized the beta-sheet conformation of KLK in water and in the presence of TFE (Figure 8C and 8F). This effect needs to be studied in more detail. In any

case, we were able to demonstrate various conformational statuses of KLK and showed that this peptide can quickly switch its conformational properties upon various environmental stimuli.

## 5.2. Membrane interacting properties of KLK

Due to their positively charged, amphipathic structures, a fundamental component of the mode of action of cationic antimicrobial peptides, such as KLK, was proposed to be their membrane-active property. Using sub-mitochondrial particles (SMPs) we demonstrated that KLK interacts with membrane vesicles without pore formation (Figure 10C). Mass spectrometric and microscopical analysis of the vesicular sub-fractions indicated that KLK preferentially stayed associated with the vesicular membrane (Figure 11). As SMPs harbour various inner-mitochondrial membrane proteins on their surface, it was important to study, whether these proteins play a role in the membrane-interacting properties of KLK. Alvarez-Bravo et al. demonstrated lytic activity of KLK measuring glucose-release from artificial liposomes (Alvarez-Bravo et al., 1994). In our experiments we used giant unilamellar vesicles derived from asolectin lipids by dialysis. As observed in the SMP-experiments, we found that the interaction of KLK with the artificial membrane occurs without release of vesicular content (Figure 10E). Therefore, membrane interaction of KLK is independent of membrane proteins and receptors.

Because of the relatively simple, homogeneous and well described membrane model offered by human erythrocytes and erythrocyte ghosts (Dodge et al., 1962), we tested the effect of KLK and KPK on the osmotic fragility of these cells as well as on their fluidity parameters. Erythrocytes and erythrocyte ghosts possess highly negatively charged sialic acid-based carbohydrate moieties (Varki, 2009) and represent therefore an ideal model to study the earlier proposed general strong charge attraction-based mechanisms in KLK action. Anisotropy-measurements of human erythrocyte ghosts revealed a strong effect of KLK but not KPK as a dramatic increase in DPH and TMA-DPH related anisotropy was seen in KLK treated samples (Figure 12B). This effect indicates a strong increase in microviscosity (or decrease in fluidity) within both the core and surface compartments of the membrane. On the other hand, the osmotic resistance was not affected by the administration of KLK confirming the lack of pore formation (Figure 12A).

One aspect of the biocydal effects of AMPs is the binding to membranes where the induce pore formation or changes of the membrane structure which finally leads to lysis of the

pathogen (Hof et al., 2001). The observed effects of KLK let us speculate whether these are also associated with ultra-structural changes of the membranes. Therefore, sub-mitochondiral particles were examined in the electron-microscope after administration of KLK or KPK. KLK induced a striking reduction in vesicle size with simultaneous enrichment of the debris-like background material. The vesicles appeared ragged-edged and often with reduction of osmophilicity in their membranes (Figure 13A). A generally disordered bilayer structure could be observed in larger magnifications, a morphology that was characteristic of nearly all vesicles in the field of view (Figure 13B). None of these effects were observed in KPK treated samples (Figure 13A). We further demonstrated that KLK strongly disturbs the membrane structure of ECV-cells. Human monocyte-derived DCs, the target cells of IC31® in the immune system also show a structural effect upon KLK administration. Here, we could observe protrusion of dendrites (Figure 14).

We assume that KLK is generally attracted to the membrane due to its charge. At the vicinity of the membrane and under specific lipid-to-peptide stoichiometric conditions KLK undergoes the previously observed conformational transitions and intercalates into the lipid bilayer. Taking the length of KLK into consideration, the peptide is too short to span the membrane. An alternative model for the interaction is the carpet-model. Here, the AMP associates with the membrane surface, parallel to it, with the hydrophilic face oriented toward the water phase. The peptide intercalation into the phospholipid head groups corresponds to an insertion of a cone-shaped molecule into the membrane (Figure 2E). Similar effects can be seen with the yeast Yop1p and Rtn1p (Khandelia et al., 2008). These molecules are important regulators of membrane curvature of the endoplasmic reticulum. The application of the carpet-model would offer an explanation of the effects seen after KLK administration. Unequal distribution of KLK at both sides of the membrane bilayer and the intercalation into the membrane could therefore lead to a disturbance of the natural membrane curvature and induce a disordered membrane structure as observed in the electron microscope.

## 5.3. Complex formation of KLK with ODN1a

Due to its backbone, the nucleotide ODN1a is negatively charged. After administration of a positively charged peptide we can expect charge interaction and formation of various size aggregates in solution. This theory was tested by a gel-retardation assay (Figure 15A). Interestingly, although KLK and KPK have the same amount of positively charged amino acids KLK but not KPK aggregated with ODN1a (Figure 15). The intermolecular beta-sheet

conformational capacity of KLK is the most obvious feature to explain this aggregation phenomenon. Thus, the potential of conformational transitions is a precondition for the observed complex formation and explains the inability of KPK to aggregate with ODN1a. Taking into account the multiple conformational transitions of KLK we speculate that peptide and nucleotide accumulate in a colloid-like complex where the β-sheet aggregates between ODN1a and KLK in the hydrophobic core are surrounded by random coil molecules towards the solvent-sorrounded surface of the aggregate. A dynamic equilibrium is assumed between the peptide pools of various conformational stages (Figure 27).

The determination of the particle size distribution revealed distinct size-fractions of the nucleotide/KLK complexes. The majority of the complexes exhibited a size between 70 μm and 250 μm. It is important to mention that the aggregates observed in the following microscopy experiments show the same diameter and therefore confirm these measurements.

# 5.4. Interaction of IC31® with dendritic cells

After our initial experiments revealing the structural features of KLK and its membrane interacting properties, we were interested to study the fate of the two components of IC31® in the presence of the target cells, the DCs. We have demonstrated that the presence of KLK increased the uptake of ODN1a into immature human and murine dendritic cells (Figure 16). This uptake was energy-dependent, as incubation on ice prevented ODN1a uptake. We assumed that the uptake of the peptide was via cellular endocytotic mechanisms. We observed rapid accumulation of ODN1a within the cell with a peak at 60 minutes. Afterwards the ODN1a signal diminished probably due to degradation of the nucleotide (Figure 17).

KLK/ODN1a based aggregates accumulate at the cell surface as large complexes spreading over numerous cells (Figure 17). Live cell laser confocal fluorescence imaging revealed dynamic interaction of the DCs with the complexes in the medium (Figure 18). Some complexes stay in close contact with its initial docking site at the DC surface, while others detach after staying associated with the cell for various length of time. These observations point to a possible dependence on specific membrane regions or even micro-domains to create a stable interaction between IC31® and a dendritic cell. Thus we hypothesize that at sites of high negative surface charges, the colloid-like complex of KLK and ODN1a is attracted to the membrane by the free positive charges of the proximal random coil molecules. These can interact with the membrane as demonstrated before and bind the whole complex to the cell-surface.

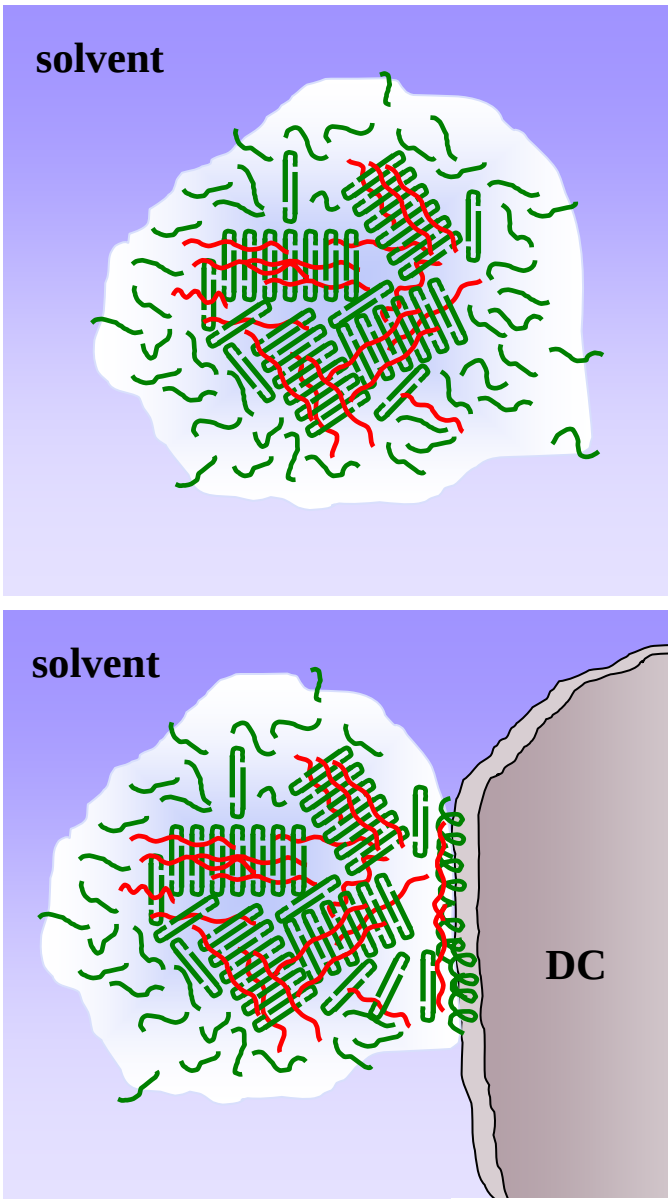


**Figure 27. Model of colloid-like aggregate formation of KLK and ODN1a**

In presence of ODN1a KLK forms a colloid-like complex in solvent. Structured interaction of KLK and ODN1 in the core allows assembly of large aggregates. In the periphery unstructured peptide is able to undergo conformational transitions and to interaction with membranes. Between core and periphery a dynamic equilibrium exists, enabling aggregate transformation and movement of peptide and nucleotide.

# 5.5. Cellular uptake of ODN1a

Multiple cellular uptake-pathways exist for the delivery of cargo molecules into the cell. All pathways except macrophagy converge at the level of early endosomes (for review see Mellman, 1996; Spang, 2009). We demonstrated that ODN1a is taken up via a mechanism that route the oligonucleotide to early and late endosomes (Figure 19). ODN1a eventually reaches compartments that are positive for TLR9 (Figure 22).

It has still to be observed whether the uptake is pathway specific. The literature offers at least three different possibilities, how ODN1a might be internalized. The function of KLK was initially claimed to be dependent on calreticulin (Cho et al., 1999), suggesting a receptor mediated uptake of ODN1a bound to KLK via calreticulin that involves macropinocytosis (Ogden et al., 2001). On the other hand, it has been demonstrated that the uptake of antigens or peptides via macropinocytosis does not necessarily need a specific receptor (Sallusto et al., 1995), indicating, that the uptake of ODN1a would be receptor independent. Further, we have clear evidence that the membrane interacting properties of KLK do not depend on the presence of any membrane protein (Figure 10E). Additionally, the co-localization with TfR points to the classical route via clathrin coated pits.

We suggest an alternative model. The membrane interacting properties of KLK assure a long lasting attachment of ODN1a at or in close vicinity to the plasma membrane. All mechanisms involving membrane turnover would now allow an uptake of the nucleotide. Therefore, the uptake is not pathway specific but appears due to general membrane turnover that is associated with all endocytic routes. This theory would also explain the localization of ODN1a within the endoplasmic reticulum (Figure 20 and 21), which would be contradictory to the co-localization in the early endosomes. It has recently been demonstrated that phagosomes of macrophages (Gagnon et al., 2002) and dendritic cells (Guermonprez et al., 2003) fuse during the process of cross presentation with the endoplasmic reticulum.

Preliminary experiments blocking the dynamine-dependent uptake routes with Dynasore and the dynamine independent pathways with chlorpromazine showed that inhibition of the specific pathways does not notably abolish the uptake of ODN1a (unpublished data) suggesting that ODN1a is taken up via multiple routes. Blocking of one particular uptake route might be compensated by the other internalization mechanisms.

If our assumption is correct, cells with low membrane turnover capacity should exhibit decreased ODN1a uptake. Thus, we administered labelled IC31® to various cell types (Figure 23). HELA-, C2C12-, CaCo- and HEK-cells did not take up the nucleotide component in

detectable amounts. Macrophages on the other hand displayed ODN1a uptake. Interestingly, the uptake was not dependent on the presence of KLK as it also occurred in untreated and KPK-treated samples. The difference between dendritic cells and macrophages regarding ODN1a uptake suggests distinct mechanisms of nucleotide uptake. To what extend the cell type specific macro-pinocytotic (Sallusto et al., 1995) and phagocytotic processes (for review see Savina and Amigorena, 2007) contribute to the observed difference, remains elusive.

## 5.6. The cellular fate of KLK

While ODN1a was taken up via various routes, we showed that at least the vast majority of KLK stayed attached to the membrane (Figure 25). Thus the peptide-nucleotide complex has to dissolve rapidly upon internalization. Taken together with the earlier findings, we assume that the alpha-helical conformation is induced at distinct negatively charged loci at the cell membrane. Recent data show that KLK is subsequently intercalating with the negatively charged inner leaflet of the plasma membrane (Weghuber et al., unpublished data), with a simultaneous disruption of the aggregates and internalization of ODN1a into distinct vesicular compartments.

The accumulation of KLK at the inner leaflet of the membrane has been demonstrated to induce a halt in the recycling of GPI-anchored proteins and the GEEC-linked pathway (Weghuber et al., unpublished data). This may induce a compensatory reaction increasing the turnover of other pathways and thus allow the efficient loading of DC cytoplasm with the immuno-stimulatory ODN1a.

## 5.7. Uptake of OVA-protein

It has been demonstrated that KLK induced the loading of APCs with various model antigens (Fritz et al., 2004). Therefore, it was our interest to see if we could reproduce this finding in our system and whether we can describe an effect of KLK on the antigen uptake of dendritic cells. When KLK and OVA-protein are administered to DCs, in the microscope a complex formation comparable to KLK/ODN1a can be observed in the cell vicinity. The aggregation of KLK and OVA captured free antigen from the medium and therefore the general staining of the cells with OVA-FITC is higher in KLK-free samples. But cells close to KLK/OVA complexes took up higher amounts of antigen than the cells in the KLK-free samples (Figure

26A). Thus, we were able to demonstrate that, when an antigen is present, efficient uptake is possible simultaneously with the KLK induced up-regulation of ODN1a internalization.

## 5.8. Working model

We suppose that KLK/ODN1a, KLK/OVA and KLK/ODN1a/OVA form a colloid-like complex in the vicinity of cells (Figure 27). The complex core is formed by a dynamic equilibrium between KLK, ODN1a and antigen. We assume that in contact with the negative charged ODN1a KLK exhibits a conformation which allows the formation of large aggregates, most probably β-sheet, but conformational transitions and exchange of molecules between core and periphery are still possible. At the periphery of the colloid-like complex we expect unbound KLK which is able to interact due to conformational changes with cell membranes. Upon charge attraction between negative charged cell surface and positive charged KLK, the complex attaches to the membrane. Here, KLK undergoes the observed conformational transition from β-sheet to α-helix and therefore stabilizes the adherence.

The long lasting attachment brings ODN1a and antigen in close proximity to the plasma membrane. Thus, membrane engulfment and pit formation during general membrane turnover leads to uptake of both components via different endocytic routes into early and late endosomes as well as tubular lysosomal compartments and the endoplasmic reticulum (Figure 28). Larger aggregates as shown in Figure 21 might be taken up via phagocytosis explaining the localization of ODN1a within the ER (Guermonprez et al., 2003). Other pathways lead to uptake into early and late endosomes and allow co-localization with TLR9 in tubular lysosomal compartments.

After KLK induced uptake, ODN1a and OVA do no fully co-localize within the cell suggesting identical as well as distinct internalization routes (Figure 26B). This further supports our model as we hypothesize that the cargo is not selected but taken up at random. The fate of KLK has to be further clarified. Why KLK is not taken up like OVA and ODN1a, and how it can avoid engulfment into endocytic vesicles has to be analyzed in more detail.

Nevertheless, our results make a significant contribution to the better understanding of the molecular action of IC31®. For the first time the functions of both the individual KLK and ODN1a molecules as well as their combination (IC31®) are understood in more details. With the work presented in this thesis IC31® becomes one of the best-understood adjuvants in current vaccine research.

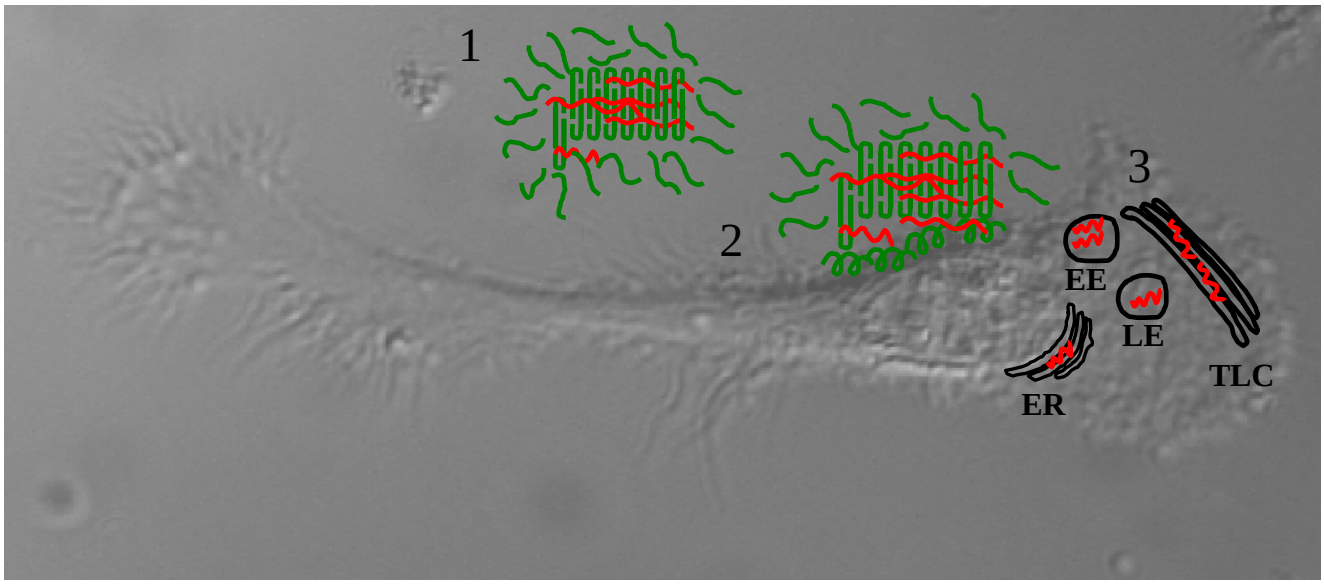


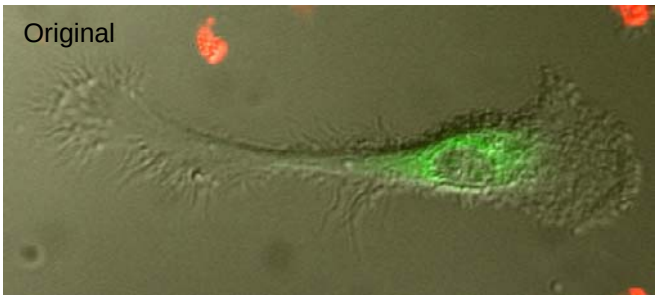


KLK (random coil)

KLK (b-sheet)

KLK (a-helix)

ODN1a

**Figure 28. Model of ODN1a internalization**

Colloid-like aggregate of KLK and ODN1a in the cell vicinity (1) is attracted to the plasma membrane due to negative surface charge. Conformational transition of KLK stabilizes the interaction of the aggregate with the membrane (2). Due to membrane turnover ODN1a is internalized via different endocytic routes and localizes within early and late endosomes (EE and LE, respectively), in tubular lysosomal compartments (TLCs) and the endoplasmic reticulum (ER).

# 6. Abbreviations

| | |
|---|---|
| AMP | Antimicrobial peptide |
| AP | Adaptor protein |
| APC | Antigen presenting cell |
| CAMP | Cationic antimicrobial peptide |
| CCL | Chemokine (C-C motif) ligand |
| CCP | Clathrin coated pits |
| CCR | Chemokine (C-C motif) receptor |
| CD | Clusters of differentiation |
| cDC | Conventional dendritic cell |
| CI | Clathrin independent |
| CLIC | Clathrin- and dynamine-independent carriers |
| Cr | Concentration ratio |
| CTL | Cytolytic T lymphocytes |
| DAMP | Danger associated molecular pattern |
| DC | Dendritic cell |
| DNA | Deoxyribonucleic acid |
| DPH | Diphenylhexatriene |
| DRM | Detergent resistant membrane |
| ECM | Extracellular matrix |
| ECV | Endosomal carrier vesicles |
| EE | Early endosome |
| ER | Endoplasmic reticulum |
| ERAAP | ER aminopeptidase associated with antigen processing |
| FRET | Fluorescence resonance energy transfer |
| G-CSF | Granulocyte colony stimulating factor |
| GEEC | GPI-AP enriched early endosomal compartment |
| GEF | Guanin exchange factor |

| | |
|---|---|
| GPI-AP | Glycosyl phosphatidylinositol-anchored proteins |
| HIV | Human immunodeficiency virus |
| HPV | Human papillomavirus |
| ICAM | Intercellular adhesion molecule |
| iDC | Immature dendritic cell |
| IFN | Interferon |
| Ig | Immunoglobulin |
| IL | Interleukin |
| ISCOM | Immune-stimulating complex |
| IS | Immunological synapse |
| KLK | KLKLLLLLKLK |
| KPK | KLKLLPLLKPK |
| LC | Langerhans cell |
| LFA | Leucocyte function associated antigen |
| LN | Lymph node |
| LPS | Lipopolysaccharide |
| LRR | Leucine rich repeat |
| MIIC | MHC II-enriched compartment |
| MHC | Major histocompatibility complex |
| mDC | Myeloid dendritic cell |
| moDC | Monocyte-derived dendritic cell |
| MVB | Multivesicular bodies |
| MyD88 | |
| NMR | Nuclear magnetic resonance |
| NLR | Nucleotide domain leucine-rich repeat containing receptor |
| NKC | Natural killer cell |
| NKTC | Natural killer T cell |

| | |
|---|---|
| ODN | Oligodoxynucleotides |
| ODN1a | Oligo-$(dIdC)_{13}$ |
| PAMP | Pathogen associated molecular pattern |
| PBFI | Potassium sensitive benzofuran isopthalate |
| PC | Phosphatidylcholin |
| pDC | Plasmacytoid dendritic cell |
| PE | Phosphatidylethanolamine |
| PI | Phosphatidylinositol |
| PKC | Protein kinase C |
| POPC | 1-palmitoyl-2-oleoyl-sn-glycero-3-phosphocholine |
| POPG | 1-palmitoyl-2-oleoyl-sn-glycero-3-phosphoglycerol |
| PRR | Pattern recognition receptor |
| PS | Phosphatidylserine |
| RE | Recycling endosome |
| RNA | Ribonucleic-acid |
| SCF | Stem cell factor |
| SM | Sphingomyelin |
| TAP | Transporter associated with antigen processing |
| TCR | T-cell receptor |
| TFE | 2,2,2-trifluoroethanol |
| TfR | Transferrin receptor |
| TGN | Trans golgi network |
| TLR | Toll like receptor |
| TMA-DPH | trimethylammonium-DPH |
| TNF | Tumor necrosis factor |
| VLP | Virus-like particle |
| VPS | Vacuolar protein sorting |

# 7. References


**Abrami, L., et al.** (2003). "Anthrax toxin triggers endocytosis of its receptor via a lipid raft-mediated clathrin-dependent process." J. Cell Biol. **160**(3): 321-328.

**Agger, E. M., et al.** (2006). "Protective immunity to tuberculosis with Ag85B-ESAT-6 in a synthetic cationic adjuvant system IC31." Vaccine **24**(26): 5452-60.

**Agostini, L., et al.** (2004). "NALP3 Forms an IL-1[beta]-Processing Inflammasome with Increased Activity in Muckle-Wells Autoinflammatory Disorder." Immunity **20**(3): 319-325.

**Aguilar, J. C. and E. G. Rodríguez** (2007). "Vaccine adjuvants revisited." Vaccine **25**(19): 3752-3762.

**Ajesh, K. and K. Sreejith** (2009). "Peptide antibiotics: An alternative and effective antimicrobial strategy to circumvent fungal infections." Peptides **30**(5): 999-1006.

**Akira, S. and H. Hemmi** (2003). "Recognition of pathogen-associated molecular patterns by TLR family." Immunology Letters **85**(2): 85-95.

**Akira, S. and K. Takeda** (2004). "Toll-like receptor signalling." Nat Rev Immunol **4**(7): 499-511.

**Alexopoulou, L., et al.** (2001). "Recognition of double-stranded RNA and activation of NF-[kappa]B by Toll-like receptor 3." Nature **413**(6857): 732-738.

**Alfonso, C. and L. Karlsson** (2000). "Nonclassical MHC class II molecules." Annu Rev Immunol **18**: 113-42.

**Almeida, J., et al.** (1975). "Formation of Virosomes from Influenza Subunits and Liposomes." The Lancet **306**(7941): 899-901.

**Alvarez-Bravo, J., et al.** (1994). "Novel synthetic antimicrobial peptides effective against methicillin-resistant Staphylococcus aureus." Biochem J **302 ( Pt 2)**: 535-8.

**Alvarez, D., et al.** (2008). "Mechanisms and Consequences of Dendritic Cell Migration." Immunity **29**(3): 325-342.

**Andreu, D. and L. Rivas** (1998). "Animal antimicrobial peptides: An overview." Peptide Science **47**(6): 415-433.

**Ariel Savina, S. A.** (2007). "Phagocytosis and antigen presentation in dendritic cells." Immunological Reviews **219**(1): 143-156.

**Asveld, L.** (2008). "Mass-vaccination programmes and the value of respect for autotonomy." Bioethics **22**(5): 245-257.

**Bals, R., et al.** (1999). "Augmentation of Innate Host Defense by Expression of a Cathelicidin Antimicrobial Peptide." Infect. Immun. **67**(11): 6084-6089.

**Banchereau, J., et al.** (2000). "Immunobiology of dendritic cells." Annu Rev Immunol **18**: 767-811.

**Banchereau, J. and R. M. Steinman** (1998). "Dendritic cells and the control of immunity." Nature **392**(6673): 245-252.

**Barbero, P., et al.** (2002). "Visualization of Rab9-mediated vesicle transport from endosomes to the trans-Golgi in living cells." J. Cell Biol. **156**(3): 511-518.

**Barral, D. C., et al.** (2008). "CD1a and MHC Class I Follow a Similar Endocytic Recycling Pathway." Traffic **9**(9): 1446-1457.

**Barton, G. M., et al.** (2006). "Intracellular localization of Toll-like receptor 9 prevents recognition of self DNA but facilitates access to viral DNA." Nat Immunol **7**(1): 49-56.

**Bazin, H.** (2003). "A brief history of the prevention of infectious diseases by immunisations." Comparative Immunology, Microbiology and Infectious Diseases **26**(5-6): 293-308.

**Bechinger, B.** (1997). "Structure and dynamics of the M13 coat signal sequence in membranes by multidimensional high-resolution and solid-state NMR spectroscopy." Proteins: Structure, Function, and Genetics **27**(4): 481-492.

**Bechinger, B.** (1997). "Structure and Functions of Channel-Forming Peptides: Magainins, Cecropins, Melittin and Alamethicin." Journal of Membrane Biology **156**(3): 197-211.

**Bechinger, B.** (1999). "The structure, dynamics and orientation of antimicrobial peptides in membranes by multidimensional solid-state NMR spectroscopy." Biochimica et Biophysica Acta (BBA) - Biomembranes **1462**(1-2): 157-183.

**Bechinger, B. and K. Lohner** (2006). "Detergent-like actions of linear amphipathic cationic antimicrobial peptides." Biochimica et Biophysica Acta (BBA) - Biomembranes **1758**(9): 1529-1539.

**Bettelli, E., et al.** (2006). "Reciprocal developmental pathways for the generation of pathogenic effector TH17 and regulatory T cells." Nature **441**(7090): 235-238.

**Betz, W. J., et al.** (1996). "Imaging exocytosis and endocytosis." Current Opinion in Neurobiology **6**(3): 365-371.

**Beutler, B.** (2004). "Inferences, questions and possibilities in Toll-like receptor signalling." Nature **430**(6996): 257-263.

**Bogner, P., et al.** (2002). "Steady-state volumes and metabolism-independent osmotic adaptation in mammalian erythrocytes." European Biophysics Journal **31**(2): 145-152.

**Bron, R., et al.** (1993). [23] Preparation, properties, and applications of reconstituted influenza virus envelopes (virosomes). Methods in Enzymology, Academic Press. **Volume 220:** 313-331.

**Brossard, C., et al.** (2005). "Multifocal structure of the T cell - dendritic cell synapse." European Journal of Immunology **35**(6): 1741-1753.

**Bryant, P. and H. Ploegh** (2004). "Class II MHC peptide loading by the professionals." Current Opinion in Immunology **16**(1): 96-102.

Bryant, P. W., et al. (2002). Proteolysis and antigen presentation by MHC class II molecules. Advances in Immunology, Academic Press. **Volume 80:** 71-114.

**Bulet, P., et al.** (2004). "Anti-microbial peptides: from invertebrates to vertebrates." Immunological Reviews **198**(1): 169-184.

**Buonaguro, L., et al.** (2006). "Baculovirus-Derived Human Immunodeficiency Virus Type 1 Virus-Like Particles Activate Dendritic Cells and Induce Ex Vivo T-Cell Responses." J. Virol. **80**(18): 9134-9143.

**Burack, W. R., et al.** (2002). "Cutting Edge: Quantitative Imaging of Raft Accumulation in the Immunological Synapse." J Immunol **169**(6): 2837-2841.

**Buschle, M., et al.** (1997). "Transloading of tumor antigen-derived peptides into antigen-presenting cells." Proc Natl Acad Sci USA **94**.

**Campbell, J. B., et al.** (2000). "Chiropractors and Vaccination: A Historical Perspective." Pediatrics **105**(4): e43-.

**Castagnola, M., et al.** (2004). "A Cascade of 24 Histatins (Histatin 3 Fragments) in Human Saliva: SUGGESTIONS FOR A PRE-SECRETORY SEQUENTIAL CLEAVAGE PATHWAY." J. Biol. Chem. **279**(40): 41436-41443.

**Chaudhuri, R., et al.** (2007). "Downregulation of CD4 by Human Immunodeficiency Virus Type 1 Nef Is Dependent on Clathrin and Involves Direct Interaction of Nef with the AP2 Clathrin Adaptor." J. Virol. **81**(8): 3877-3890.

**Chavali, S. R., et al.** (1987). "An in vitro study of immunomodulatory effects of some saponins." Int J Immunopharmacol **9**: 675-683.

**Chen, Y., et al.** (2005). "Rational Design of Alpha-Helical Antimicrobial Peptides with Enhanced Activities and Specificity/Therapeutic Index." J. Biol. Chem. **280**(13): 12316-12329.

**Cheng, Z.-J., et al.** (2006). "Distinct Mechanisms of Clathrin-independent Endocytosis Have Unique Sphingolipid Requirements." Mol. Biol. Cell **17**(7): 3197-3210.

**Cho, J.-H., et al.** (1999). "Activation of human neutrophils by a synthetic anti-microbial peptide, KLKLLLLLKLK-NH via cell surface calreticulin." European Journal of Biochemistry **266**(3): 878-885.

**Cluff, C. W., et al.** (2005). "Synthetic Toll-Like Receptor 4 Agonists Stimulate Innate Resistance to Infectious Challenge." Infect. Immun. **73**(5): 3044-3052.

**Cox, J. C. and A. R. Coulter** (1997). "Adjuvants--a classification and review of their modes of action." Vaccine **15**(3): 248-256.

**Creusot, R. J. and N. A. Mitchison** (2004). "How DCs control cross-regulation between lymphocytes." Trends in Immunology **25**(3): 126-131.

**Cutts, F., et al.** (2007). "Human papillomavirus and HPV vaccines: a review." Bulletin of the World Health Organization **85**: 719-726.

**Damke, H., et al.** (1995). "Clathrin-independent pinocytosis is induced in cells overexpressing a temperature-sensitive mutant of dynamin." J. Cell Biol. **131**(1): 69-80.

**David van Duin, A. C. S.** (2007). "Toll-Like Receptors in Older Adults." Journal of the American Geriatrics Society **55**(9): 1438-1444.

**Deng, G.-M., et al.** (1999). "Intra-articularly localized bacterial DNA containing CpG motifs induces arthritis." Nat Med **5**(6): 702-705.

**Diebold, S. S., et al.** (2004). "Innate Antiviral Responses by Means of TLR7-Mediated Recognition of Single-Stranded RNA." Science **303**(5663): 1529-1531.

**Dodge, J. T., et al.** (1962). "The preparation and chemical characteristics of Hb-free ghosts of human erythrocytes." J Biol Chem **34**: 119-130.

**Dong, C.** (2008). "TH17 cells in development: an updated view of their molecular identity and genetic programming." Nat Rev Immunol **8**(5): 337-348.

**Donner, M. and J. F. Stoltz** (1985). "Comparative study on fluorescent probes distributed in human erythrocytes and platelets." Biorheology **22**(5): 385-97.

**Doray, B., et al.** (2007). "The {gamma}/{sigma}1 and {alpha}/{sigma}2 Hemicomplexes of Clathrin Adaptors AP-1 and AP-2 Harbor the Dileucine Recognition Site." Mol. Biol. Cell **18**(5): 1887-1896.

**Drab, M., et al.** (2001). "Loss of Caveolae, Vascular Dysfunction, and Pulmonary Defects in Caveolin-1 Gene-Disrupted Mice." Science **293**(5539): 2449-2452.

**Duarte C Barral, M. C., Peter J McCormick, Salil Garg, Anthony I Magee, Juan S Bonifacino, Gennaro De Libero, Michael B Brenner,** (2008). "CD1a and MHC Class I Follow a Similar Endocytic Recycling Pathway." Traffic **9**(9): 1446-1457.

**Dürr, U. H. N., et al.** (2006). "LL-37, the only human member of the cathelicidin family of antimicrobial peptides." Biochimica et Biophysica Acta (BBA) - Biomembranes **1758**(9): 1408-1425.

**Dustin, M. L., et al.** (2006). "T cell-dendritic cell immunological synapses." Current Opinion in Immunology **18**(4): 512-516.

**Dyer, M. R., et al.** (2006). "A second vaccine revolution for the new epidemics of the 21st century." Drug Discovery Today **11**(21-22): 1028-1033.

**Ennio De Gregorio, E. T., Rino Rappuoli,** (2008). "Alum adjuvanticity: Unraveling a century old mystery." European Journal of Immunology **38**(8): 2068-2071.

**Ericsson, H.** (1946). "Purification and adsorption of diphtheria toxoid." Nature **158**: 350-351.

**Espinoza-Delgado, I.** (2002). "Cancer Vaccines." Oncologist **7**(90003): 20-33.

**Fine, P. E. M.** (1993). "Herd Immunity: History, Theory, Practice." Epidemiol Rev **15**(2): 265-302.

**Flacher, V., et al.** (2006). "Human Langerhans Cells Express a Specific TLR Profile and Differentially Respond to Viruses and Gram-Positive Bacteria." J Immunol **177**(11): 7959-7967.

**Foged, C., et al.** (2004). "Interaction of dendritic cells with antigen-containing liposomes: effect of bilayer composition." Vaccine **22**(15-16): 1903-1913.

**Frecer, V., et al.** (2004). "De Novo Design of Potent Antimicrobial Peptides." Antimicrob. Agents Chemother. **48**(9): 3349-3357.

**Fritz, J. H., et al.** (2004). "The artificial antimicrobial peptide KLKLLLLLKLK induces predominantly a TH2-type immune response to co-injected antigens." Vaccine **22**(25-26): 3274-3284.

**Frohm, M., et al.** (1997). "The Expression of the Gene Coding for the Antibacterial Peptide LL-37 Is Induced in Human Keratinocytes during Inflammatory Disorders." J. Biol. Chem. **272**(24): 15258-15263.

**Froschauer, E., et al.** (2005). "Electroneutral K+/H+ exchange in mitochondrial membrane vesicles involves Yol027/Letm1 proteins." Biochimica et Biophysica Acta (BBA) - Biomembranes **1711**(1): 41-48.

**Fynan, E. F., et al.** (1993). "DNA vaccines: protective immunizations by parenteral, mucosal, and gene-gun inoculations." Proceedings of the National Academy of Sciences of the United States of America **90**(24): 11478-11482.

**Gagnon, E., et al.** (2002). "Endoplasmic Reticulum-Mediated Phagocytosis Is a Mechanism of Entry into Macrophages." Cell **110**(1): 119-131.

**Galiana-Arnoux, D. and J. Imler** (2006). "Toll-like receptors and innate antiviral immunity." Tissue Antigens **67**(4): T267 - 276.

**Gamvrellis, A., et al.** (2004). "Vaccines that facilitate antigen entry into dendritic cells." Immunol Cell Biol **82**(5): 506-516.

**García-Olmedo, F., et al.** (1998). "Plant defense peptides." Peptide Science **47**(6): 479-491.

**Garneau, S., et al.** (2002). "Two-peptide bacteriocins produced by lactic acid bacteria." Biochimie **84**(5-6): 577-592.

**Gauthier, N. C., et al.** (2005). "Helicobacter pylori VacA Cytotoxin: A Probe for a Clathrin-independent and Cdc42-dependent Pinocytic Pathway Routed to Late Endosomes." Mol. Biol. Cell **16**(10): 4852-4866.

**Gazit, E., et al.** (1996). "Structure and Orientation of the Mammalian Antibacterial Peptide Cecropin P1 within Phospholipid Membranes." Journal of Molecular Biology **258**(5): 860-870.

**Gennaro, R. and M. Zanetti** (2000). "Structural features and biological activities of the cathelicidin-derived antimicrobial peptides." Biopolymers **55**(1): 31-49.

**Gheysen, D., et al.** (1989). "Assembly and release of HIV-1 precursor Pr55gag virus-like particles from recombinant baculovirus-infected insect cells." Cell **59**(1): 103-112.

**Girao, H., et al.** (2008). "Actin in the endocytic pathway: From yeast to mammals." FEBS Letters **582**(14): 2112-2119.

**Glenny, A., et al.** (1926). "Immunological notes XVII to XXIV." J Path **29**: 31-40

**Goodman, M., et al.** (1969). "Sensitive criteria for the critical size for helix formation in oligopeptides." Proc Natl Acad Sci U S A **64**(2): 444-50.

**Granucci, F., et al.** (1999). "Early events in dendritic cell maturation induced by LPS." Microbes and Infection **1**(13): 1079-1084.

**Grundy, I.** (2000). "Montagu's variolation." Endeavour **24**(1): 4-7.

**Guermonprez, P., et al.** (2003). "ER-phagosome fusion defines an MHC class I cross-presentation compartment in dendritic cells." Nature **425**(6956): 397-402.

**Guha, A., et al.** (2003). "shibire mutations reveal distinct dynamin-independent and -dependent endocytic pathways in primary cultures of Drosophila hemocytes." J Cell Sci **116**(16): 3373-3386.

**Guy, B.** (2007). "The perfect mix: recent progress in adjuvant research." Nat Rev Micro **5**(7): 505-517.

**H. Bowen, A. K., T. Lee, P. Lavender,** (2008). "Control of cytokine gene transcription in Th1 and Th2 cells." Clinical & Experimental Allergy **38**(9): 1422-1431.

**Hagensee, M. E., et al.** (1993). "Self-assembly of human papillomavirus type 1 capsids by expression of the L1 protein alone or by coexpression of the L1 and L2 capsid proteins." J. Virol. **67**(1): 315-322.

**Hamaoka, T., et al.** (1973). "Hapten-specific lgE antivody responses in mice: I. Secondary IgE responses in irradiated recipients of synergeneic primed spleen cells." J. Exp. Med. **138**(1): 306-311.

**Hanzal-Bayer, M. F. and J. F. Hancock** (2007). "Lipid rafts and membrane traffic." FEBS Letters **581**(11): 2098-2104.

**Hartmann G., J. B., Hendrik Poeck, Moritz Wagner, Miren Kerkmann, Norbert Lubenow, Simon Rothenfusser, Stefan Endres,** (2003). "Rational design of new CpG oligonucleotides that combine B cell activation with high IFN-&agr; induction in plasmacytoid dendritic cells." European Journal of Immunology **33**(6): 1633-1641.

**Hayat, M. A.** (1989). "Principles and techniques of electron microscopy (3rd edition)." MacMillan Press.

**Heeg, K., et al.** (2008). "Structural requirements for uptake and recognition of CpG oligonucleotides." International Journal of Medical Microbiology **298**(1-2): 33-38.

**Heil, F., et al.** (2004). "Species-Specific Recognition of Single-Stranded RNA via Toll-like Receptor 7 and 8." Science **303**(5663): 1526-1529.

**Helmerhorst, E. J., et al.** (1999). "The Cellular Target of Histatin 5 on Candida albicans Is the Energized Mitochondrion." J. Biol. Chem. **274**(11): 7286-7291.

**Hemmi, H., et al.** (2002). "Small anti-viral compounds activate immune cells via the TLR7 MyD88-dependent signaling pathway." Nat Immunol **3**(2): 196-200.

**Hemmi, H., et al.** (2000). "A Toll-like receptor recognizes bacterial DNA." Nature **408**(6813): 740-745.

**Henning, L. N., et al.** (2008). "Pulmonary Surfactant Protein A Regulates TLR Expression and Activity in Human Macrophages." J Immunol **180**(12): 7847-7858.

**Henrik, W. B., et al.** (1997) A new approach to secondary structure evaluation: Secondary structure prediction of porcine adenylate kinase and yeast guanylate kinase by CD spectroscopy of overlapping synthetic peptide segments. Biopolymers 213-231 DOI: 10.1002/(SICI)1097-0282(199702)41:2<213::AID-BIP8>3.0.CO;2-W

**Henson, P. M., et al.** (2001). "The phosphatidylserine receptor: a crucial molecular switch?" Nat Rev Mol Cell Biol **2**(8): 627-633.

**Heuser, J.** (1980). "Three-dimensional visualization of coated vesicle formation in fibroblasts." J. Cell Biol. **84**(3): 560-583.

**Hill, E., et al.** (2001). "The Role of Dynamin and Its Binding Partners in Coated Pit Invagination and Scission." J. Cell Biol. **152**(2): 309-324.

**Hinrichsen, L., et al.** (2006). "Bending a membrane: How clathrin affects budding." Proceedings of the National Academy of Sciences **103**(23): 8715-8720.

**Hoene, V., et al.** (2006). "Human monocyte-derived dendritic cells express TLR9 and react directly to the CpG-A oligonucleotide D19." J Leukoc Biol **80**(6): 1328-1336.

**Hof, W. v. t., et al.** (2001). "Antimicrobial Peptides: Properties and Applicability." Biological Chemistry **382**(4): 597-619.

**Holbrook, I. B. and P. C. Molan** (1973). "A further study of the factors enhancing glycolysis in human saliva." Archives of Oral Biology **18**(10): 1275-82.

**Horazdovsky, B., et al.** (1997). "A sorting nexin-1 homologue, Vps5p, forms a complex with Vps17p and is required for recycling the vacuolar protein-sorting receptor." Mol. Biol. Cell **8**(8): 1529-1541.

**Hornung, V., et al.** (2008). "Silica crystals and aluminum salts activate the NALP3 inflammasome through phagosomal destabilization." Nat Immunol **9**(8): 847-856.

**Huckriede, A., et al.** (2005). "The virosome concept for influenza vaccines." Vaccine **23**(Supplement 1): S26-S38.

**Huleatt, J. W., et al.** (2007). "Vaccination with recombinant fusion proteins incorporating Toll-like receptor ligands induces rapid cellular and humoral immunity." Vaccine **25**(4): 763-775.

**Idrissi, F.-Z., et al.** (2008). "Distinct acto/myosin-I structures associate with endocytic profiles at the plasma membrane." J. Cell Biol. **180**(6): 1219-1232.

**Ilangumaran, S., et al.** (2000). "Microdomains in lymphocyte signalling: beyond GPI-anchored proteins." Immunology Today **21**(1): 2-7.

**Infante-Duarte, C., et al.** (2000). "Microbial Lipopeptides Induce the Production of IL-17 in Th Cells." J Immunol **165**(11): 6107-6115.

**Isogai, E., et al.** (2008). "Antimicrobial activity of three tick defensins and four mammalian cathelicidin-derived synthetic peptides against Lyme disease spirochetes and bacteria isolated from the midgut." Experimental and Applied Acarology.

**Iwasaki, A. and R. Medzhitov** (2004). "Toll-like receptor control of the adaptive immune responses." Nat Immunol **5**(10): 987-95.

**Janes, P. W., et al.** (1999). "Aggregation of Lipid Rafts Accompanies Signaling Via the T Cell Antigen Receptor." J. Cell Biol. **147**(2): 447-461.

**Jin, M. S. and J.-O. Lee** (2008). "Structures of TLR-ligand complexes." Current Opinion in Immunology **20**(4): 414-419.

**Johannes, L. and B. Goud** (1998). "Surfing on a retrograde wave: how does Shiga toxin reach the endoplasmic reticulum?" Trends in Cell Biology **8**(4): 158-162.

**Jones, D. and C. Bevins** (1992). "Paneth cells of the human small intestine express an antimicrobial peptide gene." J. Biol. Chem. **267**(32): 23216-23225.

**Jones, D. E. and C. L. Bevins** (1993). "Defensin-6 mRNA in human Paneth cells: implications for antimicrobia peptides in host defense of the human bowel." FEBS Letters **315**(2): 187-192.

**Jones, G. L., et al.** (1990). "Peptide vaccines derived from a malarial surface antigen: effects of dose and adjuvants on immunogenicity." Immunology Letters **24**(4): 253-260.

**Jörg Vollmer, R. W., Paul Payette, Marion Jurk, Christian Schetter, Meike Laucht, Tanja Wader, Sibylle Tluk, Ming Liu, Heather L. Davis, Arthur M. Krieg,** (2004). "Characterization of three CpG oligodeoxynucleotide classes with distinct immunostimulatory activities." European Journal of Immunology **34**(1): 251-262.

**Kagan, B. L., et al.** (1990). "Antimicrobial defensin peptides form voltage-dependent ion-permeable channels in planar lipid bilayer membranes." Proc Natl Acad Sci USA **87**(1): 210-214.

**Kamath, A. T., et al.** (2008). "Adult-like anti-mycobacterial T cell and in vivo dendritic cell responses following neonatal immunization with Ag85B-ESAT-6 in the IC31 adjuvant." PLoS ONE **3**(11): e3683.

**Kang, S., et al.** (2009). "Toll-like receptor 4 in lymphatic endothelial cells contributes to LPS-induced lymphangiogenesis by chemotactic recruitment of macrophages." Blood **113**(11): 2605-2613.

**Keller, G. A., et al.** (1992). "Endocytosis of glycophospholipid-anchored and transmembrane forms of CD4 by different endocytic pathways." EMBO J **11**(3): 863-74.

**Kerri A. Mowen, L. H. G.** (2004). "Signaling pathways in Th2 development." Immunological Reviews **202**(1): 203-222.

**Khan, S., et al.** (2007). "Distinct Uptake Mechanisms but Similar Intracellular Processing of Two Different Toll-like Receptor Ligand-Peptide Conjugates in Dendritic Cells." J. Biol. Chem. **282**(29): 21145-21159.

**Khandelia, H., et al.** (2008). "The impact of peptides on lipid membranes." Biochimica et Biophysica Acta (BBA) - Biomembranes **1778**(7-8): 1528-1536.

**Khelfaoui, M., et al.** (2009). "Inhibition of RhoA pathway rescues the endocytosis defects in Oligophrenin1 mouse model of mental retardation." Hum. Mol. Genet.: ddp189.

**Kirkham, M., et al.** (2005). "Ultrastructural identification of uncoated caveolin-independent early endocytic vehicles." J. Cell Biol. **168**(3): 465-476.

**Kitani, H., et al.** (2009). "Synthetic nonamer peptides derived from insect defensin mediate the killing of African trypanosomes in axenic culture." Parasitology Research **105**(1): 217-225.

**Kleijmeer, M., et al.** (2001). "Reorganization of multivesicular bodies regulates MHC class II antigen presentation by dendritic cells." J Cell Biol **155**(1): 53-63.

**Knorr, R., et al.** (2009). "Endocytosis of MHC molecules by distinct membrane rafts." J Cell Sci **122**(10): 1584-1594.

**Kokkinopoulos, I., et al.** (2005). "Toll-like receptor mRNA expression patterns in human dendritic cells and monocytes." Molecular Immunology **42**(8): 957-968.

**Kolls, J. K., et al.** (2008). "Cytokine-mediated regulation of antimicrobial proteins." Nat Rev Immunol **8**(11): 829-835.

**Kool, M., et al.** (2008). "Cutting Edge: Alum Adjuvant Stimulates Inflammatory Dendritic Cells through Activation of the NALP3 Inflammasome." J Immunol **181**(6): 3755-3759.

**Kosaka, T. and K. Ikeda** (1983). "Reversible blockage of membrane retrieval and endocytosis in the garland cell of the temperature-sensitive mutant of Drosophila melanogaster, shibirets1." J. Cell Biol. **97**(2): 499-507.

**Krieg, A. M.** (2006). "Therapeutic potential of Toll-like receptor 9 activation." Nat Rev Drug Discov **5**(6): 471-484.

**Krieg, A. M., et al.** (1999). "Mechanisms and therapeutic applications of immune stimulatory CpG DNA." Pharmacology & Therapeutics **84**(2): 113-120.

**Krisanaprakornkit, S., et al.** (1998). "Expression of the Peptide Antibiotic Human beta - Defensin 1 in Cultured Gingival Epithelial Cells and Gingival Tissue." Infect. Immun. **66**(9): 4222-4228.

**Lahiri, A., et al.** (2008). "Engagement of TLR signaling as adjuvant: Towards smarter vaccine and beyond." Vaccine **26**(52): 6777-6783.

**Lamaze, C., et al.** (2001). "Interleukin 2 Receptors and Detergent-Resistant Membrane Domains Define a Clathrin-Independent Endocytic Pathway." Molecular Cell **7**(3): 661-671.

**Langerhans, P.** (1868). "Über die Nerven der menschlichen Haut."

**Lanzavecchia, A. and F. Sallusto** (2001). "Antigen decoding by T lymphocytes: from synapses to fate determination." Nat Immunol **2**(6): 487-492.

**Larrick, J. W., et al.** (1995). "Human CAP18: a novel antimicrobial lipopolysaccharide-binding protein." Infect. Immun. **63**: 1291-1297.

**Latz, E., et al.** (2004). "TLR9 signals after translocating from the ER to CpG DNA in the lysosome." Nat Immunol **5**(2): 190-8.

**Laulagnier, K., et al.** (2004). "Mast cell- and dendritic cell-derived exosomes display a specific lipid composition and an unusual membrane organization." Biochem. J. **380**(1): 161-171.

**Lehrer, R. I., et al.** (1989). "Interaction of human defensins with Escherichia coli. Mechanism of bactericidal activity." J Clin Invest **84**(2): 553-561.

**Leippe, M.** (1999). "Antimicrobial and cytolytic polypeptides of amoeboid protozoa - effector molecules of primitive phagocytes." Developmental & Comparative Immunology **23**(4-5): 267-279.

**Lindblad, E. B.** (2004). "Aluminium adjuvants--in retrospect and prospect." Vaccine **22**(27-28): 3658-3668.

**Lingnau, K., et al.** (2007). "IC31 and IC30, novel types of vaccine adjuvant based on peptide delivery systems." Expert Rev Vaccines **6**(5): 741-6.

**Lipardi, C., et al.** (1998). "Caveolin Transfection Results in Caveolae Formation but Not Apical Sorting of Glycosylphosphatidylinositol (GPI)-anchored Proteins in Epithelial Cells." J. Cell Biol. **140**(3): 617-626.

**Lipford, G. B., et al.** (1997). "Immunostimulatory DNA: sequence-dependent production of potentially harmful or useful cytokines." Eur J Immunol **27**.

**Liu, Y.-J.** (2005). "IPC: Professional Type 1 Interferon-Producing Cells and Plasmacytoid Dendritic Cell Precursors." Annual Review of Immunology **23**(1): 275.

**Ludtke, S. J., et al.** (1996). "Membrane Pores Induced by Magainin&#x2020." Biochemistry **35**(43): 13723-13728.

**Ludtke, S. J., et al.** (1996). "Membrane Pores Induced by Magainin†" Biochemistry **35**(43): 13723-13728.

**Lundberg, M. and M. Johansson** (2002). "Positively Charged DNA-Binding Proteins Cause Apparent Cell Membrane Translocation." Biochemical and Biophysical Research Communications **291**(2): 367-371.

**Luque-Ortega, J. R., et al.** (2008). "Human antimicrobial peptide histatin 5 is a cell-penetrating peptide targeting mitochondrial ATP synthesis in Leishmania." FASEB J. **22**(6): 1817-1828.

**M. A. M. Willart, B. N. L.** (2009). "The danger within: endogenous danger signals, atopy and asthma." Clinical & Experimental Allergy **39**(1): 12-19.

**MacKay, B. J., et al.** (1984). "Growth-inhibitory and bactericidal effects of human parotid salivary histidine-rich polypeptides on Streptococcus mutans." Infect. Immun. **44**(3): 695-701.

**Mallard, F., et al.** (1998). "Direct Pathway from Early/Recycling Endosomes to the Golgi Apparatus Revealed through the Study of Shiga Toxin B-fragment Transport." J. Cell Biol. **143**(4): 973-990.

**Mann, A., et al.** (2008). "Peptides in DNA delivery: current insights and future directions." Drug Discovery Today **13**(3-4): 152-160.

**Marc S. Lamphier, C. M. S., ANJALI VERMA, DOUGLAS T. GOLENBOCK, EICKE LATZ,** (2006). "TLR9 and the Recognition of Self and Non-Self Nucleic Acids." Annals of the New York Academy of Sciences **1082**(Oligonucleotide Therapeutics: First Annual Meeting of the Oligonucleotide Therapeutics Society): 31-43.

**Marciani, D. J., et al.** (2003). "Fractionation, structural studies, and immunological characterization of the semi-synthetic Quillaja saponins derivative GPI-0100." Vaccine **21**(25-26): 3961-3971.

**Marckmann, G.** (2008). "Impfprogramme im Spannungsfeld zwischen individueller Autonomie und allgemeinem Wohl." Bundesgesundheitsblatt - Gesundheitsforschung - Gesundheitsschutz **51**(2): 175-183.

**Martin-Fontecha, A., et al.** (2003). "Regulation of Dendritic Cell Migration to the Draining Lymph Node: Impact on T Lymphocyte Traffic and Priming." J. Exp. Med. **198**(4): 615-621.

**Martinez, G. J., et al.** (2008). "Regulation and Function of Proinflammatory TH17 Cells." Annals of the New York Academy of Sciences **1143**(The Year in Immunology 2008): 188-211.

**Matsumoto, M. and T. Seya** (2008). "TLR3: Interferon induction by double-stranded RNA including poly(I:C)." Advanced Drug Delivery Reviews **60**(7): 805-812.

**Matthew J. Hawryluk, P. A. K., Sanjay K. Mishra, Simon C. Watkins, John E. Heuser, Linton M. Traub,** (2006). "Epsin 1 is a Polyubiquitin-Selective Clathrin-Associated Sorting Protein." Traffic **7**(3): 262-281.

**Mattner, F., et al.** (2002). "Vaccination with poly-L-arginine as immunostimulant for peptide vaccines: induction of potent and long-lasting T-cell responses against cancer antigens." Cancer Res **62**.

**Maurer, W.** (2008). "Impfskeptiker - Impfgegner. Von einer anderen Realität im Internet." Pharmazie in unserer Zeit **37**(1): 64-70.

**May, T. and R. D. Silverman** (2005). "Free-Riding, Fairness, and the Rights of Minority Groups in Exemption from Mandatory Childhood Vaccination." human Vaccines **1**(1): 11-14.

**Mayor, S. and R. E. Pagano** (2007). "Pathways of clathrin-independent endocytosis." Nat Rev Mol Cell Biol **8**(8): 603-612.

**Mayor, S. and M. Rao** (2004). "Rafts: Scale-Dependent, Active Lipid Organization at the Cell Surface." Traffic **5**(4): 231-240.

**McCarthy, E. F.** (2006). "The toxins of William B. Coley and the treatment of bone and soft-tissue sarcomas." The Iowa orthopaedic journal **26**: 154-8.

**Meier, M. and J. Seelig** (2007). "Thermodynamics of the Coil [two left arrows] [beta]-Sheet Transition in a Membrane Environment." Journal of Molecular Biology **369**(1): 277-289.

**Mellman, I.** (1996). "ENDOCYTOSIS AND MOLECULAR SORTING." Annual Review of Cell and Developmental Biology **12**(1): 575-625.

**Merad, M. and M. G. Manz** (2009). "Dendritic cell homeostasis." Blood **113**(15): 3418-3427.

**Merrifield, C. J., et al.** (2005). "Coupling between Clathrin-Coated-Pit Invagination, Cortactin Recruitment, and Membrane Scission Observed in Live Cells." **121**(4): 593-606.

**Mineo, C. and R. Anderson** (2001). "Potocytosis." Histochemistry and Cell Biology **116**(2): 109-118.

**Miseta, A., et al.** (1995). "Effect of non-lytic concentrations of Brij series detergents on the metabolism-independent ion permeability properties of human erythrocytes." Biophysical Journal **69**(6): 2563-2568.

**Moraes, L. G. M., et al.** (2007). "Conformational and functional studies of gomesin analogues by CD, EPR and fluorescence spectroscopies." Biochimica et Biophysica Acta (BBA) - Biomembranes **1768**(1): 52-58.

**Moser, M. and K. M. Murphy** (2000). "Dendritic cell regulation of TH1-TH2 development." Nat Immunol **1**(3): 199-205.

**Mosmann, T., et al.** (1986). "Two types of murine helper T cell clone. I. Definition according to profiles of lymphokine activities and secreted proteins." J Immunol **136**(7): 2348-2357.

**Mueller, P.** (1975). "Membrane excitation through voltage-induced aggregation of channel precursors." Annals of the New York Academy of Sciences **264**(Carriers and Channels in Biological Systems): 247-264.

**Muscat, M., et al.** (2009). "Measles in Europe: an epidemiological assessment." The Lancet **373**(9661): 383-389.

**Nagai, Y., et al.** (2006). "Toll-like Receptors on Hematopoietic Progenitor Cells Stimulate Innate Immune System Replenishment." Immunity **24**(6): 801-812.

**Nagao, J.-i., et al.** (2006). "Lantibiotics: Insight and foresight for new paradigm." Journal of Bioscience and Bioengineering **102**(3): 139-149.

**Nakajima, Y., et al.** (1997). "Chemotherapeutic activity of synthetic antimicrobial peptides: correlation between chemotherapeutic activity and neutrophil-activating activity." FEBS Letters **415**(1): 64-66.

**Nichols, B.** (2003). "Caveosomes and endocytosis of lipid rafts." J Cell Sci **116**(23): 4707-4714.

**Nicklas, W., et al.** (2002). "Recommendations for the health monitoring of rodent and rabbit colonies in breeding and experimental units." Lab Anim **36**(1): 20-42.

**Norbury, C. C.** (2006). "Drinking a lot is good for dendritic cells." Immunology **117**(4): 443-51.

**Nowikovsky, K., et al.** (2004). "The LETM1/YOL027 Gene Family Encodes a Factor of the Mitochondrial K+ Homeostasis with a Potential Role in the Wolf-Hirschhorn Syndrome." J. Biol. Chem. **279**(29): 30307-30315.

**Núñez, L. F. a. G.** (2008). "The Nlrp3 inflammasome is critical for aluminium hydroxide-mediated IL-1&bgr; secretion but dispensable for adjuvant activity." European Journal of Immunology **38**(8): 2085-2089.

**Ogden, C. A., et al.** (2001). "C1q and Mannose Binding Lectin Engagement of Cell Surface Calreticulin and CD91 Initiates Macropinocytosis and Uptake of Apoptotic Cells." J. Exp. Med. **194**(6): 781-796.

**Oren, Z. and Y. Shai** (1998). "Mode of action of linear amphipathic &agr;-helical antimicrobial peptides." Peptide Science **47**(6): 451-463.

**Palade, G. E.** (1953). "Fine structure of blood capillaries." Journal of applied Physics **24**: 1424.

**Park, B., et al.** (2008). "Proteolytic cleavage in an endolysosomal compartment is required for activation of Toll-like receptor 9." Nat Immunol **9**(12): 1407-1414.

**Parton, R. G.** (2003). "Caveolae [mdash] from ultrastructure to molecular mechanisms." Nat Rev Mol Cell Biol **4**(2): 162-167.

**Parton, R. G. and K. Simons** (2007). "The multiple faces of caveolae." Nat Rev Mol Cell Biol **8**(3): 185-194.

**Pavelka, M., et al.** (2008). "Retrograde traffic in the biosynthetic-secretory route." Histochemistry and Cell Biology **129**(3): 277-288.

**Pelkmans, L., et al.** (2001). "Caveolar endocytosis of simian virus 40 reveals a new two-step vesicular-transport pathway to the ER." Nat Cell Biol **3**(5): 473-483.

**Peter Cresswell, A. L. A., Alessandra Giodini, David R. Peaper, Pamela A. Wearsch,** (2005). "Mechanisms of MHC class I-restricted antigen processing and cross-presentation." Immunological Reviews **207**(1): 145-157.

**Podda, A. and G. Del Giudice** (2003). "MF59-adjuvanted vaccines: increased immunogenicity with an optimal safety profile." Expert Review of Vaccines **2**(2): 197-204.

**Poethko-Müller, C., et al.** (2009). "Vaccination coverage against measles in German-born and foreign-born children and identification of unvaccinated subgroups in Germany." Vaccine **27**(19): 2563-2569.

**Pollock, J. J., et al.** (1984). "Fungistatic and fungicidal activity of human parotid salivary histidine-rich polypeptides on Candida albicans." Infect. Immun. **44**(3): 702-707.

**Pouny, Y., et al.** (1992). "Interaction of antimicrobial dermaseptin and its fluorescently labeled analogues with phospholipid membranes." Biochemistry(31): 12416-23.

**Presicce, P., et al.** (2009). "Human defensins activate monocyte-derived dendritic cells, promote the production of proinflammatory cytokines, and up-regulate the surface expression of CD91." J Leukoc Biol: jlb.0708412.

**Pulendran Bali** (2004). "Modulating vaccine responses with dendritic cells and Toll-like receptors." Immunological Reviews **199**(1): 227-250.

**Qian, S., et al.** (2008). "Structure of the Alamethicin Pore Reconstructed by X-Ray Diffraction Analysis." Biophysical Journal **94**(9): 3512-3522.

**Qiu, Q., et al.** (2008). "Induction of multispecific Th-1 type immune response against HCV in mice by protein immunization using CpG and Montanide ISA 720 as adjuvants." Vaccine **26**(43): 5527-5534.

**Raj, P. A., et al.** (1998). "Structure of human salivary histatin 5 in aqueous and nonaqueous solutions." Biopolymers **45**(1): 51-67.

**Rajput, Z., et al.** (2007). "Adjuvant effects of saponins on animal immune responses." Journal of Zhejiang University - Science B **8**(3): 153-161.

**Ralph Nossal** (2001). "Energetics of Clathrin Basket Assembly." Traffic **2**(2): 138-147.

**Rapoport, I., et al.** (1998). "Dileucine-based sorting signals bind to the beta chain of AP-1 at a site distinct and regulated differently from the tyrosine-based motif-binding site." EMBO J **17**(8): 2148-55.

**Razani, B., et al.** (2002). "Caveolin-1-deficient Mice Are Lean, Resistant to Diet-induced Obesity, and Show Hypertriglyceridemia with Adipocyte Abnormalities." J. Biol. Chem. **277**(10): 8635-8647.

**Reipert, S., et al.** (2008). "Rapid Microwave Fixation of Cell Monolayers Preserves Microtubule-associated Cell Structures." J. Histochem. Cytochem. **56**(7): 697-709.

**Reutterer, B., et al.** (2008). "Type I IFN are host modulators of strain-specific Listeria monocytogenes virulence." Cellular Microbiology **10**(5): 1116-1129.

**Riedl, K., et al.** (2008). "The novel adjuvant IC31 strongly improves influenza vaccine-specific cellular and humoral immune responses in young adult and aged mice." Vaccine **26**(27-28): 3461-8.

**Roohvand, F., et al.** (2007). "HCV core protein immunization with Montanide/CpG elicits strong Th1/Th2 and long-lived CTL responses." Biochemical and Biophysical Research Communications **354**(3): 641-649.

**Roth, T. F. and K. R. Porter** (1964). "Yolk protein uptake in the oocyte of the mosquito Aedes Aegypti.. L." J. Cell Biol. **20**(2): 313-332.

**Rothberg, K., et al.** (1990). "Cholesterol controls the clustering of the glycophospholipid-anchored membrane receptor for 5-methyltetrahydrofolate." J. Cell Biol. **111**(6): 2931-2938.

**Sabharanjak, S., et al.** (2002). "GPI-Anchored Proteins Are Delivered to Recycling Endosomes via a Distinct cdc42-Regulated, Clathrin-Independent Pinocytic Pathway." Developmental Cell **2**(4): 411-423.

**Sailaja, G., et al.** (2007). "Human immunodeficiency virus-like particles activate multiple types of immune cells." Virology **362**(2): 331-341.

**Salaun, B., et al.** (2009). "Toll-like receptor 3 is necessary for dsRNA adjuvant effects." Vaccine **27**(12): 1841-1847.

**Sallusto, F., et al.** (1995). "Dendritic cells use macropinocytosis and the mannose receptor to concentrate macromolecules in the major histocompatibility complex class II compartment: downregulation by cytokines and bacterial products." J Exp Med **182**(2): 389-400.

**Sallusto, F., et al.** (1995). "Dendritic cells use macropinocytosis and the mannose receptor to concentrate macromolecules in the major histocompatibility complex class II compartment: downregulation by cytokines and bacterial products." J Exp Med **182**(2): 389-400.

**Satyajit Mayor, M. R.** (2004). "Rafts: Scale-Dependent, Active Lipid Organization at the Cell Surface." Traffic **5**(4): 231-240.

**Savina, A. and S. Amigorena** (2007). "Phagocytosis and antigen presentation in dendritic cells." Immunological Reviews **219**(1): 143-156.

**Schafmeister, C., et al.** (1993). "Structure at 2.5 A of a designed peptide that maintains solubility of membrane proteins." Science(262): 734-8.

**Schellack, C., et al.** (2006). "IC31, a novel adjuvant signaling via TLR9, induces potent cellular and humoral immune responses." Vaccine **24**(26): 5461-72.

**Schmid D., H. H., S Abele, S Kasper, S König, S Meusburger, H Hrabcik, A Luckner-Hornischer, E Bechter, A DeMartin, Jana Stirling, A Heißenhuber, A Siedler, H Bernard, G Pfaff , D Schorr, M S Ludwig, HP Zimmerman, Ø Løvoll, P Aavitsland, F Allerberger** (2008). "An ongoing multi-state outbreak of measles linked to non-immune anthroposophic communities in Austria, Germany, and Norway, March-April 2008." Eurosurveillance **13**(16).

**Schmidt, W., et al.** (1997). "Cell-free tumor antigen peptide-based cancer vaccines." Proc Natl Acad Sci USA **94**.

**Schnitzer, J. and P. Oh** (1994). "Albondin-mediated capillary permeability to albumin. Differential role of receptors in endothelial transcytosis and endocytosis of native and modified albumins." J. Biol. Chem. **269**(8): 6072-6082.

**Scott, R. W., et al.** (2008). "De novo designed synthetic mimics of antimicrobial peptides." Current Opinion in Biotechnology **19**(6): 620-627.

**Seaman, M. N. J., et al.** (1998). "A Membrane Coat Complex Essential for Endosome-to-Golgi Retrograde Transport in Yeast." J. Cell Biol. **142**(3): 665-681.

**Seelig, J.** (2004). "Thermodynamics of lipid-peptide interactions." Biochimica et Biophysica Acta (BBA) - Biomembranes **1666**(1-2): 40-50.

**Segawa, S., et al.** (1991). "Local structures in unfolded lysozyme and correlation with secondary structures in the native conformation: helix-forming or -breaking propensity of peptide segments." Biopolymers **31**(5): 497-509.

**Serwold, T., et al.** (2002). "ERAAP customizes peptides for MHC class I molecules in the endoplasmic reticulum." Nature **419**(6906): 480-483.

**Shai, Y.** (1999). "Mechanism of the binding, insertion and destabilization of phospholipid bilayer membranes by [alpha]-helical antimicrobial and cell non-selective membrane-lytic peptides." Biochimica et Biophysica Acta (BBA) - Biomembranes **1462**(1-2): 55-70.

**Sharma, P., et al.** (2002). "Endocytosis of lipid rafts: an identity crisis." Seminars in Cell and Developmental Biology **13**(3): 205-214.

**Shi, J., et al.** (2007). "A Novel Role for Defensins in Intestinal Homeostasis: Regulation of IL-1beta Secretion." J Immunol **179**(2): 1245-1253.

**Shortman, K. and S. H. Naik** (2007). "Steady-state and inflammatory dendritic-cell development." Nat Rev Immunol **7**(1): 19-30.

**Sigismund, S., et al.** (2005). "Clathrin-independent endocytosis of ubiquitinated cargos." Proceedings of the National Academy of Sciences of the United States of America **102**(8): 2760-2765.

**Simons, K. and E. Ikonen** (1997). "Functional rafts in cell membranes." Nature **387**(6633): 569-572.

**Simpson, J. C., et al.** (1998). "Expression of Mutant Dynamin Protects Cells against Diphtheria Toxin but Not against Ricin." Experimental Cell Research **239**(2): 293-300.

**Skene, C. D. and P. Sutton** (2006). "Saponin-adjuvanted particulate vaccines for clinical use." Methods **40**(1): 53-59.

**Smet, K. and R. Contreras** (2005). "Human Antimicrobial Peptides: Defensins, Cathelicidins and Histatins." Biotechnology Letters **27**(18): 1337-1347.

**Smith, J. L., et al.** (2008). "Caveolin-1-Dependent Infectious Entry of Human Papillomavirus Type 31 in Human Keratinocytes Proceeds to the Endosomal Pathway for pH-Dependent Uncoating." J. Virol. **82**(19): 9505-9512.

**Spang, A.** (2009). "On the fate of early endosomes." Biological Chemistry **0**(ja): ---.

**Sparwasser, T., et al.** (1997). "Bacterial DNA causes septic shock." Nature **1997**(386).

**Stebbing, S. R., et al.** (2008). "Sizing, stoichiometry and optical absorbance variations of colloidal cadmium sulphide nanoparticles." Advances in Colloid and Interface Science **147-148**: 272-280.

**Steinman, R., et al.** (1976). "Membrane flow during pinocytosis. A stereologic analysis." J. Cell Biol. **68**(3): 665-687.

**Steinman, R., et al.** (1983). "Endocytosis and the recycling of plasma membrane." J. Cell Biol. **96**(1): 1-27.

**Steinman, R. M., et al.** (1999). "Antigen capture, processing, and presentation by dendritic cells: recent cell biological studies." Human Immunology **60**(7): 562-567.

**Stella, L., et al.** (2007). "Alamethicin Interaction with Lipid Membranes: A Spectroscopic Study on Synthetic Analogues." Chemistry & Biodiversity **4**(6): 1299-1312.

**Stirling, L., et al.** (2009). "Dual Roles for RHOA/RHO-Kinase In the Regulated Trafficking of a Voltage-sensitive Potassium Channel." Mol. Biol. Cell: E08-10-1074.

**Sturm, L. A., et al.** (2005). "Parental Beliefs and Decision Making About Child and Adolescent Immunization: From Polio to Sexually Transmitted Infections." Journal of Developmental & Behavioral Pediatrics **26**(6): 441-452.

**Terzi, E., et al.** (1997). "Interaction of Alzheimer β-Amyloid Peptide(1−40) with Lipid Membranes&#x2020." Biochemistry **36**(48): 14845-14852.

**Terzi, E., et al.** (1997). "Interaction of Alzheimer Î²-Amyloid Peptide(1âˆ’40) with Lipid Membranesâ€ " Biochemistry **36**(48): 14845.

**Thiele, L., et al.** (2001). "Evaluation of particle uptake in human blood monocyte-derived cells in vitro. Does phagocytosis activity of dendritic cells measure up with macrophages?" Journal of Controlled Release **76**(1-2): 59-71.

**Tieleman, D., et al.** (2002). "Analysis and evaluation of channel models: simulations of alamethicin." Biophysical Journal **83**(5): 2393-2407.

**Torgersen, M. L., et al.** (2001). "Internalization of cholera toxin by different endocytic mechanisms." J Cell Sci **114**(20): 3737-3747.

**Traub, L. M. and G. L. Lukacs** (2007). "Decoding ubiquitin sorting signals for clathrin-dependent endocytosis by CLASPs." J Cell Sci **120**(4): 543-553.

**Ungewickell, E. J. and L. Hinrichsen** (2007). "Endocytosis: clathrin-mediated membrane budding." Current Opinion in Cell Biology **19**(4): 417-425.

**van der Bliek, A. M. and E. M. Meyerowrtz** (1991). "Dynamin-like protein encoded by the Drosophila shibire gene associated with vesicular traffic." Nature **351**: 411 - 414.

**Varki, A.** (2009). "Multiple changes in sialic acid biology during human evolution." Glycoconjugate Journal **26**(3): 231-245.

**Videira, P., et al.** (2008). "Surface α2-3- and α2-6-sialylation of human monocytes and derived dendritic cells and its influence on endocytosis." Glycoconjugate Journal **25**(3): 259-268.

**Vogel, H.** (1981). "Incorporation of Melittin into phosphatidylcholine bilayers: Study of binding and conformational changes." FEBS Letters **134**(1): 37-42.

**Wagner, H.** (2004). "The immunobiology of the TLR9 subfamily." Trends in Immunology **25**(7): 381-386.

**Wagner, H.** (2008). "The sweetness of the DNA backbone drives Toll-like receptor 9." Current Opinion in Immunology **20**(4): 396-400.

**White, S. H., et al.** (1995). "Structure, function, and membrane integration of defensins." Current Opinion in Structural Biology **5**(4): 521-527.

**Wichmann, O., et al.** (2007). "Large Measles Outbreak at a German Public School, 2006." The Pediatric Infectious Disease Journal **26**(9): 782-786 10.1097/INF.0b013e318060aca1.

**Wright, C. A., et al.** (2004). "Tapasin and other chaperones: models of the MHC class I loading complex." Biological Chemistry **385**(9): 763-778.

**Wu, L. and Y.-J. Liu** (2007). "Development of Dendritic-Cell Lineages." Immunity **26**(6): 741-750.

**Yamada, E.** (1955). "The Fine Structure of the Gall Bladder Epithelium of the Mouse." J. Cell Biol. **1**(5): 445-458.

**Yeung, T. and S. Grinstein** (2007). "Lipid signaling and the modulation of surface charge during phagocytosis." Immunological Reviews **219**(1): 17-36.

**Yoder, A., et al.** (2003). "Tripalmitoyl-S-Glyceryl-Cysteine-Dependent OspA Vaccination of Toll-Like Receptor 2-Deficient Mice Results in Effective Protection from Borrelia burgdorferi Challenge." Infect. Immun. **71**(7): 3894-3900.

**Young, K. R., et al.** (2006). "Virus-like particles: Designing an effective AIDS vaccine." Methods **40**(1): 98-117.

**Yu, L., et al.** (2009). "Interaction of an artificial antimicrobial peptide with lipid membranes." Biochimica et Biophysica Acta (BBA) - Biomembranes **1788**(2): 333-344.

**Zaiou, M.** (2007). "Multifunctional antimicrobial peptides: therapeutic targets in several human diseases." Journal of Molecular Medicine **85**(4): 317-329.

**Zanetti, M., et al.** (1995). "Cathelicidins: a novel protein family with a common proregion and a variable C-terminal antimicrobial domain." FEBS Letters **374**(1): 1-5.

**Zeya, H. I. and J. K. Spitznagel** (1966). "Cationic Proteins of Polymorphonuclear Leukocyte Lysosomes I. Resolution of Antibacterial and Enzymatic Activities." J. Bacteriol. **91**(2): 750-754.

**Zhao, Q., et al.** (1996). "Effect of different chemically modified oligodeoxynucleotides on immune stimulation." Biochemical Pharmacology **51**(2): 173-182.

**Zhou, M., et al.** (2009). "Toll-like receptor expression in normal ovary and ovarian tumors." Cancer Immunology, Immunotherapy.

**Zimet, G. D., et al.** (2006). "Chapter 24: Psychosocial aspects of vaccine acceptability." Vaccine **24**(Supplement 3): S201-S209.

**Zimmet, P. Z. and K. G. M. M. Alberti** (2006). "Introduction: Globalization and the Non-communicable Disease Epidemic." Obesity **14**(1): 1-3.

**Zinser, E. and G. Daum** (1995). "Isolation and biochemical characterization of organelles from the yeast, Saccharomyces cerevisiae." Yeast **11**(6): 493-536.

# 8. Curriculum vitae

**Personal Information:**

| | |
|---|---|
| Date of Birth: | September 23rd, 1980 |
| Place of Birth: | Wels |
| Citizenship: | Austria |
| Marital status: | Married |

**Education:**

| | |
|---|---|
| **2005–2009** | PhD thesis:<br>*"Interaction between the cationic antimicrobial peptide-derivative KLKLLLLLKLK (KLK) and biological membranes. Investigation of the immuno-biological effects of KLK on dendritic cells"* (University of Vienna; Lab of Prof. Rudolf Schweyen in collaboration with Intercell) |
| **2004–2005** | Diploma thesis:<br>*"Ynl086w, a new factor in Alr1 degradation."* (University of Vienna; Lab of Prof. Rudolf Schweyen, Vienna Biocenter) |
| **2000–2005** | Study of Microbiology and Genetics<br>at the University of Vienna |
| **1999–2000** | Military service, Hörsching |
| **1999, July 27th** | Final examination (Matura) |
| **1991–1999** | Grammar school, Stiftsgymnasium Wilhering |
| **1987–1991** | Elementary school in Eferding |

**Publications:**

**2009** Paper submitted: *"Adjuvanting the Adjuvant: Facilitated delivery of the immunomodulatory oligonucleotide, ODN1a, to TLR9 by the cationic antimicrobial peptide, KLK, in dendritic cells."*

**2008** *"Unique membrane-interacting properties of the immunostimulatory cationic peptide KLKL(5)KLK (KLK)"* (Aichinger et al.; Cell Biology International, 32(11):1449-58)

**2006** *"Oligomerization of the Mg2+-transport proteins Alr1p and Alr2p in yeast plasma membrane"* (Wachek et al.; FEBS J., 273(18):4236-49)

# 9. Acknowledgements

I would like to thank **Tamás Henics** for supervising my work and for his scientific input. I am grateful for his open mind and his straightforward ideas, but above all, his positive aura that created an excellent working atmosphere.

Further, I owe thanks to the whole **MRS-group** for input, for chats at the lunchtime, for cookies and everything else.

This thesis would not have been possible without many people from Intercell, who supported me in various ways:
**Karin and Rosi Riedl**, for discussions and for the bone marrow
**Ursula Schlosser** and **Michael Ginzler**, for the essential assistance generating human dendritic cells
Great thanks **to Karen Lingnau**, who helped a lot in defining new research strategies and who offered help, when I needed it
**Eszter Nagy**, who was always providing her scientific knowledge to bring this work forward

A special "thank you" to **Alexander van Gabain**, for is support, for his uncomplicated but precise way of analyzing the data and last but not least for his visions.

I must not forget **Prof. Thomas Decker** who kindly took over the position as supervising professor and who helped me in the last period of my thesis. Also **Renate Kastner** and **Lisa Kernbauer** for coffee, chats and killing the mice.

At this point, I have to thank **Rudolf Schweyen**. When I started my studies, his lesson was the first I visited. His motivation brought me to genetics. I am still glad that I had the opportunity to work in his lab and to learn from his attitude towards research.

I would like to thank my **family** and my **friends** for their support, the drinks together, the parties and everything else.

If you want to emphazise someone, you have to put his name at the beginning, or at the end of a chapter. Therefore, here is the best place to say "thank you" to my wife, Sandra Illibauer-Aichinger. **Sandra** thank you for everything.